UNIVERSITÀ DI PARMA

UNIVERSITÀ DEGLI STUDI DI PARMA

DOTTORATO DI RICERCA IN

Scienza e Tecnologia dei Materiali

CICLO XXXIII

Towards a Closed Nuclear Fuel Cycle: Ligands for the Actinide-Lanthanide Separation

Coordinatore:

Chiar.mo Prof. Enrico Dalcanale

Tutore:

Chiar.mo Prof. Alessandro Casnati

Dottoranda: Maria Chiara Gullo

Anni Accademici 2017/2018 – 2019/2020

CONTENTS

List of Abbreviations

An	Actinides
BTBP	Bis-Triazinyl-BiPyridine
BTP	Bis-Triazinyl-Pyridine
BTPhen	Bis-Triazinyl-Phenantroline pyridine
CEA	Commissariat de l'énergie atomique & alternatives
CMPT	Methyl 2,6-bis(1-octyl-1H-1,2,3-triazol-4-yl)isonicotinate
CO_2	Carbonic anhydride
CuAAC	Copper(I)-catalyzed Azide-Alkyne Cycloaddition
DEHiBA	*N, N*-di-(ethyl-2-hexyl)isobutyramide
DGAs	Diglycolamides
DIAMEX	Diamide extraction
DMDBTDMA	*N,N'*-dimethyl- *N,N'*-dibutyl-2-tetradecylmalonamide
DMDOHEMA	*N,N'*-dimethyl-*N,N'*-dioctyl-2-hexylethoxymalonamide
DP	Degradation product
ESI-MS	ElectroSpray Ionization Mass Spectroscopy
EU	European Union
FPs	Fission Products
GANEX	Grouped actinide extraction
HLW	High Level Waste
HAR	High Active Raffinate
IAEA	International Atomic Energy Agency
IEA	International Energy Agency
KIT	Karlsruhe Institute of Technology
Ln	Lanthanides
MA	Minor Actinides (Np, Am, Cm)
MOx	Mixed Oxide Fuel
NMR	nuclear Magnetic Resonance
NOx	New uranium Oxide fuel
P&T	Partitioning and Transmutation
POLIMI	Politecnico di Milano
PTA	2-(1-(propan-3-ol)-1,2,3-triazol-4-yl)-6-ethynylpyridine
PTC	8,8'-(4,4'-(Pyridine-2,6-diyl)bis(1H-1,2,3-triazole-4,1-diyl))-dioctanoic acid
PTD	2,6-(propan-3-ol)-1,2,3-triazol-4-yl)pyridine
PTD-OMe	2,6-(propan-3-ol)-1,2,3-triazol-4-yl)-4-methoxypyridine

PTDO	2,6-Bis(1-dodecyl-1H-1,2,3-triazol-4-yl)pyridine
PTEH	2,6-Bis[1-(2-ethylhexyl)-1H-1,2,3-triazol-4-yl]pyridine
PTID	2,6-bis(1-(2,7-dimethyloctyl)-1H-1,2,3-triazol-4-yl)pyridine
PTO	2,6-Bis(1-octyl-1H-1,2,3-triazol-4-yl)pyridine
PTTO	2,6-bis(1-(2,4,4-trimethylpentyl)-1H-1,2,3-triazol-4-yl)pyridine
PyTri	2,6-bis(1,2,3-triazol-4-yl)pyridine
PUREX	Plutonium and Uranium Reduction Extraction
SANEX	Selective actinide extraction
i-SANEX	Innovative selective actinide extraction
1c-SANEX	1 cycle selective actinide extraction
SNF	Spent Nuclear Fuel
SO3-Ph-BTP	bis(di-sulfo-phenyl)-triazine-pyridine
TBP	Tri-n-butylphosphate
TODGA	*N',N',N',N'*-tetraoctyldiglycolamide
TPH	Hydrogenated tetrapropene
TRLFS	Time Resolved Laser-induced Fluorescence Spectroscopy
TRU	Transuranic
UNIPR	Università degli Studi di Parma
UV-Vis	UltraViolet Visible spectrophotometry

Abstract

The present PhD thesis mainly focused on the design, synthesis and characterization of novel lipophilic and hydrophilic ligands for actinides and lanthanides separation from nuclear waste. The properties of these ligands in terms of extraction efficiency and metal selectivity are extensively studied with liquid-liquid extraction tests and with Time-Resolved Laser-induced Fluorescence Spectroscopy. Most of the research work was focused on the development of An selective ligands, either hydrophilic or lipophilic, based on the 2,6-bis(1,2,3-triazol-4-yl)pyridine, PyTri, chelating unit. The extractants were obtained exploiting the Copper(I)-catalyzed azide-alkyne cycloaddition (CuAAC) reaction between the 2,6-diethynyl pyridine (para functionalized as needed) and a proper azide. After a first introductory chapter on the state of the art of spent nuclear fuel reprocessing, Chapter 2 deals with studies aimed at the industrial scale implementation of the hydrophilic PTD stripping agent consisting in its scale-up synthesis and investigations on its degradation products under processing conditions. In Chapter 3, in order to enhance PTD complexation properties, a revised ligand, PTD-OMe, is presented. The influence of the presence of the electron-donating methoxy group in para position of the pyridine ring on the metal ion complexation and extraction properties is studied. In Chapter 4, seven different lipophilic ligands based on the PyTri chelating moiety were synthetized and their properties exhaustively described. Among all, the PTEH is the most promising lipophilic extracting agent. For this reason, a preorganized calixarene-based ligand was prepared bearing three PTEH moieties at the lower rim. Preliminary studies on its extraction properties and on the cooperation effect of the PyTri units are also reported.

The last part of the work, described in Chapter 5, was carried out at the University of Twente during a three months secondment. The work is focused on the design and synthesis of novel An and Ln lipophilic ligands based on diglycolamide (DGA) chelating unit, prepared via the Schotten-Baumann reaction, and exploiting a novel stereochemical control on metal ion binding.

Chapter 1
General Introduction

1.1 Overview

1.1.1 Nuclear power in Europe

One of the ever-present topics in public debates is global warming. Indeed, climate change is the most critical issue facing humanity today. On this basis, one of the current worldwide challenges is the production of clean energy through an increase in the use of alternative energy sources to fossil fuels. The development of renewable energies such as hydro, wind and solar is increasing, as these are supposed to be the future leaders in an ambitious program of clean power production. Despite this, a large number of technologies will be needed in order to cope with rapidly growing global energy demand. According to the International Energy Agency (IEA), global electricity requirements will double between 2007 and 2030.[1] Global population growth is not the only determining factor of this rise. In fact, over the last few years a variety of fuel-based processes have been replaced by electricity-based ones, e.g. in public transportation, in order to restrict the use of fossil fuels and achieve environmental sustainability. Together with the already cited alternative energy sources, nuclear power -which cannot commonly be considered as an alternative renewable energy mainly due to safety issues- can play an important role in limiting greenhouse gas emissions, the primary driver of climate change. If we analyze the advanced economies as a whole, nuclear energy can be considered the largest low-carbon source of electricity in the world.[2] As it can be seen in Figure 1.1, nuclear power counts for 40% of the energy produced in advanced economies excluding carbon and other combustibles. In a wider view, that is considering also carbon and other combustibles, 10% of the global electricity supply in 2018 was provided by nuclear power.

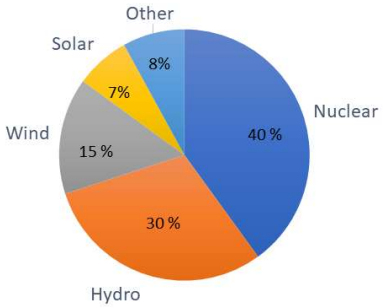

Figure 1.1. Percentage of low-carbon electricity generated in advanced economies in 2018. Data from IEA

We can assert that renewable energies and nuclear power are the most powerful tools to mitigate climate change and satisfy the growing energy demand.

On the basis of the data provided by the International Atomic Energy Agency (IAEA), there are 448 nuclear power plants operating in 31 countries all over the world while 61 are in construction.[3] Most of these operating plants are in Europe where 25% of total electricity demand is obtained from nuclear reactors. As a result, nuclear energy plays a fundamental role in limiting European's emissions of CO_2 and contributes to the EU's independence, security and diversity of energy sources. The main producer of nuclear power in the European Union is France, with its 58 nuclear power plants, followed by Sweden and Germany with 10 and 8 respectively, but the situation in Italy is entirely different.[2] Italy used to have 4 reactors (Caorso, Garigliano, Latina, Trino Vercellese) but they were all closed after the referendum of 1987, just a year after the Chernobyl disaster. In 2011 there was an attempt to reintroduce nuclear energy with another referendum, yet this culminated with the complete abolition of all Italian nuclear ambitions. Despite this, Italy - one of the major importers of electricity - buys a high percentage of energy directly from French nuclear plants. After some nuclear accidents, Switzerland and Germany followed Italy by announcing the temporary decommissioning of their nuclear programmes, in most part due to a strong internal pressure of the public opinion and media. The adoption of nuclear power to acquire zero carbon emission power, is a sound strategy, but its use remains a controversial topic in the European Union's energy debate, mainly due to public skepticism and economic factors. About this last aspect, most of the European nuclear reactors were built in the 1970's and 80's, and designed to last 30 to 40 years, so their lifetime is now almost over. The hypothesis of extending their lifetime is surely cheaper than the construction of new reactors, even though it is expensive and cost-competitive with the investment in other electricity producing

technologies (hydro, wind, solar).[2] On this basis one quarter of the reactors in advanced economies are expected to shut down by 2025. According to IAEA report, at this time, 162 reactors are being decommissioned around the world.[3]

The public acceptance for the employing of nuclear power is mainly related to safety issues and waste handling. Renewable energy sources produce more medium-level chemical waste compared to nuclear reactors, however the latter ones generate high level radioactive waste not produced by the former ones.[4] Safety and environmental issues related to the use of nuclear power plants are currently some of the most discussed topics in the energy industry. A safe, permanent solution in the management of contaminated waste is a hard goal to reach, and many technological advances still have to be attained. Moreover, it is worth noting that we cannot focus exclusively on upcoming waste production whilst forgetting about the already existing one. Whatever the decision by European governments about the future of nuclear power plants will be, one of the most important scientific and social challenges we face today is to ease the disposal of radioactive wastes accumulated over the last decades not only from nuclear plants but also from nuclear weapon and waste from hospitals.[5]

1.1.2 Recycling of nuclear waste

Uranium, with its high fission cross section for thermal neutrons, is the fundamental constituent of the fuel employed in modern nuclear reactors. Since the natural isotopic composition of uranium is 99.3% of ^{238}U and only 0.7 % of fissile ^{235}U usually the fuel is enriched in ^{235}U up to 5%. Currently there are many kinds of atomic reactors all based on nuclear fission. The main reactions that take place in a reactor, and that contribute to the composition of the spent fuel are: 1) fission of the fissile nuclei such as ^{235}U and ^{239}Pu, and 2) neutron capture followed by β decay reactions. The fertile ^{238}U can be converted into fissile nuclides through neutron capture and β decay leading to the formation of transuranic elements (TRU) and, among those, the most abundant is fissile ^{239}Pu. (Neutron capture and β decay $^{1}n_0 + {}^{238}U \rightarrow {}^{239}U + {}^{239}Np \rightarrow {}^{239}Pu$).

^{239}Pu is a fissile nuclide and can be used as fuel in nuclear reactors together with ^{235}U providing up to one third of the total energy produced. The possibility to use both ^{238}U and ^{235}U as starting material makes uranium an inexhaustible energy source. Indeed, the amount of exhausted uranium stored worldwide, and recoverable from

spent fuel, can provide energy for hundreds of years.[6]

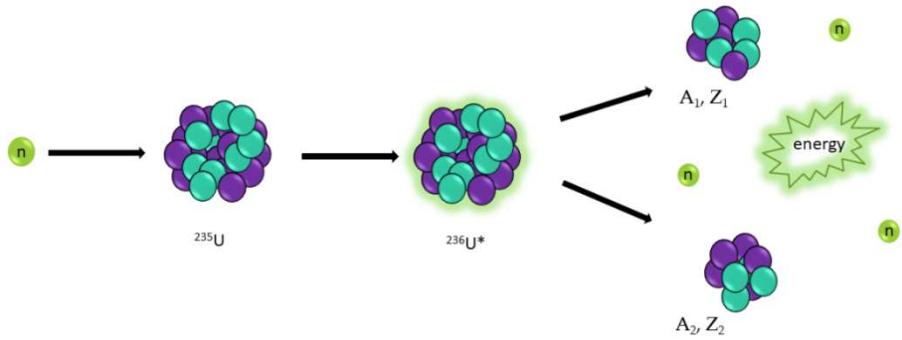

Figure 1.2. Representation of a fission reaction starting from ^{235}U

$^{1}n_0 + ^{235}U \rightarrow ^{236}U^* \rightarrow (A_1, Z_1) + (A_2, Z_2) + N\,^{1}n_0 + energy$

The final composition of the spent nuclear fuel (SNF) depends on the initial fuel type and its enrichment grade; commonly it is made of 93% of ^{238}U, 1% of ^{235}U, 5 % of short-lived fission products (FPs), 1% of transuranic actinides (Np, Pu, Am, Cm). In regards to minor actinides, Am and Cm account for ca. 0.1% of the total waste and having a $t_{1/2}$ of 10^3 to 10^6 years are recognized as the main responsible for the long-term radiotoxicity of the spent fuel.[7,8,9] In recent decades new innovative technologies created to recycle spent fuel have been explored. Some of them, which are in an advanced stage of development, can help to reduce the volume of the waste and the related radioactive hazard, making nuclear energy a more sustainable power source.[6]

There are currently two options for the management of spent fuel: the open nuclear fuel cycle and the closed nuclear fuel cycle. The first one requires that the used fuel is directly sent to geological disposal facilities, while the second one is based on the recovery of fissile U and Pu followed by the reprocessing of the minor actinides.[9] Which of these two alternatives would be the best one for the handling of spent fuel has been discussed for decades, and this debate has become more important in recent years due to the increasing accumulation of both used fuel and high active raffinate (HAR) derived from the reprocessing. The main problem related to the deep geological storage is that wastes containing long-lived radionuclides remain radioactive for hundreds of thousands of years.[10] That way, ensuring a safe storage for this extended period of time is both challenging and expensive, and public opinion is hesitant.[11] Nowadays, one of the proposed solutions for HLW are deep boreholes and mined repositories but the technologies for the construction of these sites are in early development and depend on the geology of the involved countries.

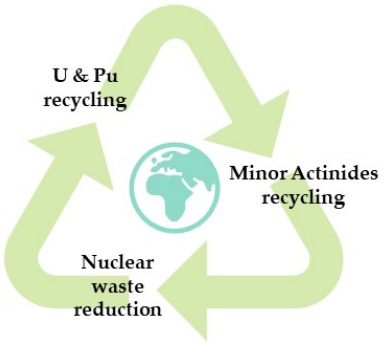

Figure 1.3. Representation of a closed nuclear fuel cycle

The closed nuclear fuel cycle approach aims at the separation of Pu, U and radionuclides contained in the HLW and their reuse as fuel in new generation reactors. Historically the reprocessing of nuclear fuels began with the early use of nuclear weapons in order to reuse fissile Pu and U, and in 1949 the PUREX process was developed by the University of Chicago.[12] PUREX (Plutonium and Uranium Recovery by Extraction) is now a worldwide known process for the recovery of U and Pu and it allows their recycling to mixed oxide fuel (MOX) for fast reactors. This process can be adapted for the separation of Np (advanced PUREX), but in order to enhance the safety and society acceptability of the nuclear energy, the recovery of Am and Cm is also mandatory. Nowadays, the most promising idea for the reprocessing of Minor Actinides is the strategy of Partitioning and Transmutation (P&T). As I have previously stated, minor actinides are responsible for the long-term radioactivity so that their transmutation allows to obtain shorter-lived or stable nuclides reducing the longevity and the volume of radioactive waste to be stored. Partitioning is necessary in order to separate actinides from lanthanides, which also exist as fission products. Indeed, due to the high neutron absorption cross-section of the majority of lanthanides, their presence can hinder an efficient transmutation of MA. The high chemical similarity of An and Ln, however, makes their partition a challenging and demanding process in the field of hydrometallurgy. Moreover, partitioned Am and Cm can be used as fuel in future IV generation (GenIV) reactors, thus closing the nuclear fuel cycle. For this reason, the idea of a closed nuclear fuel cycle employing the P&T strategy could be the right solution to handle nuclear wastes and make nuclear power more sustainable.

The recycling of spent fuel is crucial in order to reduce the waste lifetime (time necessary to

go back to the radioactivity of a uranium ore) from hundreds of thousands to hundreds of years. The estimated time for the decay of radioactive waste send to geological repository without recycling is more than 1,000,000 years. The recycling of U and Pu allows to come to 100,000 whilst the entire reprocessing, including the MA recycling, lead to a time lower than 1,000 years for radioactive decay.[13]

Europe is leading in terms of scientific research and technological progresses for waste management, although a lot of efforts still have to be done. The nuclear power will either be discarded or employed as a future energy source, but in both cases, recycling remains the key for a much-improved environmental sustainability of the radioactive waste generated up to now.

1.2 Reprocessing of nuclear waste

1.2.1 Hydrometallurgy

The main technologies for the reprocessing of nuclear waste can be distinguished in Pyrometallurgy and Hydrometallurgy and are categorized respectively as dry and wet processes. Pyrometallurgy is based on chemical operations carried out at high temperature while hydrometallurgy relies on solvent extraction methods.[14] These processes have already been used for a long time in Europe and they can count on a long-lasting experience at industrial level. Therefore liquid/liquid separation methods are currently considered the reference technology for the achievement of metal ions partition from spent nuclear fuel.[15] Since they deal with organic/aqueous extraction they require always new research in extractants, diluents and organic solvents. The extraction method shown in Figure 1.4 relies on a selective extraction of the element of our interest from a phase to another immiscible one.[14,16] In the case of nuclear application, metal ions are diffused in an acidic aqueous phase while the extracting agent is dissolved in a suitable organic diluent. The two solutions are mixed in order to enhance the contact area between them. During this mixing phase the metal ion to be extracted binds to the chelating agent forming a complex soluble in the organic phase. Once the chemical equilibrium is reached, the phases can be separated. This way, it is possible to have an aqueous phase containing all the undesired chemical species and an organic phase, hopefully, containing only/mainly the interested metal ion with the achievement of a full separation. To complete the recovery of the metal ions it is often necessary and desirable to apply a second step consisting in the back

extraction process called stripping. The organic phase is washed with a clean aqueous phase able to bring in the metal ions back in water. This step is often very important because it allows to reuse the extracting solvent in a hypothetical industrial plant further increasing the repeatability of the entire recycling process without the need to change or refill the extracting agent.

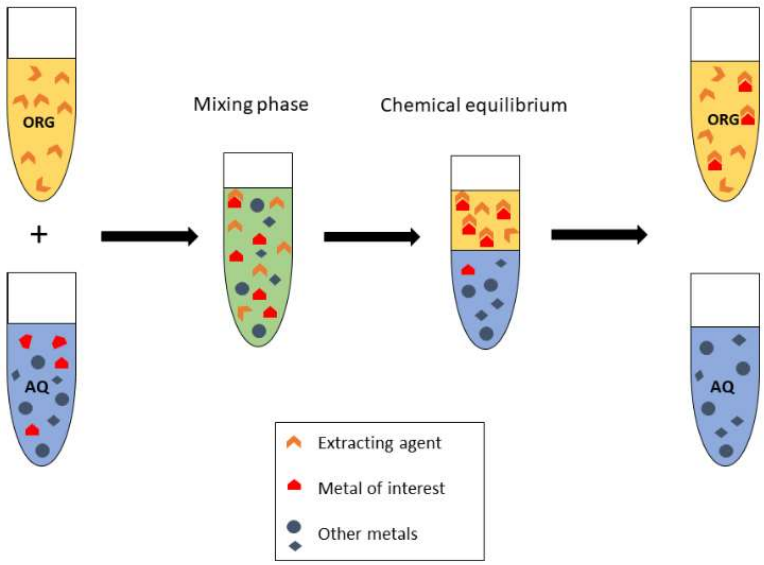

Figure 1.4. Solvent/solvent extraction concept. An organic phase (yellow) containing the extracting agent is contacted with an aqueous phase (blue) containing the metal ions to be separated. After the chemical equilibrium is reached the yellow and blue solutions can be separated

Thanks to the hydrometallurgical processes for the treatment of spent fuel, it is possible to distinguish between homogenous and heterogenous recycling. The heterogenous recycling is based on the partitioning of Pu and U first followed by minor actinides separation. On the other side, in the homogenous recycling, uranium is the only metal separated during the first stage, while plutonium is extracted together with all the minor actinides in the second process as shown on the left side of Figure 1.5.[17]

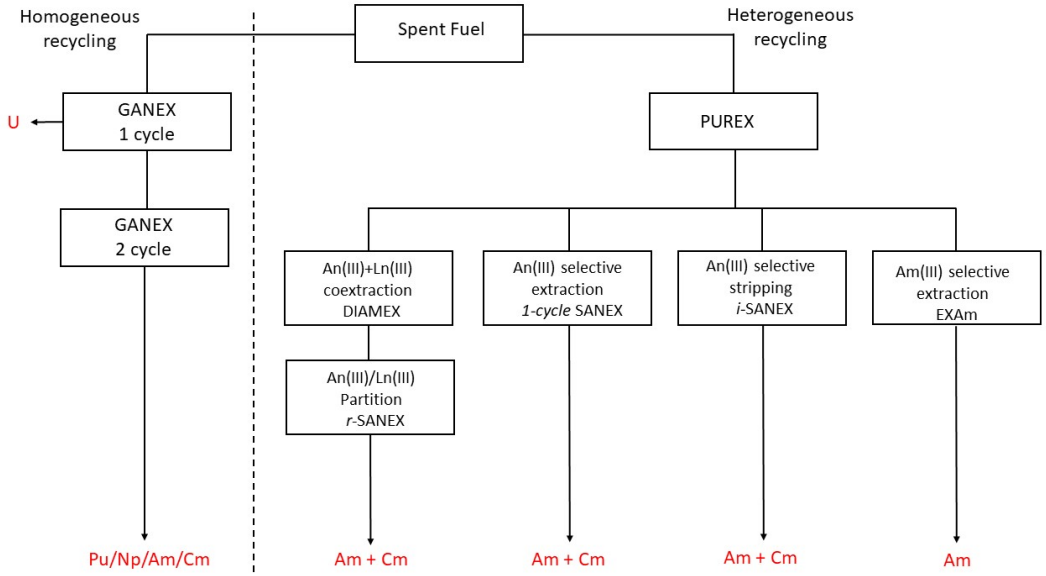

Figure 1.5. European hydrometallurgical processes for the reprocessing of spent nuclear fuel

1.2.2 U and Pu recovery

All reprocessing cycles related to the heterogeneous recycling start with the recovery of U and Pu employing the previously cited PUREX process. Said solvent extraction technology allows to separate valuable uranium and plutonium from other fission products and in the final stage also from each other, leading to the recycling of both metals as NOx or MOx fuel for faster reactors. PUREX has been well-known since the early '50s and it is now worldwide industrially employed, representing a solid base for the development of innovative recycling processes. The starting phase of this multi-step system is the dissolution of the used fuel in aqueous concentrated HNO_3 to form Pu(IV) and U(VI) nitrates according to the following reactions: $PuO_2 + 4HNO_3 \rightarrow Pu(NO_3)_4 + 2H_2O$ and $UO_2 + 4HNO_3 \rightarrow UO_2(NO_3)_2 + 2H_2O + 2NO_2$.[2] $Pu(NO_3)_4$ and $UO_2(NO_3)_2$ are then contacted with an organic phase containing TBP (Tri-*n*-butyl phosphate, Figure 1.7) as extracting agent. The TBP is able to extract Pu(IV) and U(VI) in the organic phase where Pu(IV) is converted into Pu(III) using a reducing agent like Fe(II) and U(IV). This last step is essential for the separation of plutonium and uranium since TBP can extract only tetravalent and hexavalent metals. In this way, it becomes possible to remove trivalent Pu into a clean acidic aqueous phase. Partitioned U and Pu are converted to U/Pu-MOX fuel that can be reused in fast reactors while MAs remain. Finally, the stripping of metals from the TBP containing organic phase

and from the acidic aqueous phase allow the recycling of both solvents.[2,5] In addition, recent studies have demonstrated the possibility to adapt PUREX process to include the separation of Np.

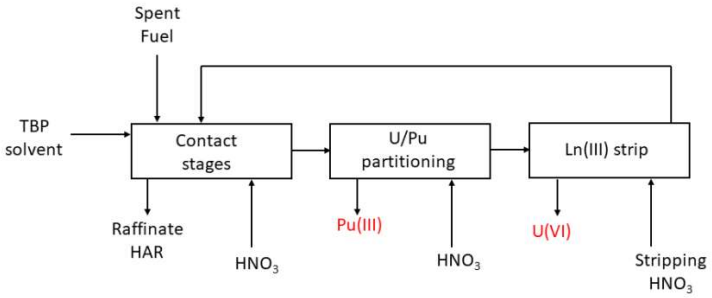

Figure 1.6. Schematic flowsheet of PUREX

Beside the inconvenient related to the presence of the reducing step needed for the separation of Pu from U (*vide supra*) the main drawback of PUREX is the use of an extracting agent containing phosphorous. TBP indeed produces non-incinerable wastes. One of the goals of the current research is to ensure a minimum generation of contaminated secondary waste and thus a highly sustainable process. The complete incinerability of the secondary wastes pushed the scientists working in this field to formulate new engineering strategy called *CHON principle*. That means that all the compounds involved in the reprocessing of the SNF must contain only Carbon, Hydrogen, Oxygen and Nitrogen atoms in order to obtain a completely incinerable organic waste.[9,10]

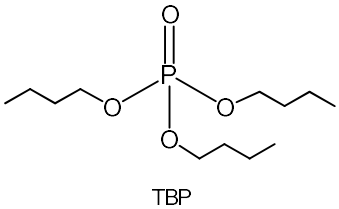

Figure 1.7. Molecular structure of tri-n-butylphosphate

The HAR (high active raffinate), aqueous phases generated in the PUREX, contains trans-plutonium elements (Am, Cm) together with lanthanides and other nontoxic fission products. The full partitioning of MA is therefore not possible with PUREX but it still urges to be the main goal of the reprocessing cycle. For this purpose, different strategies are being studied all around the world. In Europe, for example, many

projects have been funded from the European Commission over the last 30 years. The most recent ones are ACSEPT, SACSSES and currently GENIORS (2017-2021). On a European level the most promising option for the recovery of MA is entirely based on liquid/liquid extraction and it requires three main stages, Figure 1.8. After the PUREX, An and Ln are co-extracted in the refining phase and only in a third step they can be separated each other's. A further step can be added for the separation of Am from Cm.

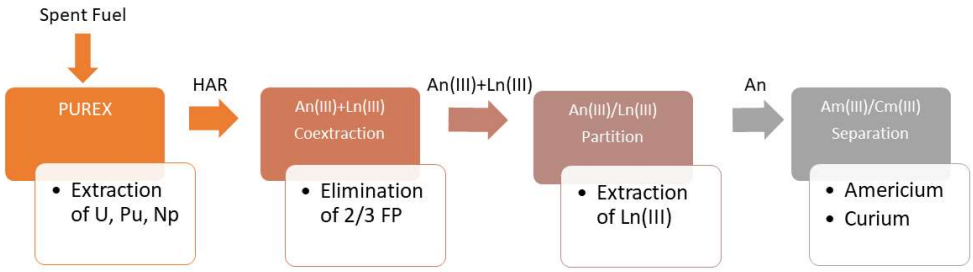

Figure 1.8. Schematic representation of the European strategy for the separation of MA

1.2.3 An and Ln co-extraction processes

The European reference process for the An and Ln co-extraction is DIAMEX, DIAMide EXtraction, developed by the French Commissariat de l' Énergie Atomique & Alternatives (CEA). The process has been tested for the first time in 1993 using real wastes at the Fontenay-aux-Roses CEA's laboratory center.[11] It requires four main steps (Figure 1.9): extraction, two scrubbing steps, An/Ln stripping. In the extraction stage the acidic aqueous phase collected from the PUREX (HAR) is contacted with an organic phase containing a diamide-based ligand able to selectively remove An and Ln from the rest. To avoid the co-extraction of Zirconium and Molybdenum, oxalic acid is added during the scrubbing stage. A further washing is necessary to fully clean the organic phase from other fission products. In the last step An and Ln are stripped with a 0,1 M HNO_3 solution, thus allowing the recycling of the organic phase.[12]

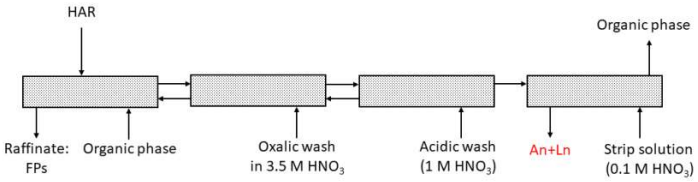

Figure 1.9. Schematic flowsheet of the DIAMEX process[18]

Two different families of ligands have been employed as co-extracting agents: malonamides and diglycolamides both respectful of the cited CHON principle. Starting from the '80s, a multitude of different malonamides were synthesized to be employed in liquid/liquid extraction experiments. Among all the others, the *N*,*N*′-dimethyl- *N*,*N*′-dibutyl-2-tetradecylmalonamide (DMDBTDMA, Figure 1.10 left) was the first one to be used in a spiked test in 1998.[19] Further studies of hydrolysis and radiolysis stability led to a valid candidate for the DIAMEX process, the *N*,*N*′-dimethyl-*N*,*N*′-dioctyl-2-hexylethoxymalonamide (DMDOHEMA, Figure 1.10), that became the molecule of reference.[8]

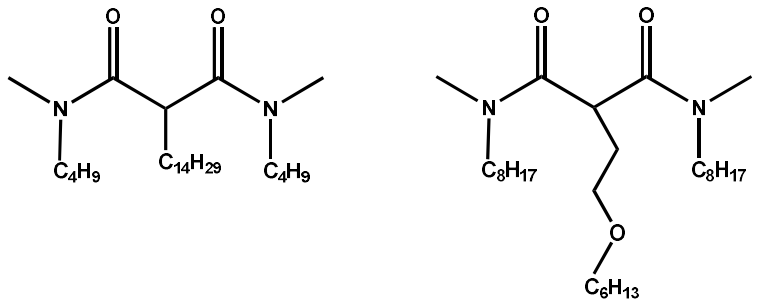

Figure 1.10. Molecular structure of DMDBTDMA (left) and DMDOHEMA (right)

More recently, another process that is being studied for the separation of An and Ln from the raffinate of PUREX counts on the use of TODGA-based solvents. A Japanese group discovered the high selectivity for An of diglycolamides during the 90's and different compounds were then synthesized. DGAs, differently from malonamides, are tridentate ligand, since the presence of an additional central oxygen atom offers the third complexing position. In addition, diglycolamides are less sensitive to acid, making it possible to operate at a lower pH range.[20,21] TODGA, *N*,*N*,*N*′,*N*′-tetraoctyldiglycolamide (Figure 1.11), showed the best affinity and solubility properties and it is now considered a valid reference molecule in a DIAMEX-like process. A successful partitioning process using TODGA was tested in 2003 by

Modolo et al. in Julich.[22] After those good results, new developments have been made and in 2006 a hot test was run at the Institute for Transuranium Elements, ITU. In these tests TBP, see Figure 1.7, was used as extractant together with TODGA but in the last variant the former ligand was replaced by *n*-octanol moving to a completely CHON compliant process. The current reference solvent for further improvements is made of 0.2 mol/L TODGA and 5% v/v octanol in kerosene.[8]

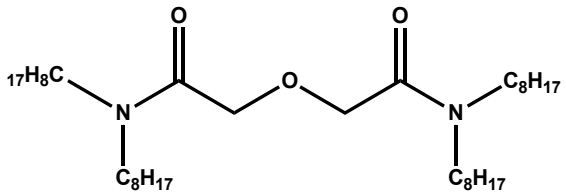

Figure 1.11. Molecular structure of TODGA

1.2.4 Selective actinide extraction processes

As described in Figure 1.8, through the DIAMEX/TODGA process it is possible to extract An and Ln from the rest of the fission products, but a further step is required to separate MA from lanthanides. The first method for the selective separation of An(III) was developed by Weaver and Kappelman[14] in the '60s. The TALSPEAK (trivalent Actinide-Lanthanide Separation by Phosphorous reagent Extraction from Aqueous Komplexes) is based on the extraction of Ln(III) with an acidic organophosphorus agent while actinides remain in the aqueous phase complexed by a polyaminocarboxylic acid. The extracting agent (2-ethylhexyl) phosphorous acid (HDEHP) is not able to distinguish between trivalent An or Ln showing high affinity for both. In order to avoid the extraction of An(III) by HDEHP, diethylenetriaminepentaacetic acid (DTPA, Figure 1.12) was added to a buffered aqueous solution. The presence of nitrogen atoms in the polyaminocarboxylic acids makes them ideal holdback reagents for trivalent actinides showing higher affinity for 5f elements.[23,14] After a few years it was developed a different version of the process. This time An(III) were extracted in the organic phase while Ln(III) remain in the aqueous solution and because of this the process was called *reverse*-TALSPEAK. After the coextraction of An and Ln by HDEHP, a selective stripping using DTPA removes selectively trivalent actinides.[24] Despite various development of this process have been done during the last decades it is not consider a viable alternative for An/Ln partitioning at industrial scale. Indeed, two are the main problems related to the

process: the necessity of a strict pH control in a limited value range and the need of a phase transfer agent to increase the extraction kinetics.

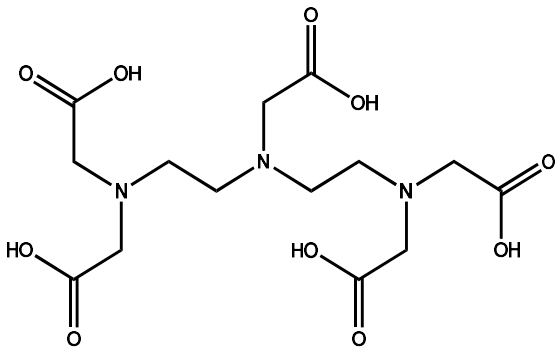

Figure 1.12. Molecular structure of DTPA

The TALSPEAK was the base for the development of a new European process entirely focused on the partitioning of An(III)/Ln(III). The SANEX (Selective Actinides Extraction) has been developed since the 2000s in different European centers and intends to selectively separate An(III) from a DIAMEX raffinate which contains both trivalent An and Ln. The general route of the process is based on a liquid/liquid extraction, where the aqueous phase collected from the DIAMEX is contacted with an organic phase containing a selective actinide extracting agent. The main difficulty of this technology is to find a high actinide selective organic ligand that complies with the CHON principle and that can operate at the rather low pH range of the DIAMEX raffinates. The first family of compound meeting these requirements was that of the bis-triazinyl-pyridines (BTP) introduced for the first time by Kolarik et al.[25] and, more recently, replaced by a new family called bis-triazinyl-bipyridine (BTBP) presented by Hudson et al.[26]. In 2013 Modolo et al.[27] performed a spiked and a hot test using $CyMe_4$-BTBP that became the current reference molecule for the process.

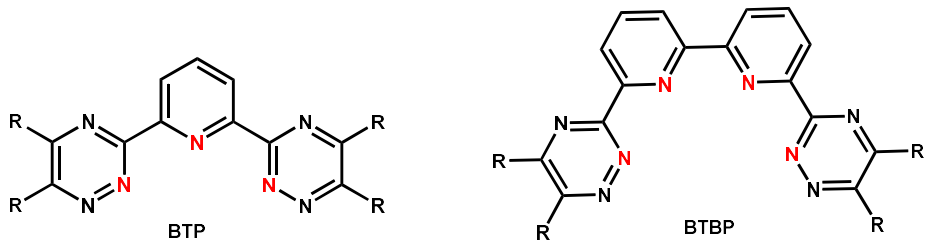

Figure 1.13. Chemical structure of Bis-Triazinyl Pyridine (left) and bis-triazinyl-bipyridine (right)

The latest version of SANEX developed and tested by Modolo et al. and presented in Figure 1.14, is a 20 stages-process. The first twelve steps are extraction stages followed by 4

scrubbing steps and 4 stripping steps. The organic phase is 15mmol/L $CyMe_4$-BTBP + 5mmol/L TODGA in *n*-octanol. For the washing stages it was used 0.7 M HNO_3 and for the back extraction a 0.5 glycolic acid solution. TODGA replaced DMDOHEMA as transfer catalyst agent which was employed in an older version of the process. The use of TODGA allows to work at low concentration and to increase the solubility of the BTBP ligand.[9,19]

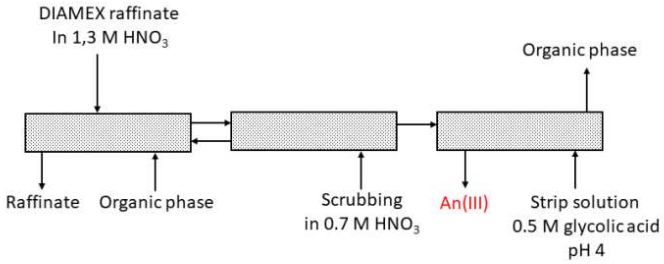

Figure 1.14. Schematic flowsheet of the latest version of r-SANEX[12]

The European strategy for the separation of actinides from the PUREX raffinate represented in Figure 1.8 is complex and involves different processes. This multiple-cycle technology could be simplified to a single cycle in order to make the reprocessing of SNF easier and less expensive. Moreover, reducing the number of stages could be a great step forward to increase the sustainability of the entire nuclear fuel cycle. Recently new SANEX-based processes have been developed in the frame of different European projects: the innovative SANEX (*i*-SANEX) and the one cycle SANEX (1-cycle SANEX). The *i*-SANEX is based on the suppression of the DIAMEX as independent process, since the selective partition of An(III) is directly made after a An(III) + Ln(III) co-extraction employing a DIAMEX-SANEX-like solvent. The flowsheet shown in Figure 1.15 includes three main stages. The first step is a co-extraction of An(III) and Ln(III) using an organic ligand like TODGA or DMDOHEMA, the following step is the selective stripping of An(III) using a hydrophilic ligand. During this phase it is necessary to introduce a further lipophilic ligand to complex Ln(III) in order to avoid their extraction in the aqueous phase. The last step is the stripping of Ln(III), which is performed using a diluted nitric acid solution. Several modifications have been made before the last variant was proposed by Geist and coll.. The coextraction of An(III) and Ln(III) is made with $CyMe_4$-BTBP + TODGA in *n*-octanol like in the DIAMEX process. The selective stripping of An(III) relies on the hydrophilic 2,6-bis(5,6-di(sulfophenyl)-1,2,4-triazin-3-yl)pyridine, SO_3-

Ph-BTP (*vide infra*). It was demonstrated that the presence of SO_3-Ph-BTP inhibits the An(III) complexation by TODGA so an additional complexing ligand is useless. The SO_3-Ph-BTP *i*-SANEX process is still being studied and it seems to be a promising technique.

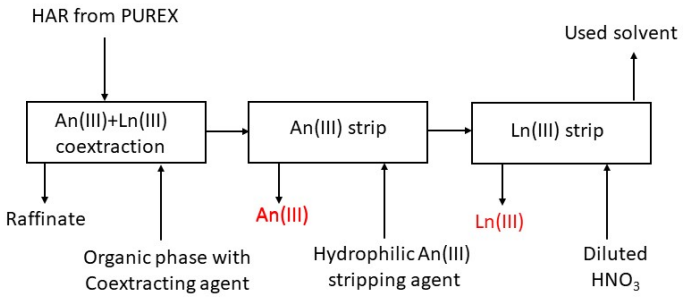

Figure 1.15. Simplified flowsheet for i-SANEX process

The second single cycle process proposed for actinides partition is the 1 cycle SANEX. This process leads to a fundamental improvement in the field of actinides separation. In fact, the extraction of An(III) takes place directly from the PUREX raffinate completely suppressing the previous coextraction step. The selective extraction exploits the properties of the already known CyMe$_4$-BTBP and *N,N,N′,N′*-tetraoctyldiglycolamide in TPH/ octanol 4:6 solution. The main related problem is to avoid the coextraction of unwanted fission products like Mo, Zr and Pd. Different masking agents can be added to the organic phase as oxalic acid and HEDTA already used in the DIAMEX. The relevance of 1 cycle SANEX was demonstrated with a test using simulated HAR solution, when 99,4% of An(III) were recovered in a single step. The last variant of the process shown in Figure 1.16 relies on 32 steps divided in three main stages: extraction, scrubbing stages and one stripping stage. The scrubbing stages are necessary in order to eliminate the unwanted fission products and the Pd which is removed through the employing of a solution of L-cysteine. The last stripping step allows to recover the An in a clean acidic aqueous phase.

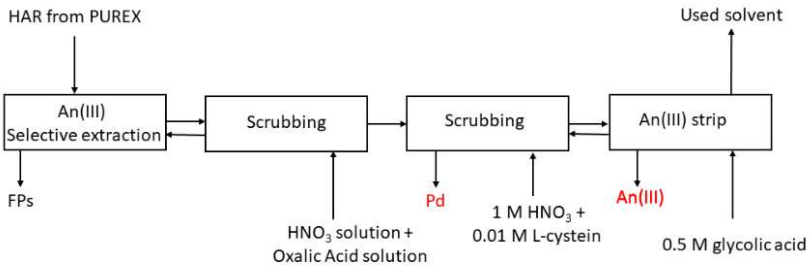

Figure 1.16. Simplified flowsheet for 1c-SANEX process

The above described processes give HOPE (hopeful options) for closing the nuclear fuel cycle. Nevertheless, further enhancements must be done to achieve the industrial scale use.

1.2.5 Co-separation of all TRU elements

Until now we have focused on the nature of heterogenous type recycling processes. In Europe homogeneous recycling (see Figure 1.5 left side) has been studied, which led to the development of a highly diverse processes. This last kind of recycling relies on two steps, first U(VI) is recovered alone then the recovery of all TRU elements occurs. The GANEX (Group Actinide Extraction) was first introduced by CEA in order to reprocess the waste of future GenIV reactors.[9] The process is made up of two cycles, the first one (GANEX 1st Cycle) is necessary for the U(VI) separation while the second (GANEX 2nd Cycle) is dedicated to the Transuranic elements recovery.

The selective separation of U(VI) is achieved by a solvent extraction process using a *N*, *N*-dialkylamide as organic extractant. GANEX first cycle is articulated in three main steps: one extraction, one scrubbing and one stripping. In the first stage the partition of hexavalent U above Pu and other fission products is possible using *N*, *N*-di-(ethyl-2-hexyl)isobutyramide (DEHiBA, Figure 1.16) that shows the best compromise between uranium loading and selectivity. The organic phase is then washed with N_2H_4 and HNO_3 to eliminate the remainder of fission products. Finally, a stripping stage allows to bring separated uranium into a clean aqueous solution and to fully clean the solvent that can be reused in the cycle.

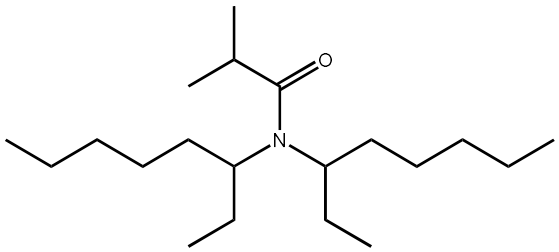

Figure 1.17. Molecular structure of DEHiBA

The 1st cycle raffinate containing An(III), Ln(III) and other fission products are sent to GANEX second cycle in order to achieve the partition of Am, Cm, Np, Pu. There are three proposals for the recovery of TRU elements: CEA GANEX, EURO-GANEX and CHALMEX.

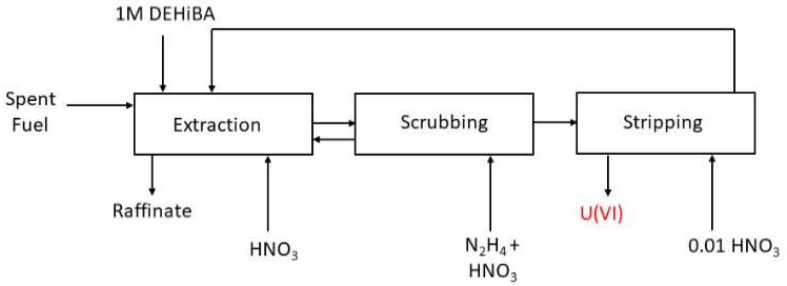

Figure 1.18. Flowsheet of GANEX 1st cycle

The CEA GANEX process, as the name suggests, was developed in Marcoule (FR) at the CEA and it is similar to the previously described DIAMEX-SANEX process. It is a five-step process: one extraction, one scrubbing, a selective stripping of Mo and Tc, a selective stripping of An and the stripping of Ln, Y, Zr, Fe. The extraction is made employing a mixture of DMDOHEMA and HDEHP in TPH solvent. The organic phase is then washed with nitric acid to eliminate the non-extractible fission products. In the third step Mo and Tc are selectively stripped by using a buffered citric acid solution, pH= 2-3. Then, the stripping of trivalent actinides is possible using a buffered solution of an aqueous complexing agent. In the laboratory test performed in 2008 a mixture of HEDTA and citric acid was employed as hydrophilic chelating ligand. The last stripping step allows the partition of Ln, Y, Zr and Fe using a nitric acid solution containing a selective complexing agent. The test performed at CEA in 2008 led to a 99,5 % yield for the TRU recovery. Nevertheless, the process is still undergoing testing at laboratory scale.

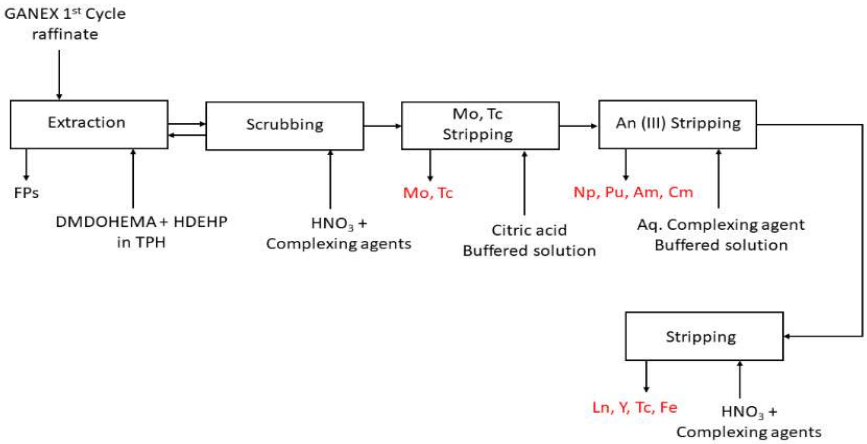

Figure 1.19. Flowsheet of CEA-GANEX process

The EURO-GANEX process is a variant of the CEA GANEX first developed in France and Germany and now under study in different European countries. The aim is always the co-separation of all TRU elements from the raffinate of the GANEX 1st cycle. The organic phase employed for the metal extraction is a mixture of DMDOHEMA and TODGA dissolved in kerosene. After the extraction stage the organic phase is washed with nitric acid (scrubbing). The organic phase is now merged with fresh solvent and then the first stripping stage occurs. Here, a solution composed of 0.055 M of SO_3-Ph-BTP and 1 M of AHA and 0.5 M nitric acid is used to strip trivalent actinides. Finally, trivalent lanthanides are stripped with a 0.5 M nitric acid solution.

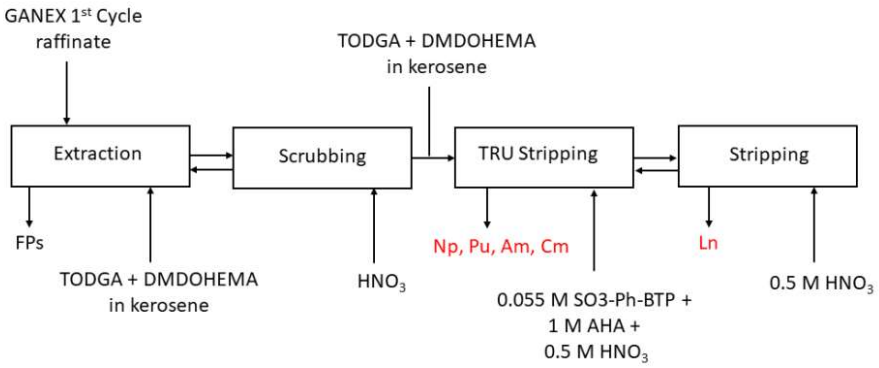

Figure 1.20. Flowsheet of EURO-GANEX process

1.3 Selective actinides extracting agents

1.3.1 An/Ln selectivity

As briefly described in the above paragraphs, Europe is a great authority in the development of innovative techniques and recycling strategies to promote radioactive waste management. Nevertheless, technologies able to selective partition minor actinides from lanthanides - or even better directly from the raffinate of the PUREX - are still under study. As stated in the first section, it is mandatory to close the nuclear cycle P&T of MA. One of the possibilities for the transmutation of An, is through a bombardment of highspeed neutrons. This procedure could transmute active isotopes of actinides with a long half-time to shorter life nuclides. Unfortunately, the majority of Ln have a high neutron absorption cross section and they can affect the transmutation process. But why is their separation so hard to achieve?[28,29] Lanthanides and Actinides are the elements of the periodic table f-block, meaning that with the increase of the atomic number of the series the occupied orbitals are respectively the 4f and the 5f. Since f orbitals are not shield ones, the increasing charge of the nucleus in the series is not adequately shielded and the outer electrons are pulled closer.[30] This determines a contraction in the atomic and ionic radii of the nuclei actually known as lanthanide or actinide contraction. The gradual decreasing in the atomic radius along the series determines a homogeneity in the properties of the corresponding elements that converts into a difficult separation intra and inter group. The light An have high stable oxidation status and they can be more easily separated whilst MA and Ln exist predominantly in trivalent oxidation state. Moreover, according to the Pearson's Hard Soft Acid Base principle, the two groups of metals are defined as hard - meaning that they both show high affinity with hard- donor ligand. Their interaction should be more efficient with oxygen or phosphorous containing compounds.[31] A considerable progress was made with the breakthrough of the major affinity of trivalent actinides for soft donor bases. It seems that the 5f orbitals of An contribute to form an interaction with some degree of covalence with nitrogen or sulfur donor ligands.[32] This last character could be the key for the development of innovative ligands able to discriminate trivalent actinides from trivalent lanthanides.

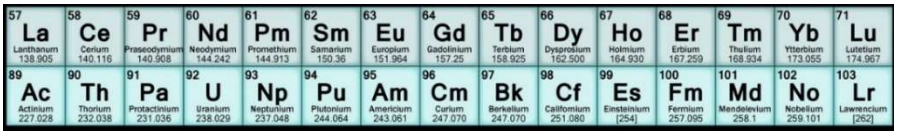

Figure 1.21. f-block of the elements periodic table

1.3.2 Ligands requirements

Many efforts have been done in the study of new ligands, but more research in this field should be done to find a suitable ligand showing the best compromise between properties, costs, and industrial scale practicability. The required characteristics for the development of an appropriate ligand are many among all the fulfillment of the cited CHON principle and obviously a pronounced An/Ln selectivity. Ligands must also show a good solubility in the solvent used, hydrolytic and radiolytic stability, fast complexation kinetics and ability to operate at low pH conditions.[33] The synthesis should be practical, aimed at large scale production, and not too expensive. The chemical stability is crucial for a possible recovery of the ligand and for the same reason also the possibility of a good stripping of the metal is considered a further needed characteristic. The parameters used to evaluate the efficiency and the selectivity of the chelating agent are respectively the Distribution Ratio D and the Separation Factor SF.[34] The D value for the extraction of a determined metal ion from an aqueous solution to an organic phase is defined as the ratio between the concentrations of the metal in the organic and in the aqueous phase, at the equilibrium. When a lipophilic ligand is used, a D value higher than 1 means that the ligand is efficient in the extraction of the metal in the organic phase. The higher the D value is, the better is the extraction efficiency. On the counterpart, a D value lower than 1 indicates that the metal remains preferably in the aqueous layer.[14] The separation factor related to two metal ions M_1/M_2, SF (M_1/M_2), is defined as the ratio between the D value of M_1 over the D value of M_2. To have a good process selectivity which allows the separation of the two species, the SF value should be greater than 10. The higher the D and SF values are, more efficient and more selective the ligand is.

$$D_{M1} = \frac{[M1]_{org}}{[M1]_{aq}} \qquad SF_{\frac{M1}{M2}} = \frac{D_{M1}}{D_{M2}}$$

1.3.3 Lipophilic selective chelating units

The study of innovative ligands to be employed in the European SANEX process has involved the investigation of many different organic binding motifs. In light of the fact that the crucial stage for the partition of trivalent actinide ions is based on the extraction of An(III) into an organic phase, the employment of a lipophilic actinide selective ligand is necessary. Structural progression of N based ligands started from TPTZ and includes TERPY and BODO which are now outdated. Indeed, remarkably important improvements in the field of SANEX ligands were done by the introduction of the Bis-triazinyl-pyridines (BTPs, Figure 1.13). This was the first family to show interesting extraction properties at high acidic concentration.[19] This group of compounds has been known for a long time but only Kolarik et al (1999)[25] introduced them as promising selective extractants for trivalent An. The core is made of a central pyridine ring flanked by two triazine rings and such an arrangement makes BTPs tridentate N-ligands for metal binding. The properties of this family of compounds can be modulated changing the substituent in position 5 and 6 of the two triazine rings. Indeed, many BTP based molecules have been synthesized bearing different alkyl chains on the triazine rings and all of them showed high D values and SF. [35] The main drawback of BTPs is their hydrolytic and radiolytic instability. Studying the stability of the molecules under operation conditions, it was found that the degradation begins with the chemical attack on the α protons of the triazine substituents. To solve this disadvantage making the ligand more robust to harsh conditions used, $CyMe_4$-BTP was synthesized. The idea that the absence of benzylic-H atoms would have reduced the hydro and radiolytic instability was appropriate and the selectivity of $CyMe_4$-BTP remained comparable to that of parent BTP. D_{Am} factor was approximately 500 and $SF_{Am/Eu}$ 5000 but the kinetics of extraction considerably decreased. This last synthesized molecule was the most promising among all the ones proposed but the high D values made the stripping of the metal ions really challenging and finally preventing the possible recycle of the organic phase in the industrial process. A detailed description of extraction and complexation experiments with BTP ligands is presented in a review by Panak and Geist.[36]

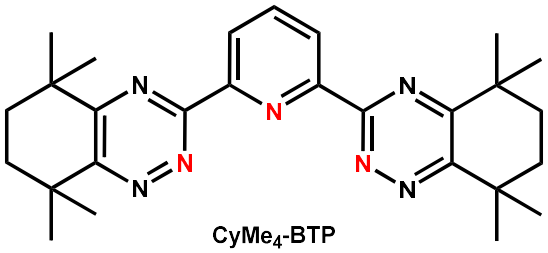

Figure 1.22. Chemical structure of CyMe4-Bis-Triazinyl Pyridine

In order to improve the kinetics, Foreman et al.[37] started to examine another class of ligand the bis-triazinyl bipyridines (BTBPs in Figure 1.23). These compounds show an extension in the aromatic core due to the presence of a bipyridine binding motif instead of a simple pyridine nucleus. The central bipyridine moiety makes them a class of tetradentate ligands. The presence of a further complexation position was thought to improve the kinetics of the An(III) extraction but the problem of degradation remained unsolved. The subsequent synthesis of CyMe4-BTBP, combines the chemical stability of the new class of ligands and the marked selectivity for An of CyMe4-BTP. Nevertheless the kinetics of extractions was still low needing the use of a phase transfer agent[38] like DMDOHEMA. CyMe4-BTBP was employed in 2008 in a SANEX hot demonstration test at the Institute for Transuranium Elements in Karlsruhe. The extracting agent was dissolved in octanol with 5mmol/L of DMDOHEMA and approximately 99,9% of An was recovered with 0,1% of Ln contamination. To better improve the kinetics, DMDOHEMA was replaced with TODGA. Since these promising results, CyMe4-BTBP is considered the reference molecule for further improvements and there is the possibility to employ it in 1-cycle SANEX and GANEX processes.

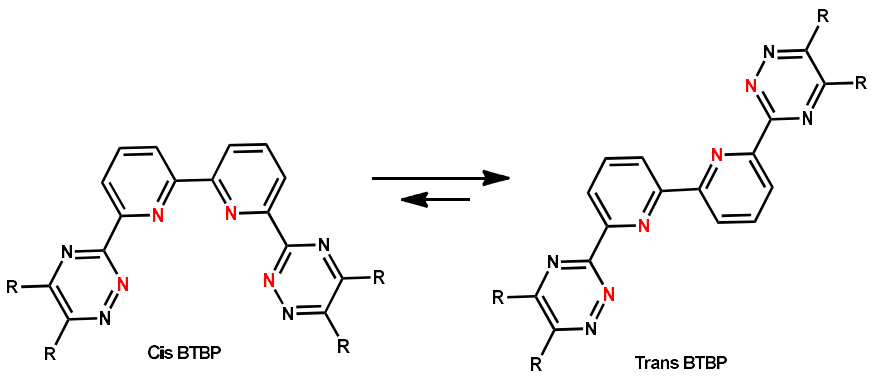

Figure 1.23. Cis-trans chemical equilibrium of BTBP

A study on these ligands hypothesized that the reason for the low extraction kinetics of CyMe4-BTBP could be due to the more stable trans conformation of the Py-Py core, Figure 1.23.[16] Different structural studies have demonstrated that it is always the nitrogen in position 2 (and not that in position 6) that complexes the metal ion and this could be explained with the α effect.[32] This effect is known among many ligands showing two or more nitrogen in sequence. The molecular orbital of the non-interacting nitrogen cooperates with the chelating one enhancing its basicity. For this reason, locking the Py-Py chelating group in cis conformation could have represented a solution to improve the extraction kinetics. CyMe4-BTPhen was therefore synthesized where the 2,2'-bipyridine moiety was replaced with a phenanthroline nucleus.[38] The cis-locked conformation of the Py-Py chelating unit in BTPhen brings to the formation of a metal-ligand bond thermodynamically favoured. The kinetics are effectively improved without the use of a transfer agent, and the D values are high. Nevertheless, the stripping of the metal with glycolic acid was challenging thus preventing the ligand from becoming a possible candidate for the industrial process.

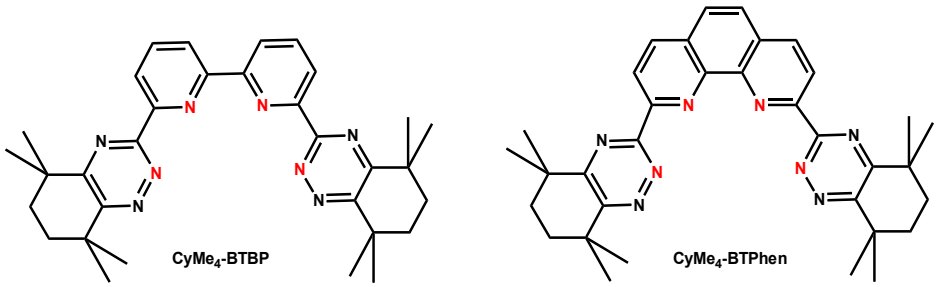

Figure 1.24. Chemical structure of CyMe4-BTBP (right) and CyMe4-BTPhen (left)

The general synthetic pathways for the preparation of bis-(1,2,4-triazine) ligands is reviewed by Hudson et al. [32]

1.3.4 Hydrophilic selective chelating units

The chelating ligands described so far are all related to the lipophilic compound family - BTP, BTBP, BTPhen. On account of the fact that the SANEX process, the current reference for the selective actinides partition, is based on the extraction of An(III) into an organic phase employing an organic lipophilic ligand. Different strategies have been proposed to develop innovative and easier ways to achieve the An partitioning based on the *reverse* TALSPEAK process. This alternative concept relies on a co-extraction step where trivalent An and Ln are carried into an organic phase followed

by a selective back extraction of An(III) into an aqueous phase. While the first step requires a non-selective organic agent, the back-extraction step needs a hydrophilic selective ligand which should meet all the requirements previously listed. Moreover, considering the homogeneous recycling, hydrophilic extractants are necessary in the EUROGANEX. Recently a hydrophilic water soluble version of BTP, BTBP and BTPhen, the corresponding bis- and tetrasulfonated ligands, were been synthesized.

The first to be synthesized and tested was the 2,6-bis(5,6-di(sulfophenyl)-1,2,4-triazin-3-yl)pyridine (SO_3-Ph-BTP) by Geist et al. in 2012.[39] The ligand showed interesting properties opening the way to further studies in this field. Lewis et al.[7] proposed the synthesis of the corresponding disulfonated BTP. To understand if the position of the phenyl sulfonated ring could affect the extraction properties or not, the two regioisomers were also synthesized.

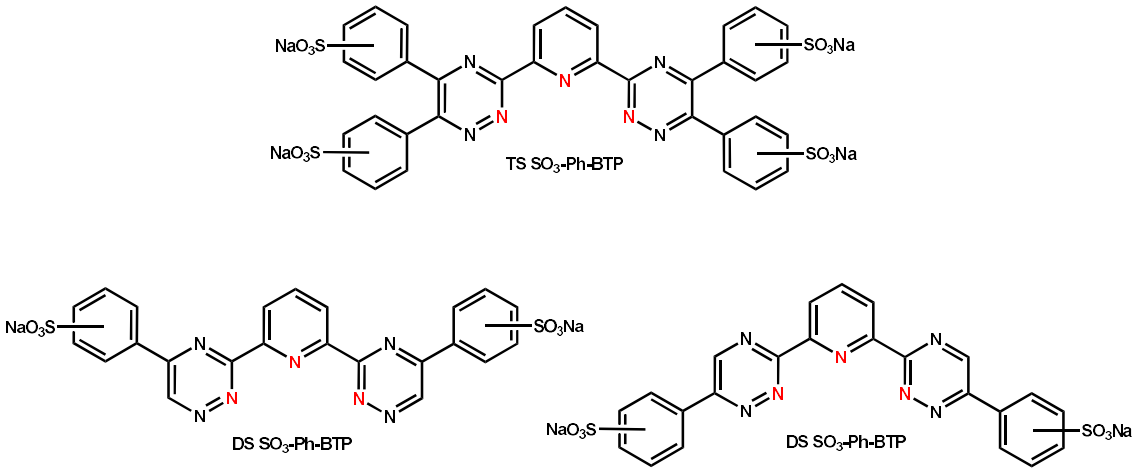

Figure 1.25. Chemical structures of tetrasulfonated phenyl BTP (above) and chemical structures of the two regioisomers of di sulfonated phenyl BTP (below)

The same group proposed the synthesis of di- and tetrasulfonated BTBP. This time, in order to verify a possible effect of the counterion, both the structure of the Na^+ salt or sulfonic acid were studied. Finally, the same research group reported the synthetic pathways of the tetrasulfonated BTPhen.[40]

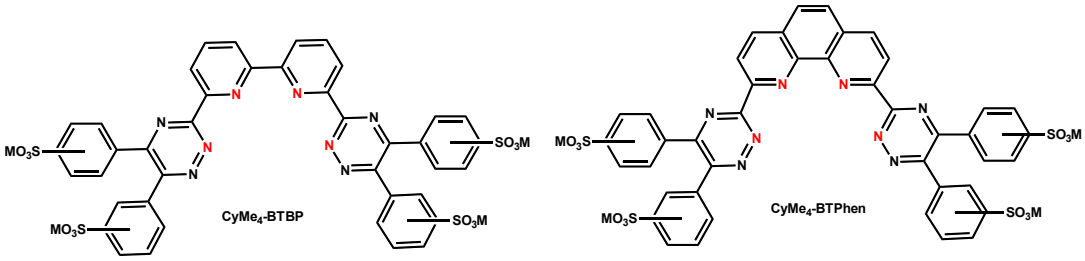

Figure 1.26. Chemical structures of tetrasulfonated phenyl BTBP (left) and of tetrasulfonated phenyl BTPhen (right)

Solubility and extraction tests were performed by different research groups. As expected, the main result is that the solubility of tetra-sulfonated ligands in aqueous solution is higher than that of the di-sulfonated ones. The extraction properties of tetra-sulfonated ligands are promising independently from the core, the position of the sulfonated phenyl ring and nature protonation-deprotonation degree. The only structural parameter that seems to affect the extraction efficiency is the number of sulfonated groups present maybe due to a decrease in the solubility observed when a lower number of sulfonated groups are present. To better understand the importance of the sulfonated groups a BTBP ligand was synthesized with four carboxylate groups, TA-BTBP. As expected, it showed a lower selectivity and lower stripping behavior compared to sulfonated BTBP, under the same extraction conditions.[35]

1.4 The 2,6-bis(1,2,3-triazolyl) pyridine motif

1.4.1 Overview

Most of the available heteroaromatic architectures for coordination chemistry requires multi-step synthesis that are both cost and time consuming. An easy, modular, high yielding method for the obtainment of a proper N donor chelating motif would be desirable.

Besides the families of BTP, other classes of pyridine centered heteroaromatic ligands have been explored. Mostly, the central pyridine ring is maintained whilst the heteroaromatic six-membered lateral rings are replaced by 5-membered ones bearing a variable number of N atoms. A collection of multidentate chelating units have been reported in literature to date, counting 2,6-di(pyrazolyl)pyridines (**bpp**), bis(1,2,4-triazolyl)pyridines (**btp'**) and 2,6-bis(tetrazol-4-yl)pyridines (**pytz**) (Figure 1.26).[41]

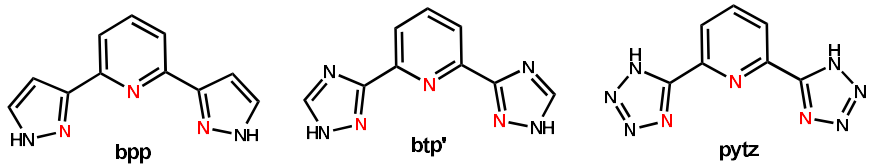

Figure 1.27. Chemical structures of 2,6-di(pyrazolyl)pyridines (left), bis(1,2,4-triazolyl)pyridines (center) and 2,6-bis(tetrazol-4-yl)pyridines (right)

One of the most recently included class of ligands is the family of 2,6-bis(1,2,3-triazolyl) pyridine, btp Figure 1.28, where the three N atoms of the triazole rings are all adjacent to each other. This heteroaromatic moiety has been intensively studied as N3 chelating agent both in supramolecular and coordination chemistry thanks to its easy synthesis and chemical modification. The bis triazolyl pyridine motif can be quickly obtained exploiting the copper catalyzed azide-alkyne cycloaddition (CuAAC) that is able to transform an acetylene group into a five membered triazole ring that encloses three adjacent nitrogen atoms.

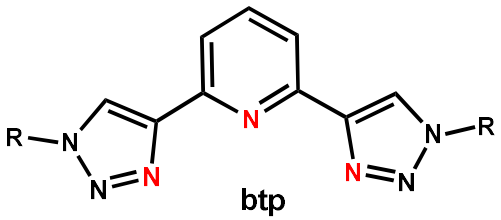

Figure 1.28. Chemical structure of 2,6-bis(1,2,3-triazolyl)pyridine

The chelating unit we are now focused on merges the renowned characteristic of pyridine centered tridentate ligands and the coordinating capability combined to the easy chemical synthetization of the triazole unit. A review of Byrne et al.- published in 2014- provides a wide overview on the employ of this recent binding motif in supramolecular and coordination chemistry.[41] The first example of a 2,6-bis(1,2,3-triazol-4-yl)pyridine was introduced by Fokin et al. in 2004.[42] On behalf of the interaction of btp based ligand with metal ions, one of the first example is referred to Flood and coworkers published in 2007. In particular they studied the formation and the stability of coordination compounds between the synthetized btp based ligands and Fe(II), Ru(II) and Eu(III).[43] In 2010 Crowley and co. published a paper listing a variety of ligands showing the cited scaffold with different alkyl chains. The compounds were obtained in high yields exploiting the CuAAC reaction and generating the hazard organic azides in situ using standard or modified Foking conditions.[44] It is possible to assert that the recent development of the 1,3-dipolar

Huisgen cycloaddition reaction could open the way to a new method for the synthesis of a variety of coordination scaffolds to be employed in a wide range of research fields and among all in the metallo-supramolecular chemistry.

In addition to cations, 1,2,3-triazoles can interact with anions using the acidic triazole CH as a direct hydrogen bond donor able to bind negatively charged guests in organic solvents providing to the btp core a high versatile coordination capability. [45,46,47] The free rotation of the C-C bond connecting the pyridyl ring and the triazoles allows an easy switch of conformation of the core.[48] X-ray crystal structure in literature demonstrate that the conformation of the free ligand is anti-anti in respect to the pyridyl N. The *anti-anti* conformation dominates in solution as well as in presence of anions while in presence of cations the *syn-syn* conformation is observed (Figure 1.29).

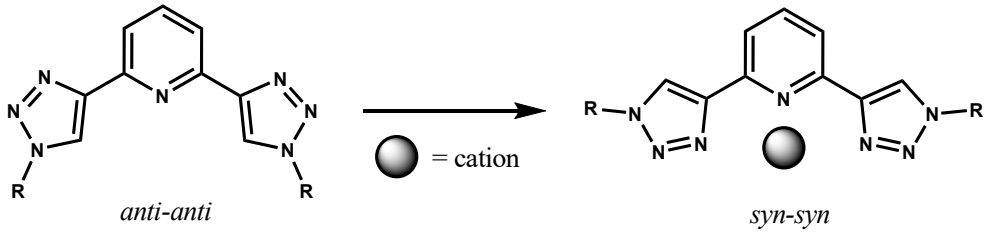

Figure 1.29. Anti-anti and syn-syn conformation of the btp core

1.4.2 Use of the btp moiety for An/Ln separation

Despite the very promising characteristics of the 2,6-bis(1,2,3-triazol-4-yl)pyridine chelating units even in coordination of Ln ions, there are nearly no examples of the use of these compounds or their derivatives in An/Ln separation until 2016 when our research group first reported the successful use of btp in the partitioning of simulated HAR.[33]

In 2007 Li et al. were able to form stable coordination compounds by using btp ligands and Eu(III). To fulfil the coordination sphere of Eu(III) three ligands are needed for a total of 9 coordination points. The complexation geometries for Eu(III) complexes were consistent with the ones obtained using terpy. These results demonstrated that the family of compounds, easily obtained by click reaction, could open the way to a vial class of terdentate ligands.[43] A further improvements on the study of the coordination capability of this class of ligands were made by Kiefer et al in 2010. They studied the properties of 2,6-Bis(1-(p-tolyl)-1H-1,2,3-triazol-4yl)pyridine (BTTP) with Eu(III) and Sm(III). As well as for the complexes obtained by Li, also in this study the Ln(III) ion is coordinated by three BTTP ligands confirming nine as the total coordination number. Some liquid/liquid extraction experiments revealed a certain selectivity of

BTTP in binding Cm(III) over Eu(III) in ACN. Although time-resolved laser fluorescence spectroscopy (TRLFS) indicate some selectivity of binding Cm over Eu in acetonitrile, the authors concluded that btp derivative is not able to extract metal ions from an acidic aqueous solution to an organic layer, probably because to its reduced complexation ability at low pH.[49]

A noteworthy step forward in the An/Ln coordination chemistry was made by Macerata et al. in 2016 when they demonstrated the possibility to employ water soluble btp ligands for the selective actinide extraction from simulate radioactive waste.[33] They synthetized a series of ligands based on the clicked triazole unit and the one which showed the best properties was the so called PTD (Figure 1.30). The selectivity of this ligand was pointed out by performing liquid-liquid extraction tests. First of all, an organic solution containing TODGA was contacted with aqueous feeds from i-SANEX (containing trivalent An) and GANEX (containing tri and tetravalent An). The TODGA ligand was able to coextract 99.9% of An and Ln from the feeds. At this point the organic phase was contacted with an aqueous layer containing the water soluble PTD. The Am concentration in the organic layer was reduced from 94% to 14% while the Eu concentration only from 99% to 96%. Interestingly, the proposed ligand is compliant with the CHON principle, is easy to synthetize and shows a great An/Ln selectivity. Further the radiolytically and hydrolytically stability of the ligand was demonstrated in the paper. The PTD can be considered the start point for further advancement in separation processes and towards a closed nuclear fuel cycle.

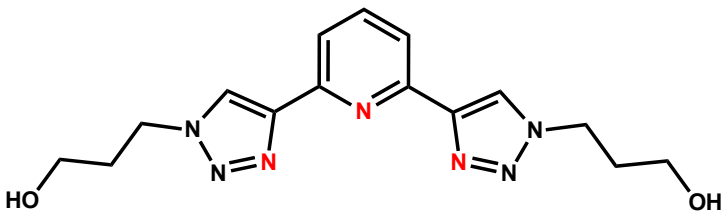

Figure 1.30. Chemical structure of PTD in syn-syn conformation

1.5 References

(1) IEA. World Energy Outlook. Paris 2006.

(2) Birkett, J. E.; Carrott, M. J.; Fox, O. D.; Jones, C. J.; Maher, C. J.; Roube, C. V; Taylor, R. J.; Woodhead, D. A. Recent Developments in the Purex Process for Nuclear Fuel Reprocessing : Complexant Based Stripping for Uranium / Plutonium Separation. *Chem. Mater. Nucl. power Prod.* **2005**, *59* (12), 898–904.

(3) Agency, I. A. E. Agency, Energy, Electricity and Nuclear Power Estimares for the

Period up to 2050. Reference Data Series No. 1: Vienna 2016.

(4) Karakosta, C.; Pappas, C.; Marinakis, V.; Psarras, J. Renewable Energy and Nuclear Power towards Sustainable Development : Characteristics and Prospects. *Renew. Sustain. energy Rev.* **2013**, *22*, 187–197. https://doi.org/10.1016/j.rser.2013.01.035.

(5) E. R: Irish; W. H. Reas. THE PUREX PROCESS - a Solvent Extraction Reprocessing Method for Irradiated Uranium. **1957**.

(6) Brook, B. W.; Alonso, A.; Meneley, D. A.; Misak, J.; Blees, T.; van Erp, J. B. Why Nuclear Energy Is Sustainable and Has to Be Part of the Energy Mix. *Sustain. Mater. Technol.* **2014**, *1*, 8–16. https://doi.org/10.1016/j.susmat.2014.11.001.

(7) Lewis, F. W.; Harwood, L. M.; Hudson, M. J.; Geist, A.; Kozhevnikov, V. N.; John, J. Hydrophilic Sulfonated Bis-1,2,4-Triazine Ligands Are Highly Effective Reagents for Separating Actinides(III) from Lanthanides(III) via Selective Formation of Aqueous Actinide Complexes. *Chem. Sci.* **2015**, *6*, 4812–4821. https://doi.org/10.1039/C5SC01328C.

(8) Lewis, F. W.; Harwood, L. M.; Hudson, M. J.; Afsar, A.; Laventine, D. M.; Šťastná, K.; John, J.; Distler, P.; Lewis, F. W.; Harwood, L. M.; Hudson, M. J.; Afsar, A.; Laventine, D. M.; Šťastná, K.; John, J.; Distler, P. Separation of the Minor Actinides Americium (III) and Curium (III) by Hydrophobic and Hydrophilic BTPhen Ligands : Exploiting Differences in Their Rates of Extraction and Effective Separations at Equilibrium Separation of the Minor Actinides Americium. *Solvent Extr. Ion Exch.* **2018**, *00* (00), 1–21. https://doi.org/10.1080/07366299.2018.1429358.

(9) Modolo, G.; Geist, A.; Miguirditchian, M. Minor Actinide Separations in the Reprocessing of Spent Nuclear Fuels: Recent Advances in Europe. In *Reprocessing and Recycling of Spent Nuclear Fuel*; Elsevier, 2015; pp 245–287. https://doi.org/10.1016/B978-1-78242-212-9.00010-1.

(10) Sharrad, C. A.; Whittaker, D. M. The Use of Organic Extractants in Solvent Extraction Processes in the Partitioning of Spent Nuclear Fuels. In *Reprocessing and Recycling of Spent Nuclear Fuel*; Elsevier, 2015; pp 153–189. https://doi.org/10.1016/B978-1-78242-212-9.00007-1.

(11) Madic, C, Blanc, P, Condamines, N, Baron, P, Berthon, L, Nicol, C, Pozo, C, Lecomte, M, Philippe, M, Masson, M, and Hequet, C. Actinide Partitioning from High Level Liquid Waste Using the Diamex Process; 1994.

(12) Pierre Joly, E. B. *Actinide Separation Processes 2015*; 2015.

(13) Horvath, A.; Rachlew, E. Nuclear Power in the 21st Century: Challenges and Possibilities. *Ambio* **2016**, *45* (1), 38–49. https://doi.org/10.1007/s13280-015-0732-y.

(14) Sypuła, M.; Michał Sypuła. *Innovative SANEX Process for Trivalent Actinides Separation from PUREX Raffinate*; 2014.

(15) Bourg, S.; Geist, A.; Narbutt, J. SACSESS – the EURATOM FP7 Project on Actinide Separation from Spent Nuclear Fuels. *Nukleonika* **2015**, *60* (4), 809–814. https://doi.org/10.1515/nuka-2015-0152.

(16) Lewis, F. W.; Harwood, L. M.; Hudson, M. J.; Drew, M. G. B.; Desreux, J. F.; Vidick, G.; Bouslimani, N.; Modolo, G.; Wilden, A.; Sypula, M.; Vu, T.-H.; Simonin, J.-P. Highly Efficient Separation of Actinides from Lanthanides by a Phenanthroline-Derived Bis-Triazine Ligand. *J. Am. Chem. Soc.* **2011**, *133* (33), 13093–13102.

https://doi.org/10.1021/ja203378m.

(17) Geist, A.; Adnet, J. M.; Bourg, S.; Ekberg, C.; Galán, H.; Guilbaud, P.; Miguirditchian, M.; Modolo, G.; Rhodes, C.; Taylor, R. An Overview of Solvent Extraction Processes Developed in Europe for Advanced Nuclear Fuel Recycling, Part 1 — Heterogeneous Recycling. *Sep. Sci. Technol.* **2020**, 1–16. https://doi.org/10.1080/01496395.2020.1795680.

(18) O. Courson, R. M.; G. Pagliosa, K. R.; B. Sätmark, J.-P. G.; Courson, O.; Malmbeck, R.; Pagliosa, G.; Römer, K.; Satmark, B.; Glatz, J.-P.; Baron, P.; Madic, C. Separation of Minor Actinides from Genuine HLLW Using the DIAMEX Process. *5th Int. Inf. Exch. Meet. Mol.* **1998**, 1–10.

(19) Modolo, G.; Wilden, A.; Geist, A.; Magnusson, D.; Malmbeck, R. A Review of the Demonstration of Innovative Solvent Extraction Processes for the Recovery of Trivalent Minor Actinides from PUREX Raffinate. *Radiochimica Acta*. August 2012, pp 715–725. https://doi.org/10.1524/ract.2012.1962.

(20) Goldberg., S. M.; Rosner, R.; Malone, J. P. *The Back-end of the Nuclear Fuel-cycle: An Innovative Storage Concept*; 2012.

(21) Iqbal, M.; Huskens, J.; Verboom, W.; Sypula, M.; Modolo, G. Synthesis and Am/Eu Extraction of Novel TODGA Derivatives. *Supramol. Chem.* **2010**, *22* (11–12), 827–837. https://doi.org/10.1080/10610278.2010.506553.

(22) Modolo, G., Vijgen, H., Schreinemachers,C., Baron, P., Dinh, B. Proceedings of GLOBAL, New Orleans, Louisiana, USA, 16-20 November. **2003**, 1926–1930.

(23) Nash, K. L. The Chemistry of TALSPEAK: A Review of the Science. *Solvent Extr. Ion Exch.* **2015**, *33* (1), 1–55. https://doi.org/10.1080/07366299.2014.985912.

(24) Moyer, B. A.; Lumetta, G. J.; Mincher, B. J. Minor Actinide Separation in the Reprocessing of Spent Nuclear Fuels: Recent Advances in the United States. In *Reprocessing and Recycling of Spent Nuclear Fuel*; Elsevier, 2015; pp 289–312. https://doi.org/10.1016/B978-1-78242-212-9.00011-3.

(25) Kolarik, Z.; Müllich, U.; Gassner, F. Selective Extraction of Am(III) over Eu(III) by 2,6-Ditriazolyl- and 2,6-Ditriazinylpyridines. *Solvent Extr. Ion Exch.* **1999**, *17* (1), 23–32. https://doi.org/10.1080/07360299908934598.

(26) Hudson, M. J.; Boucher, C. E.; Braekers, D.; Desreux, J. F.; Drew, M. G. B.; Foreman, M. R. S. J.; Harwood, L. M.; Hill, C.; Madic, C.; Marken, F.; Youngs, T. G. A. New Bis(Triazinyl) Pyridines for Selective Extraction of Americium(III). *New J. Chem.* **2006**, *30* (8), 1171–1183. https://doi.org/10.1039/b514108g.

(27) Modolo, G.; Wilden, A.; Daniels, H.; Geist, A.; Magnusson, D.; Malmbeck, R. Development and Demonstration of a New SANEX Partitioning Process for Selective Actinide(III)/Lanthanide(III Separation Using a Mixture of CyMe 4BTBP and TODGA. *Radiochim. Acta* **2013**, *101* (3), 155–162. https://doi.org/10.1524/ract.2013.2016.

(28) Karl A. Gschneidner, J.; L. E. G. R. C.; Lander, G. H. Beitz, J. V. Chapter 120 Similarities and Differences in Trivalent Lanthanide- and Actinide-Ion Solution Absorption Spectra and Luminescence Studies. In *Handbook on the Physics and Chemistry of Rare Earths*; 1994; Vol. 18, pp 159–195.

(29) Nash, K. L. AQUEOUS COMPLEXES IN SEPARATIONS OF F-ELEMENTS:

OPTIONS AND STRATEGIES FOR FUTURE DEVELOPMENT. Separation Science and Technology 34 (6). **1999**, 911–929.

(30) Nash, K. L. A Review of the Basic Chemistry and Recent Developments in Trivalent F-Elements Separations. *Solvent Extr. Ion Exch.* **1993**, *11* (4), 729–768. https://doi.org/10.1080/07366299308918184.

(31) Pearson, R. G. Hard and Soft Acids and Bases. *J. Am. Chem. Soc.* **1963**, *85* (22), 3533–3539.

(32) Hudson, M. J.; Harwood, L. M.; Laventine, D. M.; Lewis, F. W. Use of Soft Heterocyclic N-Donor Ligands to Separate Actinides and Lanthanides. *Inorg. Chem.* **2013**, *52* (7), 3414–3428. https://doi.org/10.1021/ic3008848.

(33) Macerata, E.; Mossini, E.; Scaravaggi, S.; Mariani, M.; Mele, A.; Panzeri, W.; Boubals, N.; Berthon, L.; Charbonnel, M.-C.; Sansone, F.; Arduini, A.; Casnati, A. Hydrophilic Clicked 2,6-Bis-Triazolyl-Pyridines Endowed with High Actinide Selectivity and Radiochemical Stability: Toward a Closed Nuclear Fuel Cycle. *J. Am. Chem. Soc.* **2016**, *138* (23), 7232–7235. https://doi.org/10.1021/jacs.6b03106.

(34) Dam, H. H.; Reinhoudt, D. N.; Verboom, W. Multicoordinate Ligands for Actinide/Lanthanide Separations. *Chem. Soc. Rev.* **2007**, *36* (2), 367–377. https://doi.org/10.1039/b603847f.

(35) Leoncini, A.; Huskens, J.; Verboom, W. Ligands for F-Element Extraction Used in the Nuclear Fuel Cycle. *Chemical Society Reviews*. Royal Society of Chemistry 2017, pp 7229–7273. https://doi.org/10.1039/c7cs00574a.

(36) Panak, P. J.; Geist, A. Complexation and Extraction of Trivalent Actinides and Lanthanides by Triazinylpyridine N -Donor Ligands. *Chem. Rev.* **2013**, *113* (2), 1199–1236. https://doi.org/10.1021/cr3003399.

(37) Foreman, M. R. S.; Hudson, M. J.; Drew, M. G. B.; Hill, C.; Madic, C. Complexes Formed between the Quadridentate, Heterocyclic Molecules 6,6′-Bis-(5,6-Dialkyl-1,2,4-Triazin-3-Yl)-2,2′-Bipyridine (BTBP) and Lanthanides(III): Implications for the Partitioning of Actinides(III) and Lanthanides(III). *Dalt. Trans.* **2006**, No. 13, 1645–1653. https://doi.org/10.1039/B511321K.

(38) Veliscek-Carolan, J. Separation of Actinides from Spent Nuclear Fuel: A Review. *J. Hazard. Mater.* **2016**, *318*, 266–281. https://doi.org/10.1016/j.jhazmat.2016.07.027.

(39) Geist, A.; Müllich, U.; Magnusson, D.; Kaden, P.; Modolo, G.; Wilden, A.; Zevaco, T. Actinide (III)/ Lanthanide (III) Separation Via Selective Aqueous Complexation of Actinides (III) Using a Hydrophilic 2 , 6- Acid. *Solvent Extr. Ion Exch.* **2012**, No. October 2014, 37–41. https://doi.org/10.1080/07366299.2012.671111.

(40) Kaufholz, P.; Modolo, G.; Wilden, A.; Sadowski, F.; Bosbach, D.; Wagner, C.; Geist, A.; Panak, P. J.; Lewis, F. W.; Harwood, L. M. Solvent Extraction and Fluorescence Spectroscopic Investigation of the Selective Am(III) Complexation with TS-BTPhen. *Solvent Extr. Ion Exch.* **2016**, *34* (2), 126–140. https://doi.org/10.1080/07366299.2016.1151308.

(41) Byrne, J. P.; Kitchen, J. A.; Gunnlaugsson, T.; Joseph P. Byrne, A.; Jonathan A. Kitchenb and Thorfinnur Gunnlaugsson. The Btp [2,6-Bis(1,2,3-Triazol-4-Yl)Pyridine] Binding Motif: A New Versatile Terdentate Ligand for Supramolecular and Coordination Chemistry. *Chem. Soc. Rev.* **2014**, *43* (15), 5302–5325.

https://doi.org/10.1039/c4cs00120f.

(42) Feldman, A. K.; Colasson, B.; Fokin, V. V. One-Pot Synthesis of 1,4-Disubstituted 1,2,3-Triazoles from In Situ Generated Azides. *Org. Lett.* **2004**, *6* (22), 3897–3899. https://doi.org/10.1021/ol048859z.

(43) Li, Y.; Huffman, J. C.; Flood, A. H. Can Terdentate 2,6-Bis(1,2,3-Triazol-4-Yl)Pyridines Form Stable Coordination Compounds? *Chem. Commun.* **2007**, No. 26, 2692–2694. https://doi.org/10.1039/b703301j.

(44) Crowley, J. D.; Bandeen, P. H.; Hanton, L. R. A One Pot Multi-Component CuAAC "Click" Approach to Bidentate and Tridentate Pyridyl-1,2,3-Triazole Ligands: Synthesis, X-Ray Structures and Copper(II) and Silver(I) Complexes. *Polyhedron* **2010**, *29* (1), 70–83. https://doi.org/10.1016/j.poly.2009.06.010.

(45) Gilday, L. C.; White, N. G.; Beer, P. D. Triazole- and Triazolium-Containing Porphyrin-Cages for Optical Anion Sensing. *Dalt. Trans.* **2012**, *41* (23), 7092. https://doi.org/10.1039/c2dt30124e.

(46) White, N. G.; Beer, P. D. A Catenane Host System Containing Integrated Triazole C–H Hydrogen Bond Donors for Anion Recognition. *Chem. Commun.* **2012**, *48* (68), 8499. https://doi.org/10.1039/c2cc34210c.

(47) White, N. G.; Beer, P. D. A Rotaxane Host System Containing Integrated Triazole C–H Hydrogen Bond Donors for Anion Recognition. *Org. Biomol. Chem.* **2013**, *11* (8), 1326. https://doi.org/10.1039/c2ob27229f.

(48) Meudtner, R. M.; Ostermeier, M.; Goddard, R.; Limberg, C.; Hecht, S. Multifunctional "Clickates" as Versatile Extended Heteroaromatic Building Blocks: Efficient Synthesis via Click Chemistry, Conformational Preferences, and Metal Coordination. *Chem. - A Eur. J.* **2007**, *13* (35), 9834–9840. https://doi.org/10.1002/chem.200701240.

(49) Kiefer, C.; Wagner, A. T.; Beele, B. B.; Geist, A.; Panak, P. J.; Roesky, P. W. A Complexation Study of 2,6-Bis(1-(p -Tolyl)-1 H -1,2,3-Triazol-4-Yl)Pyridine Using Single-Crystal X-Ray Diffraction and TRLFS. *Inorg. Chem.* **2015**, *54* (15), 7301–7308. https://doi.org/10.1021/acs.inorgchem.5b00803.

Chapter 2
Hydrophilic Ligands for Selective An Separation

2.1 Introduction

In the first chapter the SANEX process has been described as the European proposed strategy to selectively recover An(III) from the nuclear waste. A breakthrough in the separation of trivalent An has been made with the development of the *i*-SANEX process as well described in Chapter 1. The selective partition of An(III) is directly made after a An(III) + Ln(III) co-extraction employing a DIAMEX-SANEX-like solvent. The main feature of the *i*-SANEX is the achievement of the An separation with the use of a water soluble ligand. Hydrophilic ligands find employment also in the EURO-GANEX process. This last technology is part of the homogeneous recycling process that relies on two steps. Specifically, the GANEX 1st cycle has the task of exclusively removing U(VI), then the raffinate goes through the GANEX 2nd cycle, the EURO-GANEX, where TRU are recovered likewise.

Considering that both the above cited systems allow the selective recovery of actinides using water soluble ligands, the exploration of diverse hydrophilic chelating agents have been encouraged in recent years. Concerning the *i*-SANEX process, the reference molecule for the selective extraction of An has been for a long time the SO_3-Ph-BTP developed by Geist et al. in 2012.[1] The presence of sulfonated phenyl groups which misses the CHON principle is the main drawback of the SO_3-Ph-BTP since large volumes of secondary waste are produced.

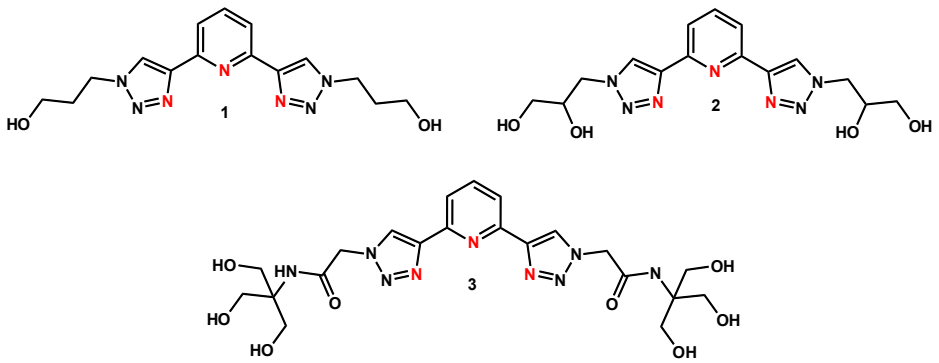

Figure 2.1. Water soluble ligands based on PyTri chelating unit

As a result this molecule has been recently replaced by the PTD which has been also selected

as possible new EURO-GANEX reference molecule.[2] The exploitation of the 2,6-bis(1,2,3-triazol-4-yl)pyridine chelating unit and in particular of PTD has been successfully introduced by Macerata et al. in 2016.[2] In their research work three water soluble ligands based on PyTri chelating unit and gathering all the industrial requirements were proposed, Figure 2.1. The ligands show an increasing number of OH groups with the aim of enhancing their solubility in aqueous solutions. In order to prove the selectivity towards An, liquid-liquid extractions tests were performed determining D_M values of Am(III) and Eu(III) and the $SF_{Eu/Am}$. D_M is defined as the ratio between the concentration of the metal (M) in organic phase over that in aqueous phase at the equilibrium, while $SF_{Eu/Am}$ is defined as the ratio between D_{Eu} and D_{Am}. The stripping phase was obtained contacting a 0.2 M TODGA solution in kerosene/ 1-octanol 95/5 with 3 M HNO_3 solution containing trivalent An (*i*-SANEX feed) and trivalent Ln. The TODGA solution was able to coextract 99.9% of both An and Ln present in the aqueous solutions. Then the TODGA-based organic solutions were contacted with the acidic solutions containing ligands **1**, **2**, **3**. The modest Ln/An selectivity of TODGA was confirm with a blank stripping experiment where the aqueous layer consists of 0.25 M HNO_3 with no ligand added. Indeed, only less than 1% of Eu and 6% of Am was released under this condition. Conversely, the introduction of ligands **1-3** in the aqueous solutions increases the back extraction of Am(III) in water. Only 14.5%, 21.2% and 37.7% of ^{241}Am remain in the organic phase with the employing of ligand **1**, **2**, **3** respectively.

Table 2.1. D_M and SF values for the stripping of Am^{3+} from a TODGA-Based organic phase into a PyTri-Based aqueous solution

Stripping phase	No ligand [HNO_3] = 0.25 M		0.1 M ligand 1 [HNO_3] = 0.25 M		0.15 M ligand 2 [HNO_3] = 0.25 M		0.15 M ligand 3 [HNO_3] = 0.25 M	
Element	**D_M**	**% in org**	**D_M**	**% in org**	**D_M**	**% in org**	**D_M**	**% in org**
^{241}Am	16.3	94.2	0.17	14.5	0.27	21.2	0.77	37.7
^{152}Eu	113	99.1	24.5	96.1	27.0	96.4	44	97.8
$SF_{Eu/Am}$	6.93		144.35		99.96		57.14	

The extraordinary selectivity of the proposed ligands for Am is confirmed by the analysis of the SF factors which increase from 7, value obtained with the blank test, to 144 for ligand **1**, 100 for ligand **2** and 57 for ligand **3**.

These data reveal that Eu remains bounded to TODGA in the organic phase while, Am is better coordinated to the PyTri ligand in aqueous phase thus promoting a strong

separation. Ligands **1** and **2** have shown comparable D_M and SF values for both Am and Eu while ligand **3**, despite of its higher water solubility, shows lower selectivity and efficiency.

In order to understand the reason of the high actinide selectivity, the stoichiometry and stability of the metal-ligand complexes were examined.[2,3] Stability constants for the formation of Am(III) and Eu(III) complexes with ligands **1** and **2** were determined by UV−VIS titrations. The spectra were fitted with the 1:1 and 1:2 complexes giving the apparent logβ'1:1 and logβ'1:2 values in Methanol/Water (75/25 v/ v), Table 2.2. These preliminary data and particularly the formation of 1:2 complexes with Am(III) support the hypothesis of a remarkable ligand affinity for An respect to Ln.

Table 2.2. Apparent stability constants (logβ'metal:ligand) for Am(III) and Eu(III) complexes with ligands 1 and 2 obtained by UV−vis titration in methanol/water (75/25 v/ v) at 25 °C and pH = 4

Metal Ion	Ligand	Logβ'1:1	Logβ'1:2	Counterion
Am(III)	**1**	3.2 ± 0.3	6.2 ± 0.3	Cl^-
Am(III)	**2**	3.1 ± 0.3	5.5 ± 0 .3	Cl^-
Eu(III)	**1**	2.4 ± 0.1		Cl^-
Eu(III)	**2**	3.0 ± 0.1		Cl^-

In 2017 the same research group published an exhaustive study on the coordination of PTD with Cm(III) and Eu(III) as representative of An(III) and Ln(III) respectively.[3] TRLFS experiments with Cm(III) in 10^{-3} M aqueous $HClO_4$ were performed. The stepwise formation of Cm(III)-PTD complexes is described by the following equation:

$[Cm(PTD)_{n-1}]^{3+} + PTD = [Cm(PTD)_n]^{3+}$ with $n = 1, 2, 3$

At low ligand concentration, the Cm(III) aqua ion is the main species. With increasing ligand concentration the amount of $[Cm(PTD)]^{3+}$ complex increases reaching a maximum fraction of 25% at 3.7 x 10^{-4} M of PTD. The $[Cm(PTD)_2]^{3+}$ is the predominant species at ligand concentrations larger than 5 × 10^{-4} M with a maximum fraction of 35% at 8.8 x 10^{-4} M of PTD. At higher ligand concentrations, ≥ 8 x 10^{-4} M, $[Cm(PTD)_3]^{3+}$ is the main component in solution.

The same experiments were carried out with Eu(III) in 10^{-3} M $HClO_4$. The formation of $[Eu(PTD)]^{3+}$ starts at a ligand concentration of 8 x 10^{-5} M and exhibits a maximum of 23% at 2.5 x 10^{-3} M PTD. $[Eu(PTD)_2]^{3+}$ is formed has a maximum fraction of 27% at 5.3 x 10^{-3} M PTD. At ligand concentration above 3.7 x 10^{-3} M, $[Eu(PTD)_3]^{3+}$ is the predominant species in solution.

The conditional stability constants for the formation of Cm(III)−PTD and Eu(III)-PTD

complexes are calculated according to:

$$\beta = [M(PTD)_n]^{3+} / [M]^{3+} \cdot [PTD]^{n}_{free}$$

Table 2.3. Comparison of conditional stability constants measured for Am(III)-PTD and Eu(III)-PTD complexes in 10^{-3} M aqueous $HClO_4$

Metal Ion	Logβ_1	Logβ_2	Logβ_3
Am(III)	3.2 ± 0.2	6.6 ± 0.2	9.7 ± 0.3
Eu(III)	2.3 ± 0.3	4.8 ± 0.3	7.3 ± 0.4

As evident, the log β_3 value of Eu(III)-PTD_3 complex (7.3 ± 0.4) is approximately 2 orders of magnitude (250 times) lower than the value of the corresponding Cm(III) complex (9.7 ± 0.3), confirming the An(III)/Ln(III) selectivity observed in extraction experiments.

These experiments demonstrated the possibility to use a hydrophilic 2,6-bis(1,2,3-triazol-4-yl)pyridine based ligand in the separation of An from Ln. PTD indeed, not only fulfils all ligand requirements but shows also an exceptional selectivity for trivalent An which augurs well for its industrial implementation.

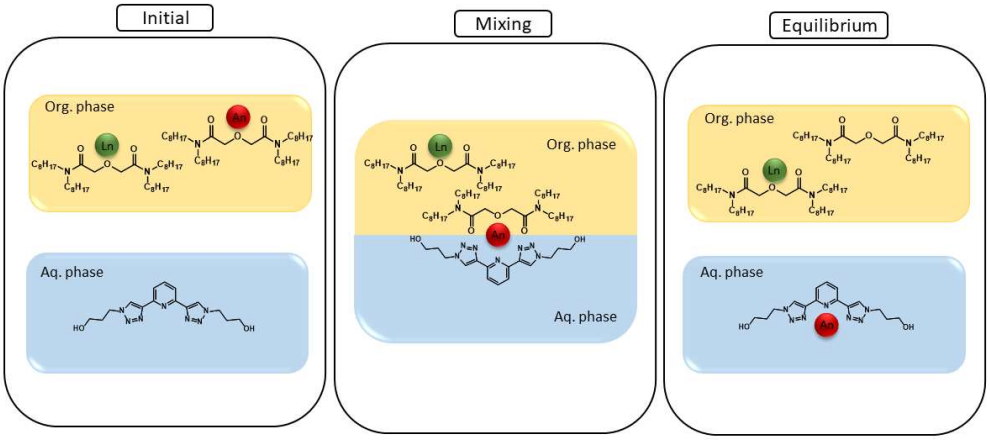

Figure 2.2. Schematic operation of PTD

2.2 PTD

The properties of PTD have been widely investigated in order to open the possibility of employing the ligand in the *i*-SANEX process at industrial scale. The MA selectivity has been demonstrated by extraction tests performed at Radiochemistry and Radiation Chemistry Lab of Politecnico di Milano and at CEA facilities (FR).[4–8]

Furthermore, TRLFS experiments performed at KIT (DE) have confirmed MA selectivity.[3] Hydrolytic and radiolytic stability was demonstrated by solvent extraction experiments, HPLC-MS and NMR analysis performed both at POLIMI and UNIPR,[2] and partly reported in the present chapter. More recently, in 2018, single stage centrifugal contactor experiments with PTD have been conducted at FZJ.[9] The encouraging results obtained from these tests demonstrated the applicability of PTD complexing agent at industrial scale. Nevertheless, an effective use at industrial level requires further experiments of plant simulations and huge quantity of ligand. In order to obtain a comprehensive overview necessary to decide for an industrial implementation of this ligand, two more aspects had to be considered and were studied in this thesis:

- The simplification of the synthesis in order to obtain the target molecule in an easier, faster and economically more convenient way
- The synthesis of the hypothesized hydrolytic and radiolytic degradation products together with the study of their extraction properties in order to assess whether they can impair the selective stripping of An(III) during the process.

2.2.1 PTD synthesis and scale up

The common procedure for the synthesis of PTD is described in the scheme below and was usually carried out on a 2.0 - 2.5 g scale. The first step is a Sonogashira reaction between 2,6-dibromopyridine and trimethylsilyacetylene, both commercially available. For this cross-coupling we used $Pd(PPh_3)_4$ and CuI as catalysts and diisopropylamine as a base in dry toluene. The intermediate **1** is obtained pure after purification by chromatography. The deprotection step is settled by the usual procedure using potassium carbonate and methanol. The 2,6-diethynylpyridine, intermediate **2**, is light and air sensitive so it should be immediately used as soon as it is produced. Finally, the target molecule is obtained under classical CuAAC reaction conditions starting from 2,6-diethynylpyridine and 3-azidopropan-1-ol (**3**) aside synthetized. The crude is purified by chromatography in 70/80% yield. The synthesis of the 3-azidopropan-1-ol (**3**) is necessary as it is not commercial. However, due to the potential explosiveness of short chain azides, large scale synthesis is not recommended. Large volumes of 3-azidopropan-1-ol solutions should not be concentrated under reduced pressure neither heated up and pure samples should be handled with care. Storage is recommended in solutions.

As described above, the synthetic route requires at least three column chromatography purifications implying large costs and long and tedious procedures. The first column is needed to remove the excess of trimethylsilyl acetylene, the monosubstituted pyridine and the products originated by the catalyst. The second column chromatography is necessary to purify the deprotected diethynylpyridine and the last one in order to isolate the target compound from the salts formed during the click reaction. Particularly essential is the last purification step. Indeed, the employ of unpurified PTD was already explored in the past, but samples impure of ascorbates or copper salts significantly decreased the selectivity of extraction.

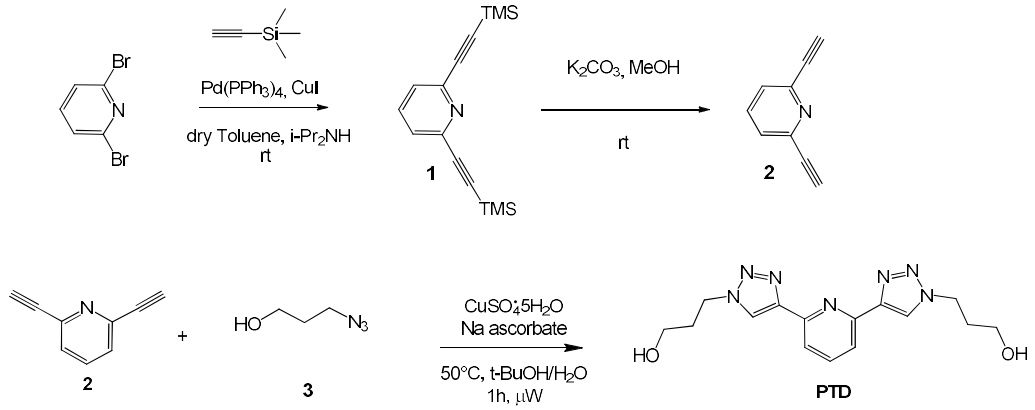

Figure 2.3. Synthesis of PTD

In view of a possible scale up of this synthesis it should be considered to:

- Reduce the number of purification steps (in the reported synthesis 3 flash column chromatography were used)
- Substitute chromatography with crystallization
- Simplify the synthetic pathways (reducing the number of reaction setup and workup procedures)
- Minimize decomposition of compound **2** (unstable to light and air)
- Minimize the amount of azide **3** present in concentrated/neat conditions,
- Minimize the amount of $Pd(PPh_3)_4$ since it is expensive
- Maintain a high purity degree of PTD to ensure high SFs

The achievement of these targets was obtained also by using the *three steps, one pot* approach hereafter proposed. This approach was firstly tested using 10 g of 2,6-dibromopyridine as starting material and then with a 25 g batch (Figure 2.4). Intermediate **1** is usually purified by column chromatography on silica gel giving 90% yield and remain the only chromatographic purification used. The purification step is

essential in order to obtain a pure compound **1** thus avoiding the formation of by-products in the following one pot procedure. Moreover, the Sonogashira cross coupling for the preparation of **1** is the only reaction which should be carried out separately, in a previous step. Starting from 25 g of 2,6-dibromopyridine, 0.006 equiv. of $Pd(PPh_3)_4$, 0.012 equiv. of CuI and 2.25 equiv. of trimethylsilyacetylene after 48 h stirring, a crude sample of **1** was obtained which was purified by filtration on silica gel pad (8 cm in diameter, 6-8 cm in high) using hexane/AcOEt 9:1 as eluent. Some experiments in order to find a better purification system have been made. The best one is a crystallization in cold MeOH. However, this method lowers the yield because of the high solubility of compound **1** in the used solvent so that, although a little bit more time consuming, a silica gel pad is recommended. Once this essential, noncommercial intermediate is prepared in large quantity, the following *three step, one pot* procedure was developed which allows to directly isolate PTD without further intermediate purification steps and without the handling of 3-azidopropanol.

In a round bottom flask 3-chloropropan-1-ol and NaN_3 in 1 : 3.5 molar ratio were dissolved in water (0.25 L). The mixture was heated up to 80 °C and stirred for 48 hours. The reaction mixture was cooled to room temperature whereupon KF (2.5 equiv.), K_2CO_3 (0.5 equiv.), 2,6-bis((trimethylsilyl)ethynylpyridine **5** (1 equiv., 25 g) and ethanol (0.25 L) were added sequentially. The mixture was stirred at room temperature until the deprotection is complete. The reaction progression is checked by TLC It is possible to heat the reaction mixture up to 35-40°C in order to shorten the reaction time. The 2,6-bis((trimethylsilyl)ethynyl)pyridine is not soluble in the solvent mixture while the deprotected intermediate is. Sodium ascorbate (0.06 eq) and $CuSO_4{\cdot}5H_2O$ (0.02 eq) were subsequently added to the mixture at room temperature. Whereupon, the mixture was stirred for one day checking the progression of the reaction by TLC (DCM/MeOH 9:1). Considering the O_2 sensitivity of the Cu (I) salt added in the last step it is advisable to use PTFE gaskets to seal the flask. If the solution turns green, it means that the copper has been oxidized and it is necessary to add more sodium ascorbate. The reaction was quenched by evaporating the ethanol under reduced pressure. Acetone is then added to precipitate the inorganic salts which are filtered off. Whereupon, the mixture was completely dried under reduced pressure. Acetone was added and the mixture was sonicated at 30 °C in order to fully dissolved the solid. An orange suspension of inorganic salts was formed and filtered off. The mixture was dried to obtain the product as a light brown solid. In this way the product could be obtained without further purification in 85% yield starting from 22.5 g (0.08 mol) of

2,6-bis((trimethylsilyl)ethynyl)pyridine.

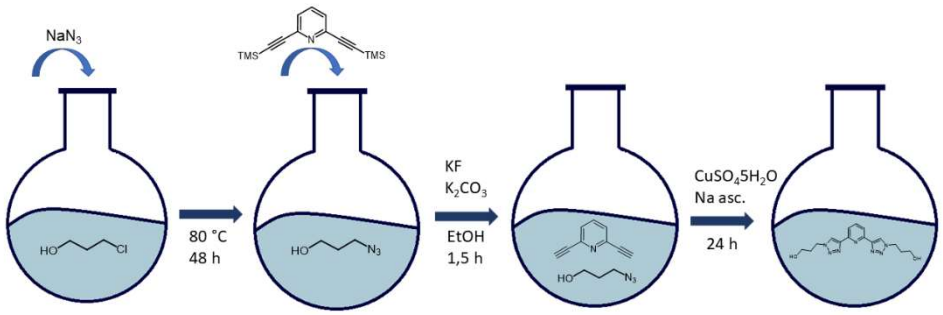

Figure 2.4. PTD synthesis through the ''three steps, one pot'' procedure

The reported NMR spectrum, Figure 2.5, is related to a crude (not purified), large scale preparation batch of PTD. At 8.62 ppm it is possible to see a single singlet related to the triazol protons demonstrating their chemical equivalence while the aromatic protons are group in one broad singlet at 7.95 ppm. A proper 2:3 ratio of the integrals of these peaks indicate the correct formation of both triazole units. The protons of the alkyl chains originate two triplets at 3.64 and 4.63 ppm related to the protons near the OH and near the N atom, respectively, and the quintuplet at 2.2 ppm related to the central CH_2 group. This pattern of signals confirms the symmetry and the purity of the final compound. The identity of the PTD was also checked by ESI-MS experiment which shows a unique peak at 352.5 *m*/*z* which corresponds to $[M + Na]^+$.

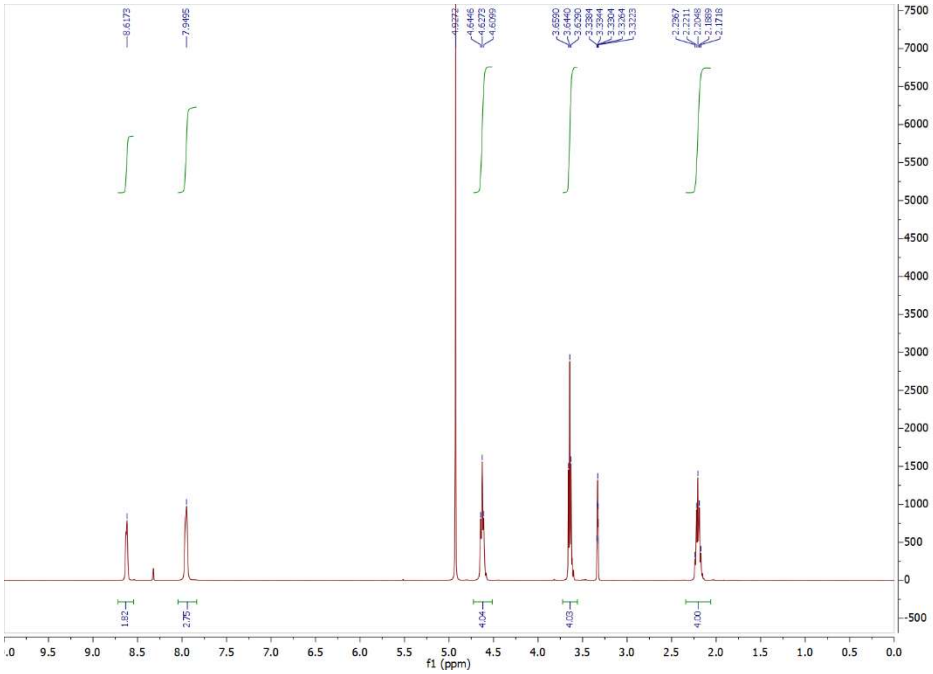

Figure 2.5. ^{1}H NMR (CD_3OD, 400 MHz) of PTD

With the aim again to avoid a further column chromatography, the crude products originated to this three step – one pot procedure were purified using different bulk procedures. In order to evaluate the level of purity of these different batches, especially in terms of performance, few extraction tests have been performed in collaboration with POLIMI. The PTD reference compound (obtained by a column chromatography) shows to have a D_{Am} value of 0.30 ± 0.030 and a $SF_{Eu/Am}$ value of 117.07. Performance of other samples are reported in Table 2.4 and 2.5. The different samples were all obtained by a three steps – one pot procedure (on a 5 g or 25 g scale as indicated between brackets) and after the following purification methods:

PTD RA 131 G: (25 g scale) sample obtained by a 1st crystallization of the crude from methanol;

PTD RA 131 V: (25 g scale) 2nd crystallization from methanol (from the mother liquor of RA 131 G);

PTD RA 119: (5 g scale) crude samples of the three step –one pot procedure without any purifications;

PTD RA 117: (5 g scale) sample obtained by a crystallization of the crude from acetonitrile;

PTD RA 117: (5 g scale) the crude was placed in a Soxhlet apparatus and continuously extracted with condensed vapors of dichloromethane for 48 hs. PTD is slowly dissolved and is collected in a round-bottomed flask.

Data in Table 2.4 reports the values of the different samples analyzed, while Table 2.5 reports, for a simpler comparison, the ratio of the DM or SF values for the observed sample and the DM or SF values for the reference PTD. Values of 1 indicated exactly the same behavior as the purified PTD reference compound, while values of 0.9, 0.8 and 0.7 indicated respectively a performance of 90%, 80% or 70% compared to the reference PTD. All the obtained data show small but, in some cases, significant deviations from the data of the pure reference compound but at different extents.

Table 2.4. D_{Am}, D_{Eu} and $SF_{Eu/Am}$ for different batches and purification methods. Organic phase: 0.2 M TODGA in kerosene + 5% 1-octanol loaded with ^{241}Am and ^{152}Eu. Aqueous phase: 0.08M PTD solution in HNO_3 0.44 M

Quant.	Batch	Purification	D_{Am}			D_{Eu}			SF Eu/Am
2 g	PTD	Chromatography	0,30	±	0,030	35,12	±	3,5	117,07
25 g	PTD RA 131 G	1st Cryst. from MeOH	0,31	±	0,031	31,59	±	3,1	101,90
25 g	PTD RA 131 V	2nd Cryst. from MeOH	0,27	±	0,027	30,34	±	3,0	112,37
5 g	PTD RA 119	Crude	0,30	±	0,030	30,30	±	3,0	101,00
5 g	PTD RA 117	1st Cryst. From ACN	0,28	±	0,028	27,94	±	2,7	99,79
5 g	PTD RA 117	Soxhlet washing	0,27	±	0,027	23,56	±	2,3	87,26

Table 2.5. Comparison of the extracting performances of PTD batches with different purity

PTD batch	Purification	D_{Am}/ $D_{Am\ ref.}$	D_{Eu}/ $D_{Eu\ ref.}$	$SF_{Eu/Am}/SF_{Eu/Am\ ref.}$
PTD RA 131 G	1st Cryst. from MeOH	**1**	0.9	0.9
PTD RA 131 V	2nd Cryst. from MeOH	0.9	0.9	**1**
PTD RA 119	Crude	**1**	0.9	0.9
PTD RA 117	1st Cryst. From ACN	0.9	0.8	0.9
PTD RA 117	Soxhlet washing	0.9	0.7	0.7

Data show that crystallization with acetonitrile or the Soxhlet washing give relative values between 0.7-0.9 of those of pure PTD, while samples obtained from methanol (either the 1st crystallization or even the 2nd one) give relative values between 1 and 0.9 and has therefore to be selected as preferred bulk purification procedure for PTD. Even the sample of crude PTD (RA 119) indeed shows very high relative values (0.9 - 1.0) suggesting it could even be used directly in the separation processes. However, in order to eliminate the inorganic salts and most of those impurities present in the NMR spectrum, at least a crystallization from methanol is recommended.

2.2.2 Safety considerations of Azides

The main drawback for obtaining and using at industrial level the 1,2,3-triazole moiety, especially in large scale, are the synthesis and handling of organic azides as reactants for the click reactions. In fact, these energy-rich synthons can be potentially explosive especially if of low molecular weight. Therefore, in view of a large-scale production of PTD, the risk in the preparation of the 3-azidopropan-1-ol is surely to be considered. The synthesis of alkyl azides is easily obtained by second order nucleophilic substitution. As leaving groups halides and sulfonates (tosylates or triflates) are preferred and DMF is the solvent of choice under thermal conditions or microwave radiations. The azide source is commonly sodium azide. It is important to remind that the N_3^- ion has a similar toxicity as the cyanide ion LD_{50} = 27 mg/kg for rats. Even though NaN_3 is quite stable in aqueous solutions it can hydrolyze with water or Bronsted acids to form HN_3 that is a high toxic and volatile gas. Sodium azide

can also react with common laboratory reagents such as bromine, CS_2 and heavy metals (Cu, Pb, Ba). NaN_3 reacts also with chloroform and dichloromethane forming di- and tri- azido methane which are highly explosive[10] so that the use of chlorinated solvents as reaction media is impossible. However, precautions relative to sodium azide are not the only ones to be taken into account since also the handling of some organic azides should be considered with care. Some of these compounds indeed can decompose explosively even with a slight input of external energy (heat). A safety rule to consider when preparing organic azides is the ''carbon to nitrogen ratio'', $N_C + N_O / N_N$) where N is the number of Carbon, Oxygen or Nitrogen atoms. When C/N is equal or more than 3 (e.g. nonyl azide) the azide derivative can be isolated and stored pure in large quantities. Azides showing a C/N value comprised between 1 and 3 can be isolated but stored as solutions in a concentration not higher than 1 M and in a maximum of 5 grams. Azides with C/N < 1 cannot be isolated since they are high explosive. They can be synthetized in situ as intermediate and with a maximum quantity of 1 gram.[11,12]

A potent technique to evaluate the risk in handling this compound is the Differential Scanning Calorimetry (DSC).[13] For this reason, we performed DSC analyses of some of these organic azide or triazole prepared and used in this chapter. The 3-azidopropan-1-ol necessary for the synthesis of PTD has a C/N ratio of 1.3 therefore the storage and preparation of large quantities should be considered with care. DSC analyses of this derivative, however, are impaired by the volatility of this compound that escapes from normal sample pans used for solids or high molecular weight liquids. In order to check however the risk associated with the manipulation of 3-azidopropan-1-ol, a similar compound in terms of C/N ratio and present in laboratory was tested. Indeed 1-azido-4-iodobutane has a C/N ratio of 1.3. Its thermogram (Figure 2.6) shows an endothermic peak at around 130 °C which is consistent with the boiling point of the compound. The absence of exothermic peak until 350°C proves that the product should be considered safe to handle.

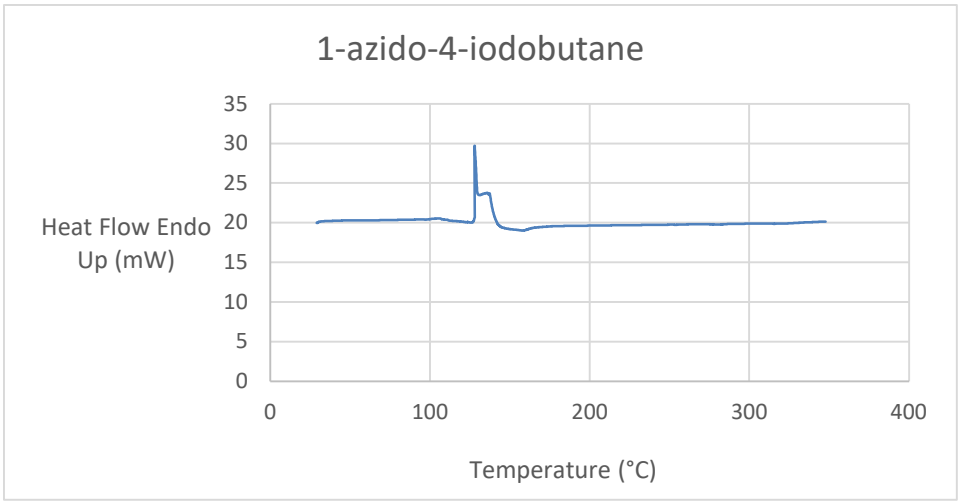

Figure 2.6. DSC of 1-azido-4-iodobutane

Particularly interesting is also the evaluation of the hazard connected with use of the bis-triazolylpyridine moiety. PTD, in particular, has a C/N ratio of 2.1 but, on the base of these preliminary data, it can be considered a safe compound to work with. A thermogram (Figure 2.7) was in fact recorded also for this compound and the results obtained indicate the presence of an endothermic peak at 109.23 °C which corresponds to the melting point of PTD. Remarkably, no exothermic peaks are present up to 350 °C ensuring that the product is not explosive, even when pure and in the solid state.

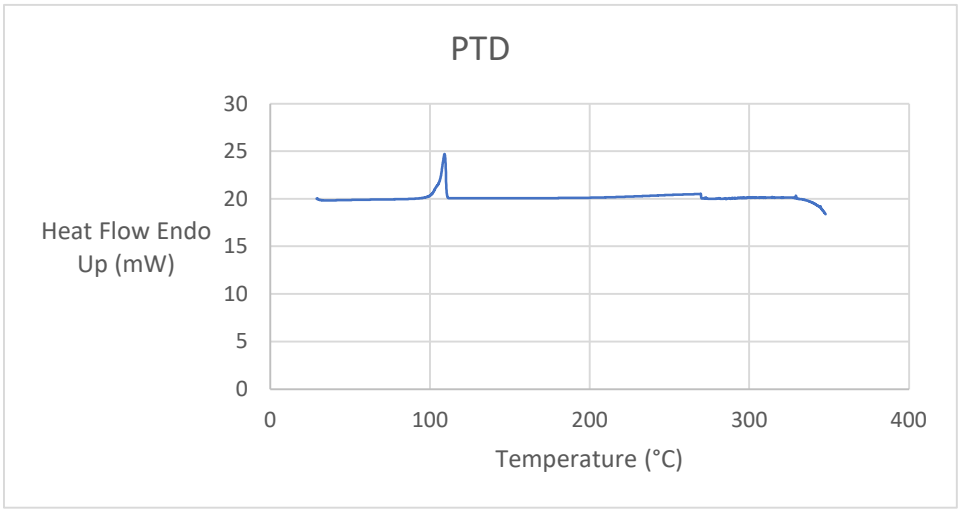

Figure 2.7. DSC of PTD

2.2.3 Identification and synthesis of PTD degradation products

The hydrolytic and radiolytic stability of the ligand is a key prerequisite in view of a possible scale-up of SNF partitioning processes. Hydrolysis and radiolysis may induce the formation of ligand by-products which might impair the separation efficiency and the process. Therefore, in order to evaluate the potential use of PTD at industrial level, this ligand was exposed to tests which simulated the operating conditions of the industrial process. The ligand should work at harsh acidic conditions ([HNO_3] = 0.1 - 4.0 M) and in presence of high γ radiation doses. Particularly, the optimized stripping solvent formulation consists in 0.08 M PTD dissolved in 0.44 M HNO_3. In order to investigate the stability in the acidic medium, PTD stripping solutions were aged in the dark at room temperature for 361 days. Solvent extraction tests and HPLC-MS analysis were performed, and no ligand by-products could be observed. PTD resistance towards hydrolysis further recommends its use in industrial scale processes.[2]

In order to investigate the ligand stability towards radiolysis, PTD stripping solutions were irradiated with two ^{60}Co sources characterized by different dose rates: 2.5 and 0.13 kGy h^{-1}. The irradiations were performed up to absorbed dose of 500 kGy with the 2.5 kGy/h ^{60}Co source and up to 100 kGy with the 0.13 kGy/h ^{60}Co source. Under these operating conditions only a rather slight decrease in the efficiency and selectivity of the ligand has been observed. Accurate analysis of the irradiated acidic aqueous phase by HPLC coupled with ESI-MS were performed by Macerata's group at POLIMI. HPLC were performed with 1100 Series (Agilent) equipped with Purospher® STAR RP-18 endcapped column (3 μm) and H_2O:CH_3CN 80:20 (or 77:23) was used as mobile phase. The obtained data showed that the decrease in ligand properties was associated to an increase in species with different molecular weights. It can therefore be inferred that the radiolysis processes which occur during extraction tests lead to the formation of degradation products (DPs) even if in rather small quantities (0.5 - 2%). These compounds were analyzed by HPLC-ESI/MS, so that only their molecular masses are known. From the molecular mass it is relatively easy to hypothesize which fragment has been lost or which moiety was added but it is quite difficult to understand in which part of the molecules the modification has taken place, especially considering that PTD has two perfectly equal propanol branches. Generally, being in presence of oxidative conditions (HNO_3, O_2, OH^-) C-C and C-H bonds are broken in favor of the formation of C=O, C-O and C-NO_2 bands. Several

hypotheses on their structures (Figure 2.8) were given based on tandem mass spectrometry. Obviously, several isomers with the same mass might be equally suggested. Observing the proposed structures of DPs the lateral branches seem to be the weakest position of the ligand while the aromatic core is apparently the most resistant one. It has been hypothesized that the degradation mechanism is mainly caused by indirect radiolysis due to ligand reactions with reactive species present in the aqueous layer such as nitric acid and hydroxyl and peroxyl radicals.[14,15]

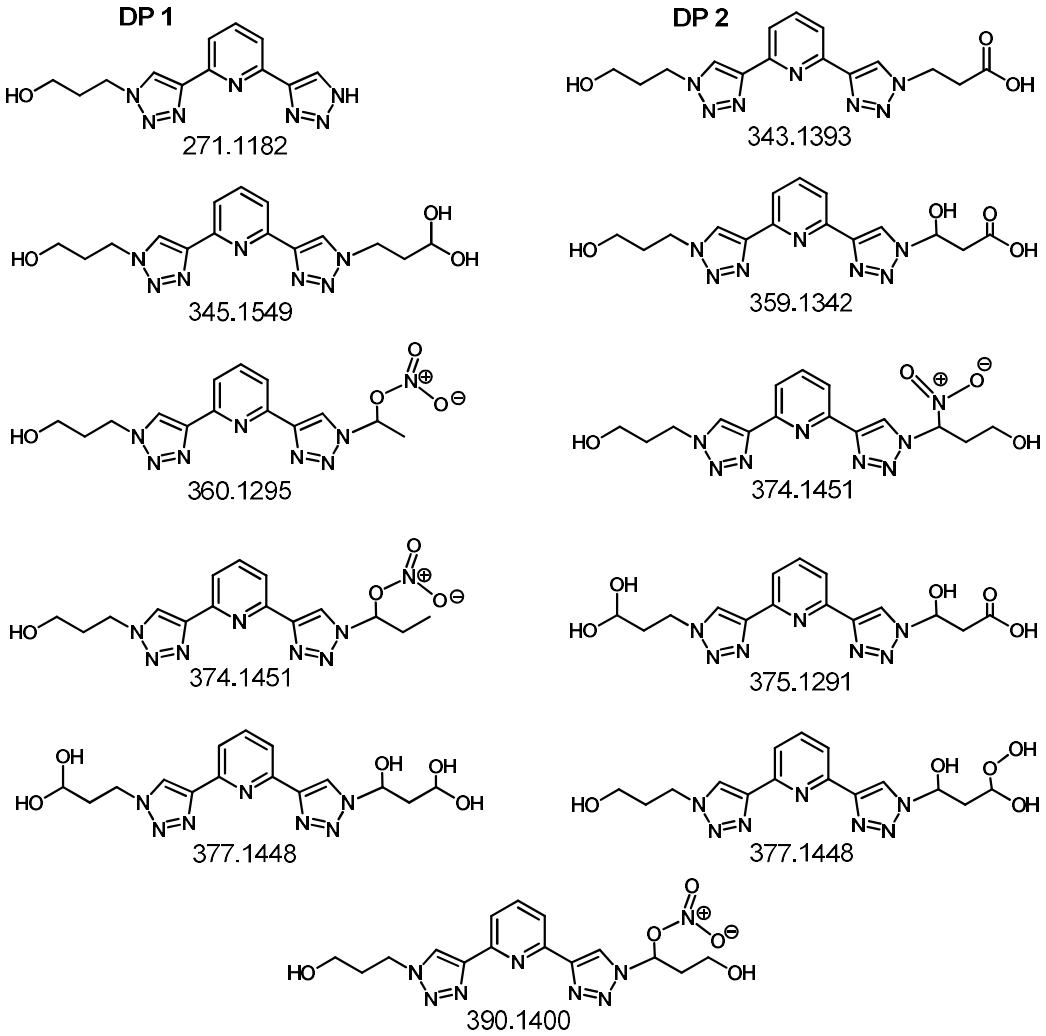

Figure 2.8. Molecular structure and calculated exact mass of the DPs as proposed by POLIMI and UNIPR. Structural isomers of the proposed structures are as well possible.

Further irradiation tests have been carried out at CEA (France) and the collected data support the structure of some of the degradation products hypothesized by POLIMI

and UNIPR. Apart from the product with m/z = 360, identified only by POLIMI, all the other peaks present in the ESI-MS spectra were evidenced by both laboratories even though different possible isomeric structure were given in this preliminary assignment.

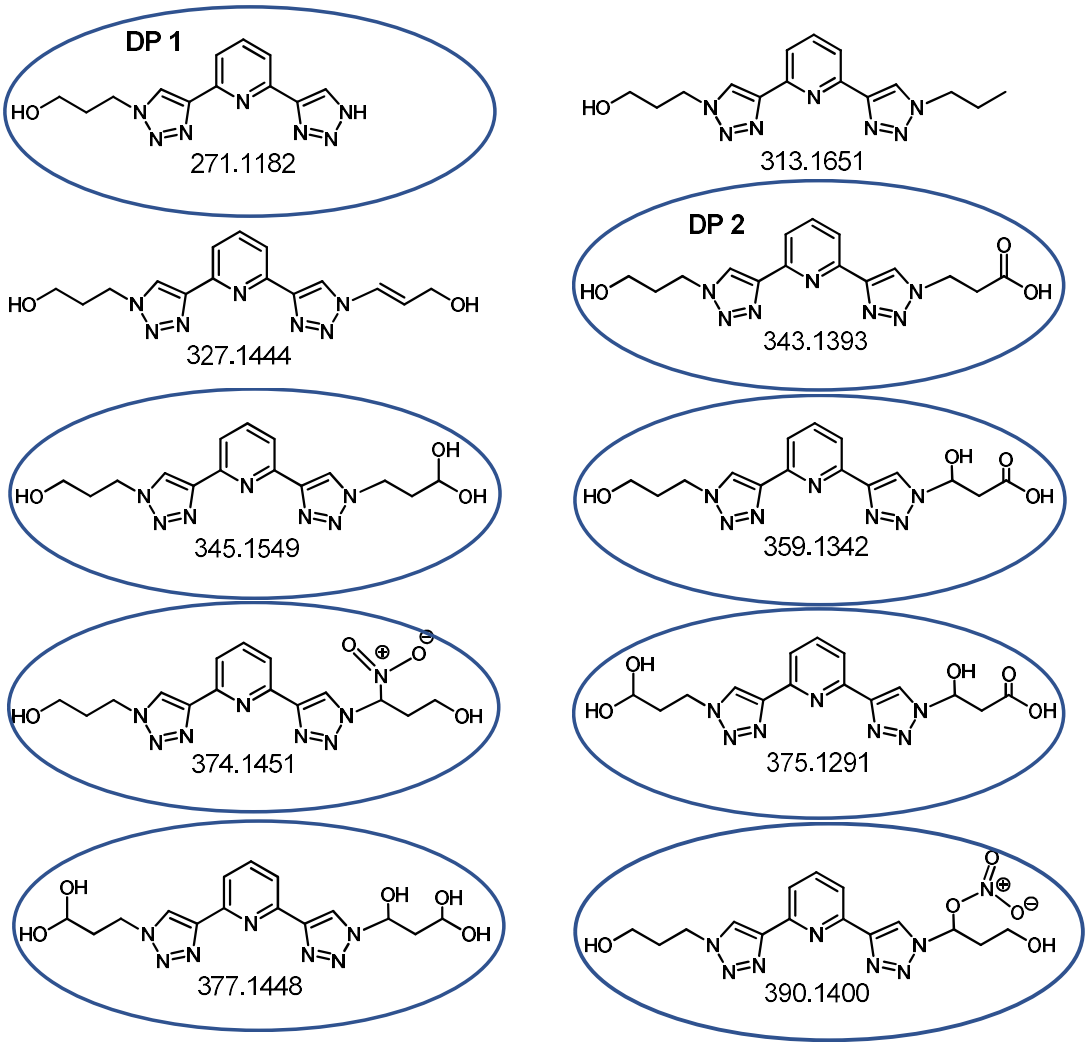

Figure 2.9. Proposed molecular structure and calculated exact mass of the DPs by CEA. Encircled products were also suggested by POLIMI-UNIPR, although in some cases thy have different structural formulas

Only the isolation of a reasonable (5 - 10 mg) amount of such compounds and their structural determination will remove all the doubts on their structure. The rather low concentration of each products makes the isolation of a significant amount by preparative HPLC very difficult and time consuming. It was therefore planned to

synthesize some of the most plausible compounds and to verify their presence in the irradiated mixture by HPLC analysis and MS/MS experiments which will hopefully help in the structure determination of degradation products.

As shown in Figure 2.8 and 2.9, most of the degradation products lost the C_{2v} symmetry of the starting PTD ligand due to a single reaction on only one of the two arms or by two reactions in two different positions of the two arms. Therefore, the most relevant problem of the synthesis of these degradation products is related to the preparation of PyTri having two different arms connected to the pyridine nucleus.

As first attempt it was tried to synthetize DP 1 and DP 2 (Figure 2.8). The former has no possibility of isomerism, so that the structure first assigned should also be the real structure of this DP. DP 2, on the other side, has three possible isomers. Since DP 2 could be the father of other degradation products, the disclosure of its structure could help in the determination of the structure of other compounds.

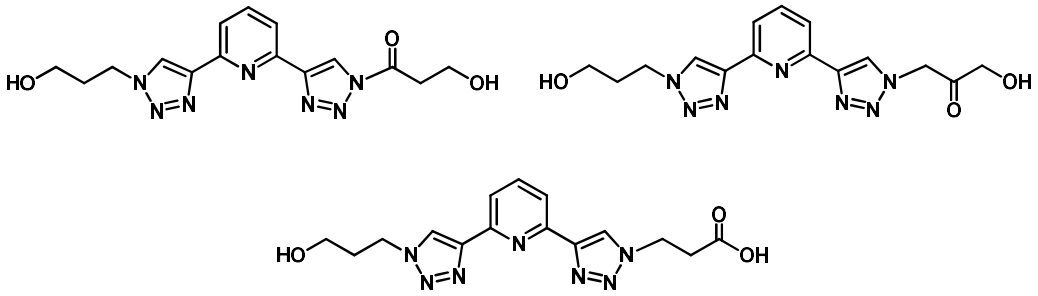

Figure 2.10. Possible isomers of DP 2

First, the 3-azidopropan-1-ol and ethyl-3-azido propanoate have been prepared by direct substitution of the halogen atom into commercially available 3-chloropropan-1-ol and ethyl-3-bromopropanoate, respectively.

The synthesis of **DP 1** is shown in Figure 2.11 and it requires the preparation of intermediate **4**. Accordingly, we tried to study the selective cycloaddition reaction with 3-azidopropan-1-ol and 2,6-diethynylpyridine but the reaction seems to be not so selective. Even in the presence of 1 equivalent (or even less) of azidopropanol, the main product of the reaction is PTD which could be recovered with the starting material and only a rather small amount of the desired monofunctionalised compound **4** could be isolated. Conditions were however developed to allow a 20% formation of **4**, which could be chromatographically separated from PTD on silica gel. Compound **4**, although obtained in low yields, represents an important intermediate since from this molecule it would be possible to obtain, upon cycloaddition with the

appropriate azide, all the degradation products of PTD having only one altered propanol arm.

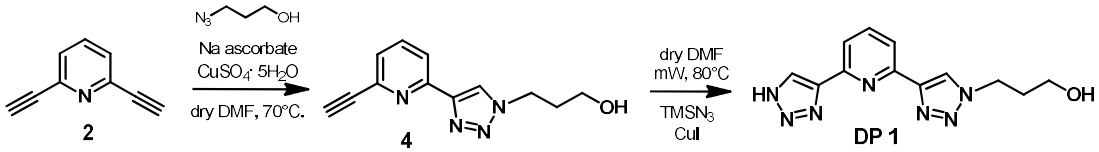

Figure 2.11. Synthesis of DP 1

Reaction of **4** with trimethylsilyl azide ($TMSN_3$) in a microwave synthesizer allowed to obtain, even if in quite low yields (37%) the desired compound, identified as **DP 1**.

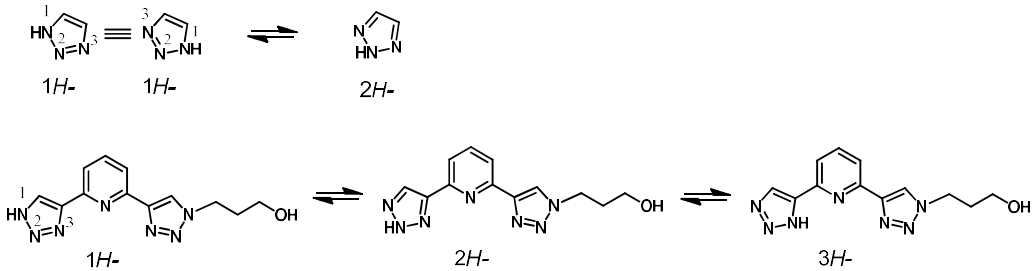

Figure 2.12. Tautomerism between 1H- and 2H- forms of unsubstituted 1,2,3-triazole (above) and between *1H-, 2H- and 3H- forms of a monofunctionalized 1,2,3-triazole in compound* ***DP 1*** (below).

It has to be noted that, as reported in the literature,[16,17] a tautomerism between the two forms 1*H* and 2*H* of unsubstituted 1,2,3-triazole is effective in water and protic solvents with a slight preference (2 parts to 1) for the 2*H* form. A similar tautomerism on 4-substituted-1,2,3-triazole, as **DP 1** (Figure 2.12 above), might result in three different forms whose distribution in solution has never been studied (to the best of our knowledge). It appears probable that the *3H-* form is the most stable because of a possible *intra*molecular dipolar interaction between the N-H group and the pyridine lone pair and this could impair the chelating ability of **DP1**.

For the synthesis of compound **DP 2** we have followed a different synthetic strategy. First, it was introduced the oxidized arm bearing the carbo-ethoxy group. The 2,6-diethynyl pyridine was reacted with ethyl 3-azidopropanoate (2.5 equiv.) in the presence of copper sulfate and ascorbic acid. Since even with only 1.0-1.5 equiv. of azide, all the three compounds (unreacted **2**, monofunctionalised **10** and difunctionalised **10b**) were present in the reaction mixture, we chose to add 2.5 equivalents of azide in order, at least, to consume all the starting dialkynylpyridine **2**. Mono and difunctionalized products indeed, are easier to separate then 2,6-diethynyl pyridine and **10**. The

reaction was stirred at room temperature for 24 hours to facilitate the product of monofunctionalization upon the difunctionalized one. After quenching and purification, the two compounds were isolated in 20% and 70% yields, respectively. Compound **10** was subsequently reacted under Huisgen cycloaddition conditions with 3-azidopropan-1-ol to obtain compound **11** (yield = 47%) and subsequently hydrolyzed under basic conditions to afford compound **12 (DP 2**) in 89% yield.

In parallel, also compound **10 b** was hydrolyzed under basic conditions and the diacid **13** was obtained quantitatively.

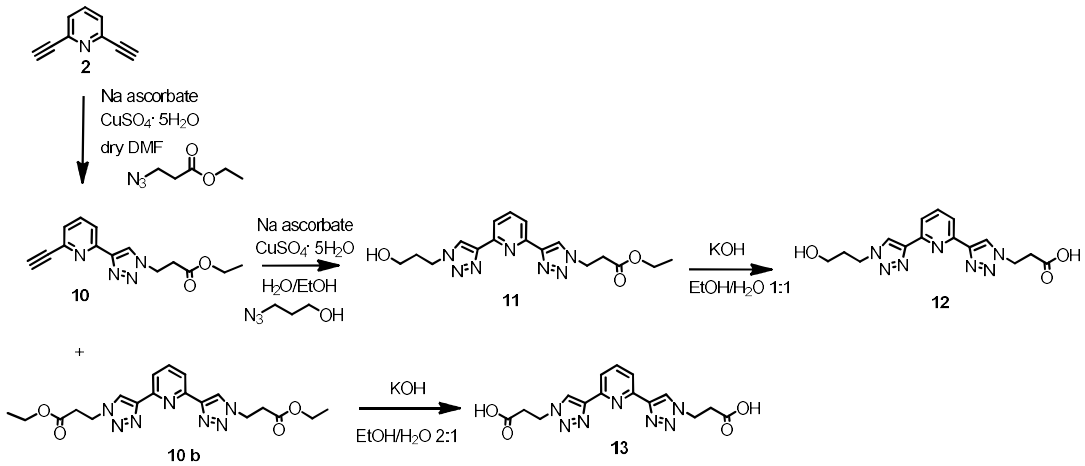

Figure 2.13. Synthesis of DP 2

The studies on the extraction properties of the DPs are undergoing at POLIMI. The extraction tests are performed using 0.2 M TODGA in kerosene + 5% 1-octanol loaded with ^{241}Am and ^{152}Eu as organic phase and 0.08 M DP solution in HNO_3 0.44 M as organic phase which are the optimal conditions used for extraction test with PTD. Data are also with the monotriazolyl monoalcohol derivative PTA, obtained as byproduct in the synthesis of PTD. Because of the insolubility of DP 2 in the used aqueous solution it was not possible to complete extraction tests for this compound.

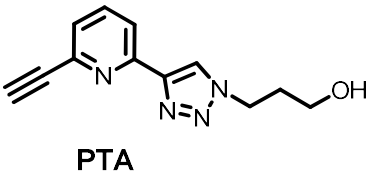

Figure 2.14. Molecular structure of the monotriazolyl monoalcohol derivative PTA

DP 1 shows D_{Am} and D_{Eu} values much higher than those of PTD indicating a considerably

drop in stripping ability of this compound for both Am(III) and Eu(III), but especially for the former one. Even worse appears the chelation ability of PTA which seems not to be able to significantly strip metal ions into the aqueous layer (cfr. last column of Table 2.6). Once more these data confirm of the exceptional ability of the PyTri chelating unit as effective and selective stripping agent for trivalent actinide ions in acidic water solution.

Table 2.6. D_M and SF values for PTD, DP 1, DP 2 and PTA. Used conditions: 0.2M TODGA in kerosene + 5% 1-octanol loaded with Am^{241} and Eu^{152} as organic phase and 0.08 M DP solution in HNO_3 0.44M as aqueous phase

	PTD	DP 1	DP 2	PTA	No stripping agent
D_{Am}	0.3	~ 2	NS	~ 15	16.3
D_{Eu}	35	78	NS	~ 100	113
SF	117	35		~ 7	6.93

NS = not soluble in the acidic aqueous phase

The confirmation of the presence of exactly these synthetized compounds **DP 1** and **DP 2** in the irradiated PTD solutions by HPLC-MS analyses is still in progress.

2.3 Experimental

2.3.1 General methods and chemicals

Reagents and solvents

All commercially available chemicals (Sigma-Aldrich, TCI, ChemPur, VWR) used in this study were analytical reagent grade and were used without further purification. All air sensitive reactions were carried out under nitrogen atmosphere using oven-dried glassware. All dry solvents were prepared according to standard procedures and stored over 3 or 4 Å molecular sieves.

Instrumentation, techniques, and common procedures

^{1}H NMR and ^{13}C NMR spectra were recorded on Bruker AV300 and AV400 or JEOL ECZ600R spectrometers (observation of ^{1}H at 300 MHz, 400 MHz and 600 MHz and of ^{13}C at 75 MHz, 100 MHz or 150 MHz). Partially deuterated solvents were used as internal standards to calculate the chemical shifts (δ values in ppm). J coupling constants are

given in Hz. All ^{13}C NMR spectra were performed with proton decoupling. The used abbreviations in these spectra are singlet (s), doublet (d), triplet (t), quadruplet (q), quintuplet (quint) and multiplet (m).

In order to monitor the progress of reactions, aluminum sheets covered with silica gel 60 F-254 provided by Merck were used. All TLC s were revealed under an ultraviolet lamp (λ= 254 nm) or using staining reagents. Merck silica gel 60 was used for flash chromatography (40-63 μm) and for preparative TLC plates 20x20cm (10-12 μm).

Electrospray ionization (ESI) mass analysis were performed on a Waters single- quadrupole instrument SQ Detector in positive mode using MeOH or CH_3CN as solvents. HR-MS spectra were registered by Dr. Andrea Faccini at "Centro Interdipartimentale Misure" of Università di Parma with an LTQ ORBITRAP XL Thermo instrument in positive mode using MeOH or CH_3CN as solvents.

Melting points were determined on an Electrothermal apparatus in sealed under nitrogen capillaries.

The liquid-liquid extraction tests were performed following a standard protocol. Equal volumes of aqueous and organic phases were contacted in closed single-use Eppendorf microtubes at room temperature (T = 22.2 °C). Once contacted, the organic and aqueous phases were vigorously shaken with a benchtop shaker for 1h. The mixing time of 1h was found to be enough for the system to reach the equilibrium. After the phase separation by centrifugation, an aliquot of 200 μL from each phase was subsampled and analysed. The ^{241}Am and ^{152}Eu specific activities were quantified by γ spectrometry (2"x2" NaI(Tl), Silena SNIP 201 N MCA) exploiting the γ lines at 59.5 keV and 121.8 keV, respectively. The ^{239}Pu and ^{244}Cm specific activities were quantified by α-spectrometry. The concentrations of stable elements (Y and Lanthanides) were determined by Inductively Coupled Plasma Mass Spectrometry (ThermoFisher X-SeriesII ICP-MS) as direct measurements on the aqueous phases after adequate dilution, and after mineralization by microwave oven for the organic phases. The activity balance was checked and the overall accuracy in the determination of DM is within few percent.

Preparation of the loaded organic phase

The extraction step simulates the first step of the *i*-SANEX process or GANEX-2 process. An and Ln are co-extracted into the organic phase, while the other fission and corrosion products remain in the aqueous phase. Thus, the loaded organic phase was used as phase to be decontaminated in the following stripping tests. Extraction experiments were performed by contacting a 0.2 M TODGA solution in kerosene/1-octanol (95/5 v/v) with an equal volume of a 3 M nitric acid aqueous feed. The lipophilic extractant

TODGA can co-extract 99.9% of An and Ln present in the aqueous phase into the organic one. The cations concentration in the loaded organic phase was then determined by ICPMS, α and γ spectrometry. Moreover, it is known that TODGA is able to extract nitric acid, that is subsequently released when contacted with aqueous solutions at lower acidity. This phenomenon has an impact on the equilibrium acidity of the stripping phase, that is an important parameter in the extraction process. Therefore, it was checked in the different steps of the experiments by potentiometric titration.

Stripping experiments

The stripping experiments consisted in contacting the loaded TODGA-based solutions with the aqueous stripping phases, that are ligand solutions in 0.25 M HNO_3. To specifically investigate the role of the hydrophilic ligands, stripping experiments with 0.25 M HNO_3 in absence of the hydrophilic ligands were performed and reported as blank experiments. First of all, the solubility of the hydrophilic extractants in the aqueous phase was ascertained by a stepwise process: a weighted quantity of compound was dissolved in diluted nitric acid solution and weighted amounts of diluent were added until the solutions were clear. Then, the losses of ligands due to their solubility in the organic phase (kerosene/1-octanol 95/5 v/v or 0.2 M TODGA in kerosene/1-octanol 95/5 v/v) were evaluated by UV-*vis* measurements of the ligand concentration. For both the ligands, a concentration variation within the experimental error was observed. Consequently, no pre-equilibration of the phases before the tests were carried out. In addition, the amount of HNO_3 released into the aqueous phase during the stripping step was evaluated by measuring the HNO_3 concentration before (initial) and after the test (equilibrium) by means of potentiometric titration with NaOH. The HNO_3 concentration, initially at 0.25 M, reached the equilibrium value at 0.44 M after the contact with the loaded organic phase. Some extraction tests were performed with 0.44 M HNO_3 stripping phases because the stripping test is preceded with a scrubbing step by 0.5 M HNO_3. During this stage the extracted nitric acid is released, so that no acidity changes were registered in the following stripping step.

2.3.2 Synthesis

3-Azidopropan-1-ol

Prepared according to literature procedure.[18] NaN_3 (9.1 g, 140 mmol) was added to water

(50 ml). Once the azide is completely dissolved, 3-chloropropan-1-ol (6.87 g, 68 mmol) was added dropwise. The reaction mixture was stirred at 80° C for 24 h. The aqueous solution was extracted three times with dichloromethane, and then the organic phases collected were dries over anhydrous Na_2SO_4. The solvent was evaporated in vacuo to obtain the product as a yellowish oil. Yield: 85%. ^{1}H NMR (400 MHz, $CDCl_3$): δ 3.76 (2H, t, *J* = 6.0 Hz, C*H*$_2$N$_3$), 3.46 (2H, t, *J* = 6.6 Hz, C*H*$_2$OH), 1.84 (2H, quint, *J* = 6.3 Hz, CH$_2$C*H*$_2$CH$_2$).

2,6-bis((trimethylsilyl)ethynyl)pyridine (1)

A solution of 2,6-dibromopyridine (25.0 g, 0.105 mol), CuI (0.24 g, 1.26 mmol), $Pd(PPh_3)_4$ (0.73 g, 0.63 mmol) and trimethylsilylacetylene (23.2 g, 0.24 mol) was stirred under N_2 at room temperature for 48 h. The reaction was quenched with 4 M HCl (500 ml). HCl was added until the organic phase has a pH ≤ 7. The aqueous phase was extracted one time with AcOEt (300 ml), then the organic phases collected were washed with water (3 x 300). The organic layer was dried over anhydrous Na_2SO_4 and the solvent was evaporated under reduced pressure to obtain a brown solid. The crude was purified by flash column chromatography using Hexane/ AcOET 9:1 as eluent. Yield: 89.6%. ^{1}H NMR (600 MHz, $CDCl_3$) δ (ppm): 7.58 (2H, t, *J* = 7.6 Hz, Ar*H*$_{para}$), 7.37 (2H, d, *J* = 7.8 Hz, Ar*H*$_{meta}$), 0.25 (18 H, s, TMS).

PTD through the three steps, one pot procedure

NaN_3 (56.9 g, 0.88 mol) was dissolved in water (250 ml) then 3-chloropropan-1-ol (23.22 g, 0.25 mol) was added. The mixture was stirred at 80 °C for 40 h. Careful must be taken as a condenser has not been used. The mixture was cooled to room temperature and 2,6-bis((trimethylsilyl)ethynyl)pyridine (22.5 g, 0.082 mol), K_2CO_3 (5.66 g, 0.041 mol) and KF (11.9 g, 0.20 mol) were added. Whereupon, EtOH (250 ml) was added and the mixture was stirred until the PyTMS was almost completely dissolved. Then, Na ascorbate (9.75 g, 4.9 mmol) and $CuSO_4 \cdot 5H_2O$ (0.41 g, 1.64 mmol) were added. The mixture was stirred at room temperature for 48 h then quenched evaporating the solvents. Acetone was added to the crude in order to precipitate the inorganic salts which were filtered off. The solvent was evaporated and the obtained solid was completely dissolved in acetone (1.0 L) sonicating at 40 °C for 2 h. The obtained solution was filtered, and the solvent evaporated to obtain a light brown solid. ^{1}H NMR (Acetone-d$_6$, 400MHz) δ (ppm)= 8.53 (2H, s, Triaz-H), 8.05 (2H, d, *J* = 7.5 Hz, PyH$_{meta}$), 7.97 (1H, t, *J* = 7.5 Hz, PyH$_{para}$), 4.63 (4H, t, *J* = 7.0 Hz, C*H*$_2$N), 3.87 (2H, t, *J* = 6.5 Hz, OH), 3.64 (4H, t, *J* = 7.5 Hz, C*H*$_2$OH), 2.20 (4H, m, *J* = 7.5 Hz, *H*$_2$CH$_2$OH). ^{13}C

NMR (Acetone-d_6, 100 MHz) = 150.7, 147.8, 137.7, 122.9, 118.2, 58.0, 47.0, 33.1. ESI-MS (+): 352.5 $[M+Na]^+$.

2-(1-(propan-3-ol)-1,2,3-triazol-4-yl)-6-ethynylpyridine (4)

2,6 diethynylpyridine **2** (0.5 g, 3.9 mmol) was dissolved in dry DMF (50 ml) under N_2. Then, $CuSO_4 \cdot 5H_2O$ (0.02 eq.), Na ascorbate (0.2 eq.) and 3-azidopropan-1-ol (0.59 g, 5.85 mmol) were added. The resulting mixture was stirred for 72 hours at 70° C. The solvent was removed under reduced pressure and the crude purified by flash column chromatography using DCM/MeOH (96:4 to 8:2) as eluent. Yield: 20%. ^{1}H NMR (400 MHz, $CDCl_3$) δ (ppm): 8.30 (1H, s, Triaz*H*); 8.20 (1H, d, J = 8 Hz, ArH_{meta}); 7.79 (1H, t, *J* = 7.8 Hz, ArH_{para}); 7.45 (d, *J* = 8 Hz, 1H, ArH_{meta}); 4.62 (t, *J* = 7 Hz, 2H, CH_2CH_2N); 3.71 (2H, t, *J* = 6 Hz, CH_2CH_2OH); 3.21 (1H, s, CC*H*); 2.20 (2H, quint, *J* = 6 Hz, $CH_2CH_2CH_2$). ^{13}C-NMR (100 MHz, $CDCl_3$) δ (ppm): 150.8; 147.7; 141.9; 137.2; 126.6; 123.1; 120.1; 82.8; 77.2; 58.6; 47.1; 32.5. ESI-MS (+): m/z 251.2 [100%; $(M+Na)^+$]; m/z 267.2 [15%; $(M+K)^+$]; m/z 229.2 [10%; $(M+H)^+$]. mp: 130°C.

Diethyl 3,3′-(4,4′-(pyridine-2,6-diyl)bis(1H-1,2,3-triazole-4,1-diyl))dipropanoate (10) and ethyl 3-(4-(6-ethynylpyridine-2-yl)-1H-1,2,3-triazol-1-yl))propanoate (10 b)

A mixture of 2,6 diethynylpyridine **2** (86 mg, 0.68 mmol) and ethyl-3-azidopropionate (0.24 g, 1.7 mmol) was dissolved in dry DMF (2 ml) under inert atmosphere. Then, $CuSO_4 \cdot 5H_2O$ (0.02 eq.) and Na ascorbate (0.2 eq.) were added. The reaction mixture was stirred for 24 hours at room temperature then quenched with water. The aqueous layer was extracted with AcOEt and the organic phases, combined, washed with water and dried over anhydrous Na_2SO_4. The crude was purified by flash column chromatography using Hex/AcOEt/MeOH 6:3:1 as eluent to obtain product **10** (yield: 20%) and **10 b** (yield: 70%).

Compound 10: ^{1}H NMR (400 MHz, $CDCl_3$) δ (ppm): 8.3 (1H, s, Triaz*H*), 8.2 (1H, d, J = 8 Hz, Ar*H*), 7.8 (1H, t, J = 8 Hz, Ar*H*), 7.4 (1H, t, J = 7 Hz, Ar*H*), 4.7 (2H, t, J = 6.4 Hz, Triaz-CH_2CH_2CO), 4.2 (4H, q, *J* = 6.8 Hz, CH_3CH_2OCO), 3.2 (1H, s, CC*H*), 3.0 (2H, t, *J* = 6.8 Hz, Triaz-CH_2CH_2CO), 1.3 (3H, t, *J* = 7.0 Hz, CH_3CH_2OCO).

Compound 10 b: ^{1}H NMR (400 MHz, $CDCl_3$) δ (ppm): 8.28 (2H, s, Triaz*H*); 8.09 (2H, d, *J* = 7.8 Hz, ArH_{meta}); 7.86 (1H, t, *J* = 7.8 Hz, ArH_{para}); 4.75 (4H, t, *J* = 6.5 Hz, Triaz-CH_2CH_2CO); 4.19 (4H, q, *J* = 7.2 Hz, CH_3CH_2OCO); 3.05 (4H, t, *J* = 6.5 Hz, Triaz-CH_2CH_2CO); 1.27 (3H, t, *J* = 7.1 Hz, CH_3CH_2OCO). ^{13}C-NMR (100 MHz, $CDCl_3$) δ (ppm): 170.5; 149.9; 148.3; 137.7; 123.1; 119.3; 61.9; 45.8; 34.7; 14.1.

3,3'-(4,4'-(pyridine-2,6-diyl)bis(1H-1,2,3-triazole-4,1-diyl))dipropanoic acid (13)

10 b (0.197 g, 0.45 mmol) and KOH (0.16 g, 2.86 mmol) were dissolved in a mixture of EtOH/H_2O (15 ml). The reaction was stirred for 72 hours at room temperature then quenched evaporating the solvents. The crude was purified by reverse phase column chromatography using H_2O as eluent to obtain the product as a white solid in a quantitative yield. ^{1}H NMR (400 MHz, $CDCl_3$) δ (ppm): 8.64 (2H, s, Triaz*H*); 7.98-7.89 (3H, m, Ar*H*); 4.75 (4H, t, *J* = 6.7 Hz, Triaz-C*H*$_2$CH$_2$CO); 2.84 (4H, t, *J* = 6.7 Hz, Triaz-CH$_2$C*H*$_2$CO). ^{13}C-NMR (100 MHz, $CDCl_3$) δ (ppm): 178.5; 162.06; 148.9; 139.2; 124.1; 120.3; 47.8; 37.5. ESI-MS: m/z 380.3 [100%; $(M+Na)^+$].

Ethyl 3-(4-(6-(1-(3-hydroxypropyl)-1H-1,2,3-triazol-4-yl)pyridin-2-yl)-1H-1,2,3-triazol-1-yl)propanoate (11)

The monoester derivative **10** (35 mg, 0.13 mmol), was dissolved in a mixture of H_2O/EtOH 1:1 (1 ml) under N_2. Then, 3-azidopropan-1-ol (15 mg, 0.15 mmol), $CuSO_4 \cdot 5H_2O$ (0.06 eq.) and Na ascorbate (0.6 eq.) were added. The reaction mixture was stirred for 5 days at room temperature then quenched evaporating the solvents. The crude was dissolved in acetone and the inorganic salts were filtered off. A further purification by preparative TLC using DCM/MeOH 9:1 allowed to obtain the product **11** in 47% yield. ^{1}H NMR (300 MHz, Acetone-d6) δ (ppm): 8.53 (1H, s, Triaz*H*); 8.51 (1H, s, Triaz*H*); 8.07-7.94 (3H, m, Ar$H_{meta,para}$); 4.79 (2H, t, *J* = 6.6 Hz, CH$_2$C*H*$_2$N); 4.63 (2H, t, *J* = 7.0 Hz, CH$_2$C*H*$_2$N); 4.14 (2H, q, *J* = 7.1 Hz, COOC*H*$_2$CH$_3$); 3.65 (2H, t, *J* = 6.0 Hz, CH$_2$C*H*$_2$OH); 3.1 (2H, t, *J* = 6.6 Hz, Triaz-CH$_2$C*H*$_2$CO); 2.18 (2H, quin, *J*= 6.5 Hz, CH$_2$C*H*$_2$CH$_2$); 1.22 (3H, t, *J* = 7.1 Hz, CH$_2$C*H*$_3$). ^{13}C-NMR (100 MHz, CD_3OD) δ (ppm): 170.3, 150.7, 150.5, 147.7, 137.7, 123.3, 122.9, 118.3, 118.2, 60.4, 58.0, 47.0, 45.7, 34.2, 33.1, 13.5. ESI-MS: m/z 394.3 [100%; $(M+Na)^+$]; m/z 410.2 [9.7%; $(M+K)^+$]; m/z 372.3 [7.7%; $(M+H)^+$]; 765.5 [7.1%; $(2MNa)^+$].

3-(4-(6-(1-(3-hydroxypropyl)-1H-1,2,3-triazol-4-yl)pyridin-2-yl)-1H-1,2,3-triazol-1-yl)propanoic acid (12)

Compound **11 (**22 mg, 0.06 mmol) was dissolved in a mixture of EtOH/H_2O 1:1 (2 ml) then KOH (6 eq.) were added. The reaction was stirred for 24 h then quenched by evaporating the EtOH. The aqueous layer was acidified until pH 2.5 then extracted with DCM (3x) and AcOEt (3x). The organic layers, combined, were dried over anhydrous Na_2SO_4 and the solvents removed *under vacuo* to obtain the product as a white solid in 89% yield. ^{1}H NMR (400 MHz, CD_3OD) δ (ppm): 8.63 (2H, s, Triaz*H*); 7.97 (3H, s, Ar$H_{meta,para}$); 4.77 (2H, t, J = 6.6 Hz, CH$_2$C*H*$_2$N); 4.63 (2H, t, J = 7.0 Hz,

CH_2CH_2N); 3.65 (2H, t, J = 6.0 Hz, CH_2CH_2OH); 3.06 (2H, t, J = 6.0 Hz, CH_2CH_2OH); 2.21 (2H, quin, J = 6.5 Hz, $CH_2CH_2CH_2$). ^{13}C-NMR (100 MHz, CD_3OD) δ (ppm): 172.7; 149.8; 147.7; 147.5; 137.8; 123.7; 123.5; 118.69; 118.6; 57.9; 46.1; 34.0; 32.6; 29.4; 22.3. ESI-MS: m/z 341.98 [28.0%; $(M+H)^-$].

2-(1-(propan-3-ol)-1,2,3-triazol-4-yl)-6-(1-H-1,2,3-triazol-4-yl)pyridine (DP 1)

Compound **4** (50 mg, 0.22 mmol) and CuI (0.3 eq) were dissolved in DMF (8 ml) then trimethylsilyl azide (0.08 ml) was added to the mixture. The reaction mixture was heated up to 90° C and stirred for 24 hours. The reaction was quenched by evaporating the solvent. The solid was dissolved in AcOEt and the organic layer was washed with water. The organic phase was dried over anhydrous Na_2SO_4 and the solvent evaporated under reduced pressure. The aqueous phase was evaporated and the obtained solid was merged to the crude. The crude was purified by preparative TLC using DCM/MeOH 9:1 as eluent. Yield 37%. ^{1}H NMR (400 MHz, CD_3OD) δ (ppm): 8.66 (1H, s, Triaz*H*); 8.47 (1H, s, Triaz*H*); 7.99-7.95 (3H, m, Ar$H_{meta,para}$); 4.64 (2H, t, J = 7.04 Hz, CH_2CH_2N); 3.65 (2H, t, J = 6 Hz, CH_2CH_2OH); 2.22 (2H, quint, J = 7 Hz, $CH_2CH_2CH_2$). ESI-MS: m/z 294.24 [100%; $(M+Na)^+$]; m/z 310.16 [6%; $(M+K)^+$]; m/z 565.33 [16%; $(2M+Na)^+$]; m/z 581.32 [7%; $(2M+K)^+$].

Eethyl-3-azidopropionate

Ethyl-3-bromopropionate (0.28 ml, 2.01 mmol) and NaN3 (0.19 g, 2.92 mmol) were dissolved in DMSO (8 ml). The mixture was stirred for 4 days at room temperature. The reaction was quenched with water and the aqueous layer extracted with diethyl ether. The combined organic phases were washed with a Na2CO3 aqueous solution then dried over anhydrous Na2SO4. The solvent was removed in vacuo to obtain the product as a yellowish oil. Yield: 92% 1H NMR (300 MHz, CDCl3) δ (ppm): 4.20 (2H, q, J = 8 Hz, COOCH2CH3); 3.59 (2H, t, J = 6 Hz, CH2CH2COO); 2.59 (2H, t, J = 6 Hz, N3CH2CH2); 1.30 (3H, t, J = 6 Hz, OCH_2CH_3).

2.4 References

(1) Bremer, A.; Ruff, C. M.; Girnt, D.; Müllich, U.; Rothe, J.; Roesky, P. W.; Panak, P. J.; Karpov, A.; Müller, T. J. J.; Denecke, M. A.; Geist, A. 2,6-Bis(5-(2,2-Dimethylpropyl)-1H-Pyrazol-3-Yl)Pyridine as a Ligand for Efficient Actinide(III)/Lanthanide(III) Separation. *Inorg. Chem.* **2012**, *51* (9), 5199–5207. https://doi.org/10.1021/ic3000526.

(2) Macerata, E.; Mossini, E.; Scaravaggi, S.; Mariani, M.; Mele, A.; Panzeri, W.; Boubals, N.; Berthon, L.; Charbonnel, M.-C.; Sansone, F.; Arduini, A.; Casnati, A. Hydrophilic

Clicked 2,6-Bis-Triazolyl-Pyridines Endowed with High Actinide Selectivity and Radiochemical Stability: Toward a Closed Nuclear Fuel Cycle. *J. Am. Chem. Soc.* **2016**, *138* (23), 7232–7235. https://doi.org/10.1021/jacs.6b03106.

(3) Wagner, C.; Mossini, E.; Macerata, E.; Mariani, M.; Arduini, A.; Casnati, A.; Geist, A.; Panak, P. J. Time-Resolved Laser Fluorescence Spectroscopy Study of the Coordination Chemistry of a Hydrophilic CHON [1,2,3-Triazol-4-Yl]Pyridine Ligand with Cm(III) and Eu(III). *Inorg. Chem.* **2017**, *56* (4), 2135–2144. https://doi.org/10.1021/acs.inorgchem.6b02788.

(4) Mossini, E. Novel I-SANEX/GANEX Formulation for Hydrometallurgical Actinide Separation from Spent Nuclear Fuel, Politecnico di Milano, 2016.

(5) Scaravaggi S. Selective Separation of Minor Actinides from Spent Nuclear Fuel in Homogeneous and Heterogeneous Recycling: Extraction Performances and Speciation Studies of CHON Hydrophilic Ligands, Politecnico di Milano, 2013.

(6) Quasucci N. Utilizzo Di Leganti Idrofili Piridinici Nei Processi Di Estrazione Selettiva Degli Attinidi, Politecnico di Milano, 2012.

(7) Ongari N. Partitioning Idrometallurgico Di Combustibile Nucleare Irraggiato: Stripping Selettivo Di An Mediante 2,6-Triazolil Piridina Idrosolubile, Politecnico di Milano.

(8) Mossini, E. Screening and Optimization of Nitrogen Ligands for the Actinides Separation from the Spent Nuclear Fuel in the I-SANEX Proces, Politecnico di Milano.

(9) Mossini, E.; Macerata, E.; Wilden, A.; Kaufholz, P.; Modolo, G.; Iotti, N.; Casnati, A.; Geist, A.; Mariani, M. Optimization and Single-Stage Centrifugal Contactor Experiments with the Novel Hydrophilic Complexant PyTri-Diol for the i-SANEX Process. *Solvent Extr. Ion Exch.* **2018**, *36* (4), 373–386. https://doi.org/10.1080/07366299.2018.1507134.

(10) Conrow, R. E.; Dean, W. D. Diazidomethane Explosion. *Org. Process Res. Dev.* **2008**, *12* (6), 1285–1286. https://doi.org/10.1021/op8000977.

(11) Kolb, H. C.; Finn, M. G.; Sharpless, K. B. Click Chemistry: Diverse Chemical Function from a Few Good Reactions. *Angew. Chemie Int. Ed.* **2001**, *40* (11), 2004–2021. https://doi.org/10.1002/1521-3773.

(12) Bräse, S.; Gil, C.; Knepper, K.; Zimmermann, V. Organic Azides: An Exploding Diversity of a Unique Class of Compounds. *Angew. Chemie Int. Ed.* **2005**, *44* (33), 5188–5240. https://doi.org/10.1002/anie.200400657.

(13) Richardson, M. B.; Brown, D. B.; Vasquez, C. A.; Ziller, J. W.; Johnston, K. M.; Weiss, G. A. Synthesis and Explosion Hazards of 4-Azido-1-Phenylalanine. *J. Org. Chem.* **2018**, *83* (8), 4525–4536. https://doi.org/10.1021/acs.joc.8b00270.

(14) Mincher, B. J.; Modolo, G.; Mezyk, S. P. Review Article: The Effects of Radiation Chemistry on Solvent Extraction: 1. Conditions in Acidic Solution and a Review of TBP Radiolysis. *Solvent Extr. Ion Exch.* **2009**, *27* (1), 1–25. https://doi.org/10.1080/07366290802544767.

(15) Mincher, B. J.; Modolo, G.; Mezyk, S. P. Review: The Effects of Radiation Chemistry on Solvent Extraction 4: Separation of the Trivalent Actinides and Considerations for Radiation-Resistant Solvent Systems. *Solvent Extr. Ion Exch.* **2010**, *28* (4), 415–436.

https://doi.org/10.1080/07366299.2010.485548.

(16) Bellagamba, M.; Bencivenni, L.; Gontrani, L.; Guidoni, L.; Sadun, C. Tautomerism in Liquid 1,2,3-Triazole: A Combined Energy-Dispersive X-Ray Diffraction, Molecular Dynamics, and FTIR Study. *Struct. Chem.* **2013**, *24* (3), 933–943. https://doi.org/10.1007/s11224-013-0206-4.

(17) Albert, A.; Taylor, P. J. The Tautomerism of 1,2,3-Triazole in Aqueous Solution. *J. Chem. Soc.{,} Perkin Trans. 2* **1989**, No. 11, 1903–1905. https://doi.org/10.1039/P29890001903.

(18) Antoni, P.; Hed, Y.; Nordberg, A.; Nyström, D.; von Holst, H.; Hult, A.; Malkoch, M. Bifunctional Dendrimers: From Robust Synthesis and Accelerated One-Pot Postfunctionalization Strategy to Potential Applications. *Angew. Chemie Int. Ed.* **2009**, *48* (12), 2126–2130. https://doi.org/10.1002/anie.200804987.

Chapter 3
Modified Hydrophilic Ligand for An Separation

3.1 Introduction

In the work presented by Macerata et al.,[1] the properties of the PTD have been largely described. Compared to its competitor, SO_3-Ph-BTP, PTD present several advantages: PTD is a CHON compound, shows a noticeable hydrolytic and radiolitic stability and has fast kinetics of stripping. On the other hand, PTD is less efficient and slightly less selective than SO_3-Ph-BTP. The experiments conducted by Wagner et al. in 2017[2] allow to assess the $\log\beta_3$ values for Cm(III)-PTD complexes and compare them with those found for Cm(III)- SO_3–Ph–BTP using the same a 10^{-3} M $HClO_4$ solution of a strong acid having a noncoordinating conjugate base. The observed value for PTD ($\log \beta_3$ = 9.7) is significantly lower than that of the water-soluble BTP ($\log \beta_3$ = 12.2) so that a higher concentration of PTD is required for the efficient and selective stripping of An(III) in biphasic extraction experiments compared to SO_3–Ph–BTP.[3] To further evaluate the properties of PTD, Cm(III) complexation in 0.44 M HNO_3 aqueous solution, and therefore closer to the conditions of the process, were also studied (Table 3.1).

Table 3.1. Conditional stability constants ($\log\beta_n$) for Cm(III) complexes with PTD at 0.44 M HNO_3 and 10^{-3} M $HClO_4$

Conditions	$\log\beta_1$	$\log\beta_2$	$\log\beta_3$
10^{-3} M $HClO_4$	3.2 ± 0.2	6.6 ± 0.2	9.7 ± 0.3
0.44 M HNO_3	1.7 ± 0.2	4.0 ± 0.2	5.7 ± 0.3

At higher acidic conditions (0.44 M HNO_3 *vs.* 10^{-3} M $HClO_4$) and in the presence of a more coordinating anion (NO_3^- *vs.* ClO_4^-) consistent decreases in the stability constant values were observed.

In order to study the effect of pH in the complexation properties of PTD, further titrations experiments were performed by Time-Resolved Laser Fluorescence Spectroscopy (TRLFS) in $HClO_4$ solutions. At 10^{-3} M $HClO_4$ concentration, all three $[Cm(PTD)_n]^{3+}$ (n = 1,2,3) complexes are observed. With the increasing of the $HClO_4$ concentration, the

Cm(III) emission spectra displays a strong decrease of the number of complexed Cm(III) species. At $HClO_4$ concentrations greater than 0.5 M, the Cm(III) aqua ion is the only observed species. These results demonstrate that the increase of the H^+ concentration in the solutions leads to a decrease of the conditional stability constants. This outcome is consistent with the difference of the conditional stability constants observed in 10^{-3} M $HClO_4$ and 0.44 M HNO_3 and emphasizes the strong influence of H^+ concentration in the complexation properties of the ligand.

In order to better evaluate the An selectivity of PTD over Ln, the complexation of Eu(III) in 0.44 M HNO_3 solution were also investigated. The observed $\log\beta_3$ value (3.7 ± 0.3) is lower than the Cm(III) value obtained at the same conditions (5.7 ± 0.3). This result confirms the An selectivity over Ln for PTD. As it is expected, due to the presence of relatively basic N atoms, the PTD efficiency in metal binding is strongly dependent on its attitude to be protonated which strongly influence its behavior and efficiency in the process conditions.[2]

In this chapter it will be described how, in order to enhance PTD complexation properties, a revised ligand has been designed and synthetized, PTD-OMe. The structure has been modified by adding a methoxy group in para position of the pyridine ring with the intention of increasing the electron density of the aromatic core and, consequently, of the pyridine N atom. According to our hypothesis, the presence of an electrondonating methoxy group in para to the pyridine N-atom should activate its basicity improving the metal ion complexation and therefore the An(III) extraction efficiency.[4]

For the same goal, similar structural modification on the aromatic core had already been explored on BTP and BTPhen ligands.[5,6,7]

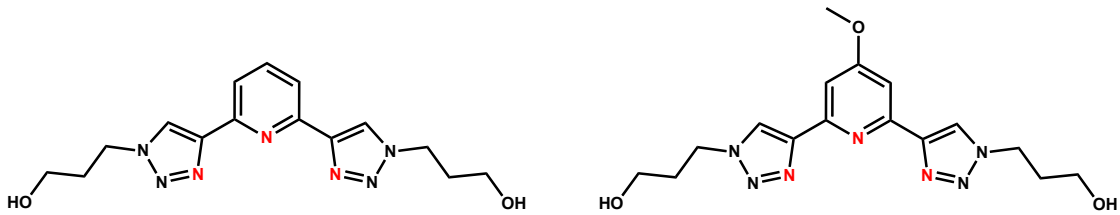

Figure 3.1. Structure of PTD (left) and PTD-OMe (right)

3.2 Results and discussion

In collaboration with Politecnico di Milano (POLIMI) and Karlsruhe Institute of Technology (KIT) PTD-OMe was studied using solvent extraction, time-resolved laser

fluorescence spectroscopy and ^{1}H NMR. It will be, herein, reported the most valuable data and experiments to characterise the extraction and complexation behavior of this novel PTD ligand. For more in depth details about solvent extraction experiments and TRLFS experiments, please refer to Annalisa Ossola's PhD thesis (POLIMI) and to our joint paper.[8]

3.2.1 Synthesis

The synthetic pathway followed for the preparation of the PTD-OMe is shown in Figure 3.2.

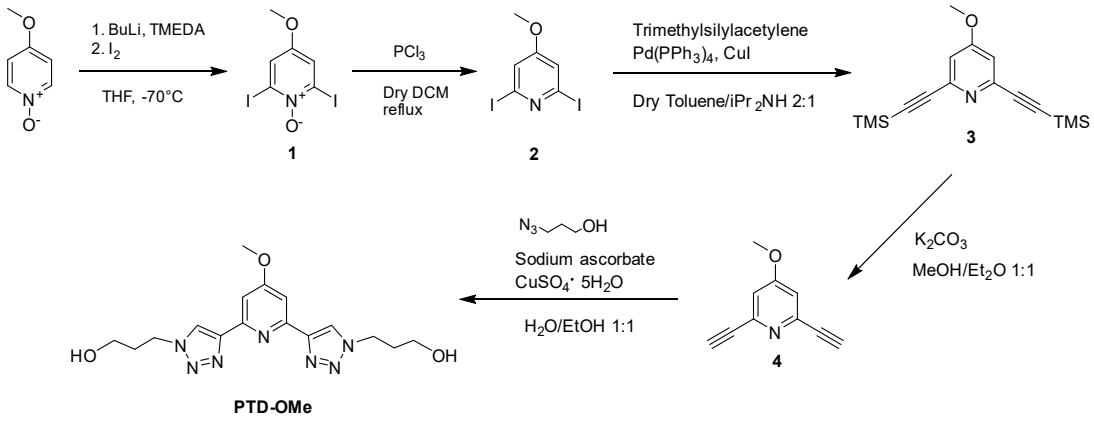

Figure 3.2. Synthesis of PTD-OMe

The target molecule has been synthetized similarly to PTD but being commercially not available a 2,6-dihalo-4-methoxypyridine such as 2, the 2,6-diiodo-4-methoxypyridine had to be synthesized starting from the commercially available 4-methoxypyridine 1-oxide used without further purification. Pyridine is a rather mild nucleophile and Iodine a rather weak electrophile so that iodine substitution needs to be activated by ortho-lithiation of the pyridine. The use of a pyridine N-oxide derivative was necessary in order to activate the pyridine ring, making the orto-lithiation faster. BuLi was added to a solution of TMEDA in THF cooled at -70 °C, whereupon the 4-methoxypyridine 1-oxide was added. Finally, a solution of I_2 in THF was added and the mixture stirred at -70 °C overnight. Intermediate 1 was obtained in 30% yield which is the lowest yield of the whole synthesis. The second step is needed in order to reduce the N-oxide by removing the oxygen from the N atom of the pyridine ring. We used PCl_3 as reducing agent and we obtained intermediate 2 in quantitative yield. For the synthesis of both intermediate 1 and 2 we adapted known literature procedures.9 4-methoxy-2,6-bis((trimethylsilyl)ethynyl) pyridine (3) was obtained by reaction of 2 with trimethylsilylacetylene through a classical Sonogashira coupling in a

very nice 92% yield. The trimethylsilyl protecting groups were subsequently removed following the standard procedure with potassium carbonate in methanol/diethyl ether 2:1 and the reaction was quantitative in roughly one hour. The NMR spectrum of compound 4 (Figure 3.3, above) shows the singlet related to the acetylene protons at 3.13 ppm and the absence of the singlet related to the TMS groups (see singlet at 0.25 ppm in Figure 3.3 below) indicating the complete conversion of the reagent into the desired product. 2,6-diethynyl-4-methoxypyridine (4) was reacted with 3-azidopropan-1-ol (synthetized as reported in chapter 2) under classical CuAAC reaction conditions with copper sulfate pentahydrate and sodium ascorbate.

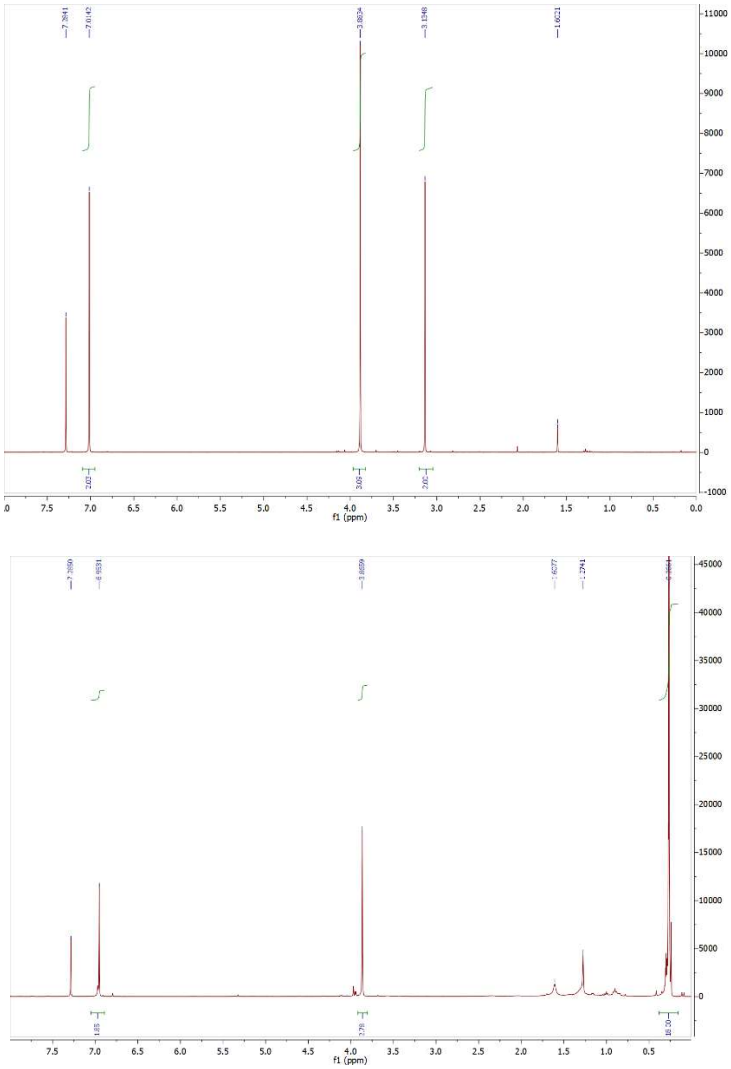

*Figure 3.3. ^{1}H NMR spectrum (CD_3OCl_3, 400 MHz) of compound **4** (above) and **3** (below)*

The NMR spectrum of PTD-OMe reflects it C_2 symmetry. We can observe at 8.57 and 7.53 the singlet related to the triazol protons and to the pyridine ring, respectively, and the diagnostic signal of the -OMe group at 4.00 ppm. The alkyl chains give rise to two triplets at 4.62 and 3.64 ppm related to the protons near the OH and near the N atom, respectively, and to the quintuplet at 2.2 ppm due to the central CH_2 protons.

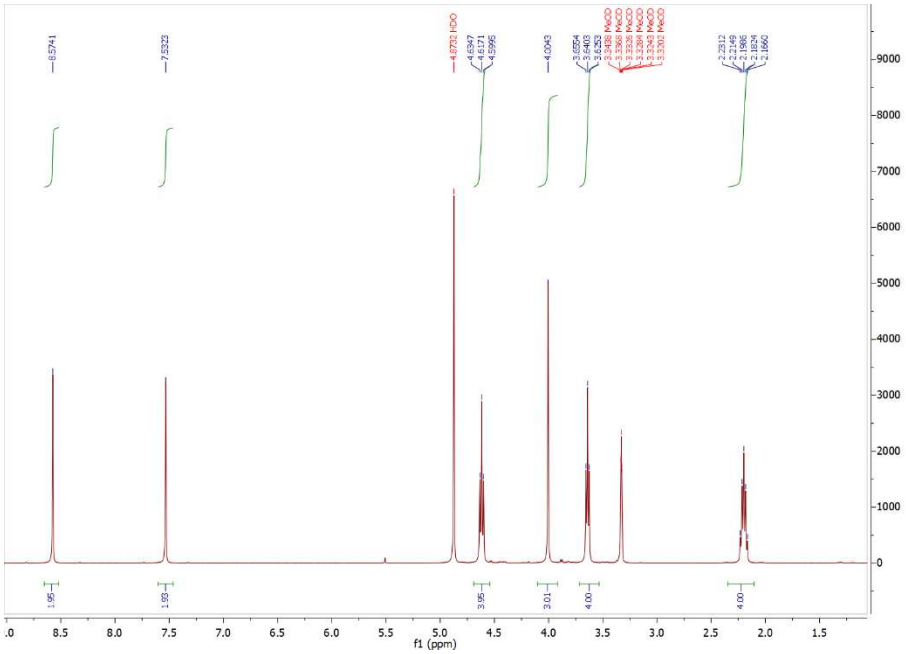

Figure 3.4. ^{1}H NMR spectrum (CD_3OD, 400 MHz) of PTD-OMe

3.2.2 Liquid-liquid extraction

The PTD-OMe affinity for trivalent An was studied trough liquid-liquid extraction tests. The insertion of an activating group on the central pyridine ring should increase the electron density of the core affecting the basicity of the ligand. Considering the high acid concentration present in the waste recovery plants it is valuable to study the effect of HNO_3 concentration on ligand extracting properties. Moreover, in order to compare the chelating behavior of PTD-OMe and PTD the liquid-liquid extraction tests were conducted taking as reference the optimal formulation for the selective extraction of PTD which is 0.08 M ligand in 0.44 M HNO_3. Therefore, the nitric acid concentration dependence of PTD-OMe has been studied operating at ligand constant concentration of 0.08 M. Am(III) and Eu(III) were used as representative of An(III) and Ln(III) metal ions, respectively. The composition of the organic phase was 0.2 mol/L

TODGA in TPH/1-octanol (5 vol %) and the one of the aqueous phases was 0.08 mol/L PTD-OMe or PTD in HNO_3.

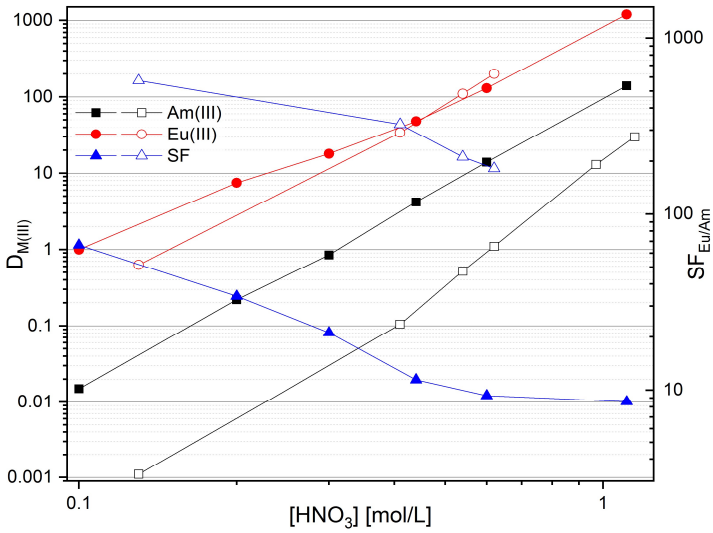

Figure 3.5. Distribution ratios for the extraction of Am(III) and Eu(III) with TODGA/PTD-OMe (solid symbols) and TODGA/PTD (open symbols)

In Figure 3.5 it is possible to compare the distribution ratios and the separation factors for the systems TODGA/PTD (open symbols) and TODGA/PTD-OMe (solid symbols). Considering the formula $D_{M(III)} = [M(III)_{org}]/[M(III)_{aq}]$, Am(III)/Eu(III) separation is achieved for $D_{Am(III)} < 1$ and $D_{Eu(III)} > 1$. Separation factors are calculated as following $SF_{Eu/Am} = D_{Eu(III)}/D_{Am(III)}$. Both ligands showed a similar extraction efficiency for Eu(III) (red lines), especially at $[HNO_3] > 0.3$ confirming that Eu(III) has little affinity for the PTD ligands and prefers to remain in the organic phase complexed to TODGA. The collected data highlight that PTD-OMe is less efficient than PTD in An(III) back extraction into the aqueous phase in the whole $[HNO_3]$ explored. This obviously strongly affects also the separation factors which indeed decrease. The only $[HNO_3]$ at which PTD-OMe could be operative is around 0.2 M, where Am(III) prefers to stay in the aqueous while Eu(III) in the organic (but with a low value od D_{Eu}). At $[HNO_3]$ of 0.1 (and presumably lower), both Eu(III) and Am(III) stay in the water layer, while at $[HNO_3] > 0.3$ both Eu(III) and Am(III) prefers the organic layer with extremely low SF. We have therefore to conclude that, contrary to expectations, PTD-OMe is less efficient and less selective than PTD and that the presence of an electron-donating MeO- group in para position to the pyridine N atom impairs the separation of An(III) from Ln(III).

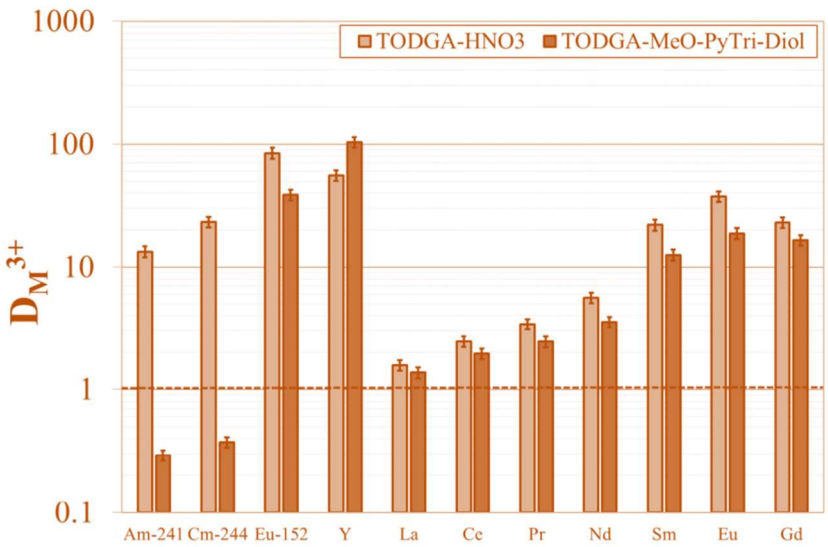

Figure 3.6. Distribution ratios of trivalent ^{241}Am, ^{244}Cm, ^{152}Eu, Y and lighter Ln (La-Gd) obtained with stripping aqueous phases without and with MeO-PyTri-Diol (0.1 M HNO_3 + 0.68 NH_4NO_3).

To further evaluate the PTD-OMe selectivity for trivalent actinides towards trivalent lanthanides, liquid-liquid extractions tests were performed. In order to simulate the PUREX raffinate composition, the aqueous phase was spiked with ^{241}Am, ^{244}Cm, ^{152}Eu and different amounts of other trivalent lanthanides, from lanthanum to gadolinium, for a total concentration of 0.02 M. The organic phase conditions were 0.2 M TODGA in kerosene + 5 vol.% 1-octanol. The aqueous phase conditions were 0.1 M HNO_3 + 0.68 NH_4NO_3 solution (light brown, Figure 3.6) and 0.08 M MeO-PyTri-Diol in 0.1 M HNO_3 + 0.68 NH_4NO_3 solution (darker brown, Figure 3.6). The distribution ratios of Y and all the observed Ln (including ^{152}Eu) were not affected significantly by the presence of PTD-OMe in the aqueous phase. On the contrary, in presence of the water soluble ligand the distribution ratios of Am and Cm decrease below one. These tests demonstrate that PTD-OMe is able to tear An(III) from TODGA and to complex it in slightly acidic water solution, at least under these specific conditions (0.1 M HNO_3 + 0.68 NH_4NO_3) while Ln(III) prefer to remain bound to the glycolamide ligand in the organic phase. This experiment also supports the hypothesis that the ligand lower efficiency is not probably due to a lower An affinity but, probably, to a higher proton affinity (basicity) compared to PTD.

3.2.3 NMR studies

In order to better compare the extraction properties of PTD and PTD-OMe the determination of the pKa value of PTD-OMe was necessary. The pKa value was determined by evaluating the shifts of its ^{1}H NMR signals as a function of measured pH. The protonation of the ligand due to the pH decrease determines a downfield shift in the ^{1}H NMR signals only observable in the pH range 4.02 – 1.25.

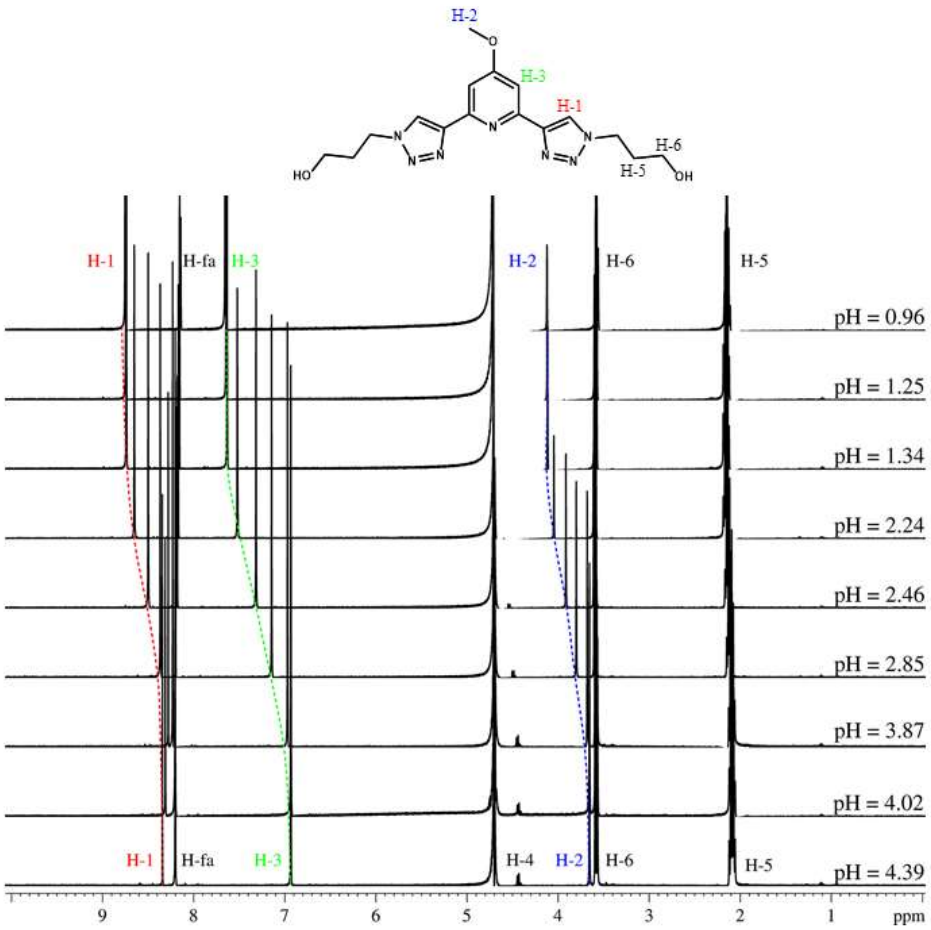

Figure 3.7. ^{1}H NMR spectra of PTD-OMe in formic acid/formate (H-fa) buffer with 10 vol % D_2O at varied pH. The water signal at δ = 4.702 ppm was suppressed using the WATERGATE technique

Beyond this range no shift is noticeable thus indicating the existence of only the protonated (pH = 0.96, Figure 3.7) or unprotonated (pH = 4.39, Figure 3.7) ligand. In 1.25 – 3.87 pH range both protonated and unprotonated species are present but only one set of

signals is observed indicating a fast proton exchange. Therefore, the average of signals of the two species is detected and used for determining the pKa values.

The relative peak shifts for all protons of PTD-OMe are shown in Figure 3.8. Shifts of the protons of the propanol chains (H-4, H-5 and H-6) are negligible while the strongest shifts are detected for the pyridine protons (H-3, $\Delta\delta_{max}$ = 0.725 ppm), followed by the triazole proton (H-1, $\Delta\delta_{max}$ = 0.552 ppm) and the methoxy protons (H-2, $\Delta\delta_{max}$ = 0.470 ppm). The large shifts of the aromatic protons and especially of the pyridine protons indicate that the protonation occurs in the aromatic region, most probably at the pyridine N atom. To estimate the pKa value, the Henderson-Hasselbalch equation below was used.

$$\mathrm{Log}\left(\frac{[LH_n^{n+}]}{[L]}\right) = -n \times pH + pKa \qquad \textit{eq. 1}$$

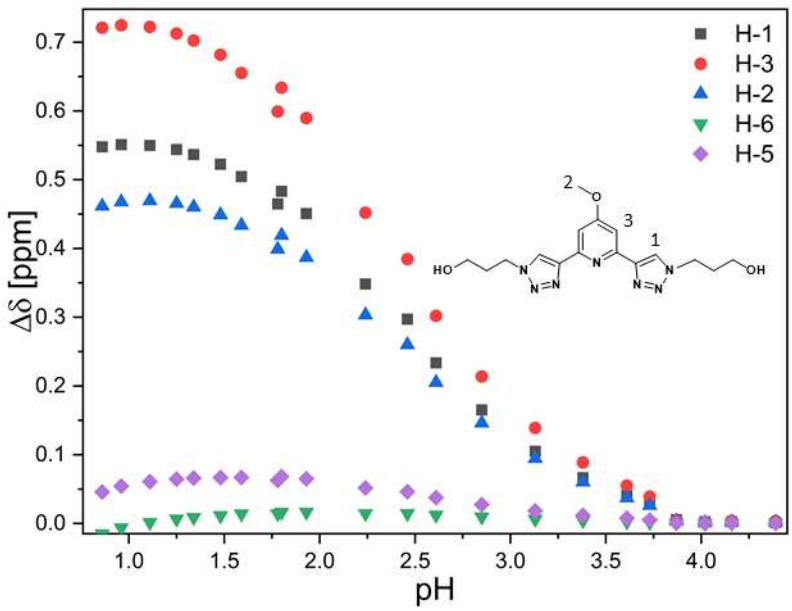

Figure 3.8. Shift of the ^1H signals in respect to the ^1H shift of the unprotonated PTD-OMe as a function of pH.

The relative species concentrations were calculated with equation 2 using proton signals H-1, H-2, and H-3 individually.

$$X = \frac{\Delta\delta i}{\Delta\delta max} \qquad \text{eq. 2}$$

Where X is the molar fraction of protonated ligand at the i-th point, while Δδi is the difference between the chemical shift observed at the i-th point and the chemical shift of the free ligand and Δδmax is the maximum shift observed.

The average pKa value, derived from the shifts of H-1, H-2 and H-3, of PTD-OMe is 2.54 ± 0.08. As expected, the presence of an electron-donating group increases the basicity of the core compared to PTD (pKa value = 2.1).[1]

Table 3.2. pKa values of the protonated PTD-OMe

Proton	pKa
H-1	2.55 ± 0.05
H-2	2.51 ± 0.03
H-3	2.57 ± 0.06

The comparison of the pKa of both PTD and PTD-OMe demonstrates that the latter one is more easily protonated. In the acidic conditions used in the extraction experiments (0.44 M HNO_3), compared to PTD, PTD-OMe is more protonated and therefore the lower stripping abilities shown by this ligand are also due to a lower concentration of the free unprotonated species.

3.2.4 Complexation studies with TRLFS

TRLFS experiments performed at KIT allowed to determine stability constants and speciation in solution of the Cm(III)–PTD-OMe complexes.

In Figure 3.9 Cm(III) fluorescence spectra as a function of PTD or PTD-OMe concentration are shown. Cm(III) was chosen as representative for An(III) because of its high fluorescence properties.

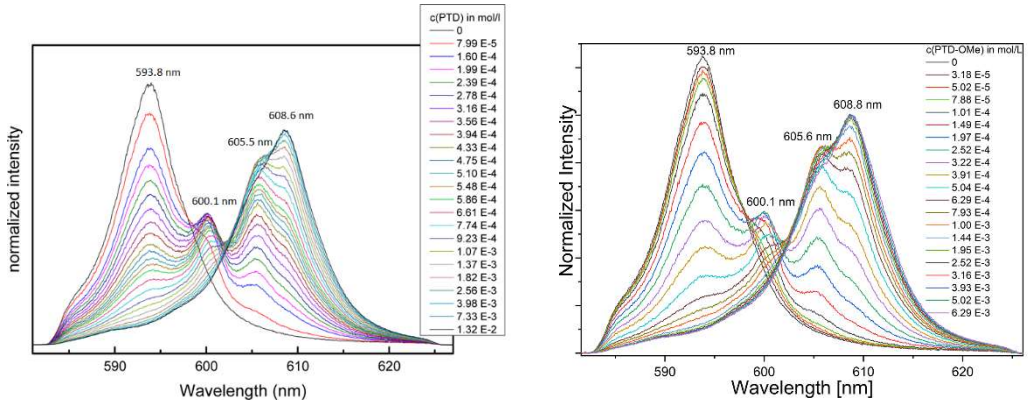

Figure 3.9. Normalized Cm(III) emission spectra in 1 × 10^{-3} M $HClO_4$ with increasing PTD (left) and PTD-OMe (right) concentrations

PTD-OMe emission bands are in agreement with those of $Cm(PTD)_n$ complexes.[2] Therefore it is possible to attribute 593.8 nm bands to Cm(III) aqua ion and 600.1 nm, 605.6 nm, 608.8 nm bands to $Cm(PTD\text{-}OMe)_1$, $Cm(PTD\text{-}OMe)_2$, $Cm(PTD\text{-}OMe)_3$ respectively.

The species distribution of the complexes as a function of the free ligand concentration were obtained analyzing the normalized spectra of the titration experiments obtained using the spectra of the pure components as described in ref 2.

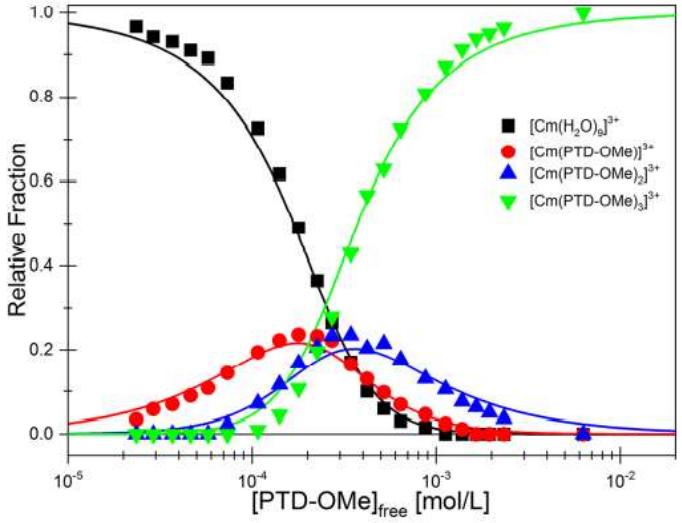

Figure 3.10. Cm(III) species distribution in 1 × 10^{-3} M $HClO_4$ as a function of the free PTD-OMe concentration.

The formation of the 1:1 complex starts at 10^{-5} ligand concentration with a maximum of 23 % at 2.5 x 10^{-4} M. The 1:2 complex has a maximum fraction of 26% at 5.3 × 10^{-4} M ligand

concentration. The 1:3 complex becomes the dominating species for PTD-OMe concentrations greater than 3.5×10^{-4} M. As for PTD (Chapter 2) the conditional stability constants for the formation of Cm(III)−PTD-OMe complexes were calculated according to:

$\log\beta = [M(PTD\text{-}OMe)_n]^{3+} / [M]^{3+} \cdot [PTD\text{-}OMe]^{n}_{free}$.

Table 3.3. Conditional stability constants of the $[Cm(PTD\text{-}OMe)n]^{3+}$ and $[Cm(PTD)n]^{3+}$ complexes, 1×10^{-3} mol/L $HClO_4$

	$Log\beta_1$	$Log\beta_2$	$Log\beta_3$	pKa
PTD	3.2 ± 0.2	6.8 ± 0.2	9.9 ± 0.5	2.1
PTD-OMe	3.4 ± 0.3	7.0 ± 0.4	10.8 ± 0.4	2.54

A comparison of the conditional stability constants and pKa values of PTD-OMe and PTD is given in Table 3.3. This higher basicity of PTD-OMe increases conditional stability constants compared to PTD, at these low acid concentrations. Stability constants for the 1:1 and 1:2 complexes are less influenced by the electron-donating -OMe substituent, while the conditional stability constant of the Cm(III) 1:3 complex is almost 0.9 order of magnitude higher for the activated ligand. The higher pKa value of PTD-OMe confirms the increased basicity of the ligand due to the presence of -OMe group on the pyridine ring and the higher stability constants at low acidic concentrations. Higher basicity determines however higher inclination to protonation at high acid concentrations and therefore a greater competition between ligand protonation and metal ion complexation is present. In this sense the higher basicity explains the lower performance of PTD-OMe in extraction tests. Indeed, due to the acidic conditions used in the extraction experiments (0.44 M HNO_3) the free ligand concentration decreases. As a result, the concentration of unprotonated ligand is lower compared to that of PTD thus determining higher value of Am(III) distribution ratios.

The positive effect of methoxy substitution is confirmed by the higher stability constants values observed for PTD-OMe. As hypothesized the activation of the aromatic core made PTD-OMe a stronger ligand. At the same time the increased susceptibility to protonation decreases PTD-OMe performances in the high acidic solvent extraction conditions (0.44 M HNO_3).

3.3 Experimental

3.3.1 General methods and chemicals

Reagents and solvents

All commercially available chemicals (Sigma-Aldrich, TCI, ChemPur, VWR) used in this study were analytical reagent grade and were used without further purification. All air sensitive reactions were carried out under nitrogen atmosphere using oven-dried glassware. All dry solvents were prepared according to standard procedures and stored over 3 or 4 Å molecular sieves.

Instrumentation, techniques, and common procedures

^{1}H NMR and ^{13}C NMR spectra were recorded on Bruker AV300 and AV400 or JEOL ECZ600R spectrometers (observation of ^{1}H at 300 MHz, 400 MHz and 600 MHz and of ^{13}C at 75 MHz, 100 MHz or 150 MHz). Partially deuterated solvents were used as internal standards to calculate the chemical shifts (δ values in ppm) and J coupling constants are given in Hz. All ^{13}C NMR spectra were performed with proton decoupling. The used abbreviations in these spectra are singlet (s), doublet (d), triplet (t), quadruplet (q), quintuplet (quint) and multiplet (m).

In order to monitor the progress of reactions, aluminum sheets covered with silica gel 60 F-254 provided by Merck were used. All aluminum sheets were revealed under an ultraviolet lamp (λ= 254 nm) or using staining reagents. Merck silica gel 60 was used for flash chromatography (40-63 μm) and for preparative TLC plates 20x20cm (10-12 μm).

Electrospray ionization (ESI) mass analysis were performed on a Waters single- quadrupole instrument SQ Detector in positive mode using MeOH or CH_3CN as solvents. HR-MS spectra were registered by Dr. Andrea Faccini at "Centro Interdipartimentale Misure" of Università di Parma with an LTQ ORBITRAP XL Thermo instrument in positive mode using MeOH or CH_3CN as solvents.

Melting points were determined on an Electrothermal apparatus in capillaries sealed under nitrogen.

Solvent Extraction.

Organic phase was 0.2 mol/L N,N,N′,N′-tetra-n-octyl-3-oxapentanediamide (TODGA) + 5 vol % 1-octanol in kerosene. Aqueous phase was 80 mmol/L PTD or PTDOMe in HNO_3 (varied concentration) spiked with each 2.5 kBq/mL ^{241}Am(III) and ^{154}Eu(III).

Each 300 μL of aqueous and organic phases were placed in 2 mL Eppendorf tubes and shaken on an orbital shaker for 60 min at 1100 rpm and 295 K. Following centrifugation for 10 min at 1000 rpm, 200 μL aliquots of both phases were analyzed on a gamma counter (Packard Cobra Auto-Gamma 5003).

TRLFS Sample Preparation.

Stock solutions containing 0.5 mol/ L PTD-OMe were prepared by dissolving 50.3 mg of PTD-OMe in 280 μL of 1 × 10−3 mol/L $HClO_4$ or 0.44 mol/L HNO_3. Solutions with lower PTD-OMe concentrations were prepared by dilution with 1 × 10−3 mol/L $HClO_4$ or 0.44 mol/L HNO_3, respectively. TRLFS samples were prepared by adding 4.7 μL of a Cm(III) stock solution (2.12 × 10−5 mol/L $Cm(ClO_4)_3$ in 0.1 mol/L $HClO_4$; ^{248}Cm: 89.7%, ^{246}Cm: 9.4%, ^{243}Cm: 0.4%, ^{244}Cm: 0.3%, ^{245}Cm: 0.1%, ^{247}Cm: 0.1%) to 995.3 μL of 1 × 10^{-3} mol/L $HClO_4$ or 0.44 mol/L HNO_3, resulting in an initial Cm(III) concentration of 1 × 10−7 mol/ L. Ligand concentration was adjusted by adding appropriate volumes of the PTD-OMe solutions. TRLFS spectra were recorded following an equilibration time of 10 min. Preliminary tests showed this to be enough to attain equilibrium. Solvent extraction samples for TRLFS measurements were prepared as described in *Solvent Extraction*, with the exception that samples were 500 μL per phase each spiked with 4.7 μL of the Cm(III) stock solution instead of ^{241}Am and ^{154}Eu. TRLFS Measurements. TRLFS measurements were performed at 298 K using a Nd:YAG (Surelite II laser, Continuum) pumped dye laser system (NarrowScan D-R; Radiant Dyes Laser Accessories GmbH). A wavelength of 396.6 nm was chosen to excite Cm(III). A spectrograph (Shamrock 303i, ANDOR) with 300, 1199, and 2400 lines per millimeter gratings was used for spectral decomposition. The fluorescence emission was detected by an ICCD camera (iStar Gen III, ANDOR) after a delay time of 1 μs to discriminate short-lived, organic fluorescence, and light scattering.

NMR Sample Preparation.

NMR samples for pKa determination contained initially 9 × 10−3 mol/L PTD-OMe in an aqueous formic acid/formate buffer containing 10 vol.% of D_2O. pH was measured with a microelectrode (Orion PerpHecT ROSS, Thermo Fisher Scientific) and a pH meter (Orion Star, Thermo Fisher Scientific) before and after NMR measurement. The pH was adjusted with 1, 0.1, or 0.01 mol/L HCl or NaOH solutions.

3.3.2 Synthesis

3-Azidopropan-1-ol

Prepared according to the procedure described in Chapter 2.

2,6-diiodo-4-methoxypyridine 1-oxide (1)

Prepared according to literature procedure[9] from 4-methoxypyridine 1-oxide in 30% yield. To a solution of dry THF (0.25 l) and TMEDA (15.4 ml) BuLi (63 ml) was added at -70 C°. After 20 min, 4-methoxypyridine 1-oxide (3.0 g, 23.98 mmol) was added. The reaction was stirred for five hours then a mixture of I_2 in THF (29.8 g in 0.2 l) was added. The mixture was stirred for 24 hours at – 70 °C then was quenched with a 0.5 M $Na_2S_2O_3$ aqueous solution (0.4 l). The aqueous layer was extracted three times with AcOEt whereupon the combined organic phases were washed twice with 0.5 M $Na_2S_2O_3$ aqueous solution and dried over anhydrous Na_2SO_4. The solvent was evaporated under vacuum to obtain a light brown solid. The crude was purified by crystallization from MeOH. Yield: 30% ^{1}H NMR (400 MHz, CD_3OD): δ 7.75 (2H, s, Py$H_{3,5}$), 3.90 (3H, s, Py-OCH_3).

2,6-diiodo-4-methoxypyridine (2)

Prepared according to literature procedure[9] from 4-methoxypyridine 1-oxide in 90% yield. 2,6-diiodo-4-methoxypyridine 1-oxide (0.65 g, 1.7 mmol) was dissolved in dry DCM (20 ml) then PCl_3 (0.45 ml, 5.2 mmol) was added. The reaction was heated up to reflux and stirred for 24 hours. The reaction mixture was quenched with ice. The aqueous layer was extracted with DCM then the combined organic phases were dried over anhydrous Na_2SO_4 and the solvent removed under vacuum. ^{1}H NMR (300 MHz, CD_3OD): δ 7.42 (2H, s, Py$H_{3,5}$), 3.86 (3H, s, Py-OCH_3).

4-methoxy-2,6-bis((trimethylsilyl)ethynyl) pyridine (3)

2,6-diiodo-4-methoxypyridine (1.30 g, 3.6 mmol) was dissolved in a dry mixture of toluene and diisopropylamine 2:1 (150 ml) under inert atmosphere. Then CuI (27.4 mg, 0.04 eq), $Pd(PPh_3)_4$ (83.2 mg, 0.02 eq), trimethylsilylacetylene (0.79, 2.25 eq) were added and the reaction mixture was stirred at room temperature for 24 h. The reaction was quenched with water and the aqueous phase extracted with AcOEt. The combined organic phases were dried over anhydrous sodium sulfate and the solvent evaporated under reduced pressure. The residue was purified by flash column chromatography using hexane/AcOEt 8.5:1.5 as eluent. Yield: 92% ^{1}H NMR (400 MHz, $CDCl_3$): δ 6.95

(2H, s, Py$H_{3,5}$), 3.87 (3H, s, Py-OCH_3), 0.27 (18H, s, Si(CH_3)$_3$). ^{13}C NMR (100 MHz, $CDCl_3$): δ 165.7, 144.4, 113.2, 103.2, 94.8, 55.5, 0.3. HR-MS (ESI+) *m*/*z* $[M + H]^+$ Calcd for $C_{16}H_{24}NOSi_2$ 302.1391; Found 302.1392. mp: 64-66 °C.

2,6-diethynyl-4-methoxypyridine (4)

4-methoxy-2,6-bis((trimethylsilyl)ethynyl) pyridine (1.0 g, 3.32) was dissolved in 70 ml of a mixture of MeOH/Et_2O 2:1 then K_2CO_3 (2.3 g, 16.64 mmol) was added. The reaction mixture was stirred for one hour and then quenched with water. The aqueous layer was extracted three times with AcOEt. The combined organic phases are dried over anhydrous Na_2SO_4 then the solvent removed under reduced pressure to obtain the product as a brownish solid in 88% yield. ^{1}H NMR (400 MHz, $CDCl_3$): δ 7.01 (2H, s, Py$H_{3,5}$), 3.88 (3H, s, Py-OCH_3), 3.13 (2H, s, CCH). ^{13}C NMR (100 MHz, $CDCl_3$): δ 165.8, 143.7, 113.7, 82.1, 77.3, 55.6. HR-MS (ESI+) *m*/*z* $[M + H]^+$ Calcd for $C_{10}H_8NO$ 158.0600; Found 158.0601. mp: 140 °C.

PTD-OMe

2,6-diethynyl-4-methoxypyridine (0.25 g, 1.59 mmol) and 1-azido-3-propanol (0.52 g, 5.2 mmol) were dissolved in a mixture of water and ethanol 1:1. Then $CuSO_4 \cdot 5H_2O$ (0.03 eq) and sodium ascorbate (0.3 eq) were added. The reaction mixture was stirred for 3 days then quenched by removing the solvents under reduced pressure. The residue was purified by flash column chromatography using dichloromethane/methanol 92/8 as eluent to obtain the product as a white solid in 57% yield. ^{1}H NMR (400 MHz, CD_3OD): δ 8.57 (2H, s, Triaz-H), 7.53 (2H, s, Py$H_{3,5}$), 4.62 (4H, t, J = 7.2 Hz, CH_2N), 4.00 (3H, s, Py-OCH_3), 3.64 (4H, t, J = 6.0 Hz, CH_2OH), 2.20 (4H, quint, J = 6.4 Hz, CH_2CH_2N). ^{13}C NMR (100 MHz, CD_3OD): δ 167.6, 151.3, 147.6, 123.6, 104.7, 57.9, 54.8, 47.09, 32.6. ESI-MS: m/z (100%): 360.4 $[(M+H)]^+$ (66.84), 382.3 $[(M+Na)]^+$ (100), 398.2 $[(M+K)]^+$ (24.7), 558.9 [(M+Na ascorbate)]$^+$ (6.22), 741.5 $[(2M+Na)]^+$ (10). HR-MS (ESI+) *m*/*z* $[M + H]^+$ Calcd for $C_{16}H_{22}N_7O_3$ 360.1779; Found 360.1786. mp: 118-120 °C.

3.4 References

(1) Macerata, E.; Mossini, E.; Scaravaggi, S.; Mariani, M.; Mele, A.; Panzeri, W.; Boubals, N.; Berthon, L.; Charbonnel, M.-C.; Sansone, F.; Arduini, A.; Casnati, A. Hydrophilic Clicked 2,6-Bis-Triazolyl-Pyridines Endowed with High Actinide Selectivity and Radiochemical Stability: Toward a Closed Nuclear Fuel Cycle. *J. Am. Chem. Soc.* **2016**, *138* (23), 7232–7235. https://doi.org/10.1021/jacs.6b03106.

(2) Wagner, C.; Mossini, E.; Macerata, E.; Mariani, M.; Arduini, A.; Casnati, A.; Geist, A.;

Panak, P. J. Time-Resolved Laser Fluorescence Spectroscopy Study of the Coordination Chemistry of a Hydrophilic CHON [1,2,3-Triazol-4-Yl]Pyridine Ligand with Cm(III) and Eu(III). *Inorg. Chem.* **2017**, *56* (4), 2135–2144. https://doi.org/10.1021/acs.inorgchem.6b02788.

(3) Geist, A.; Müllich, U.; Magnusson, D.; Kaden, P.; Modolo, G.; Wilden, A.; Zevaco, T. Actinide(III)/Lanthanide(III) Separation Via Selective Aqueous Complexation of Actinides(III) Using a Hydrophilic 2,6-Bis(1,2,4-Triazin-3-Yl)-Pyridine in Nitric Acid. *Solvent Extr. Ion Exch.* **2012**, *30* (5), 433–444. https://doi.org/10.1080/07366299.2012.671111.

(4) Acids, I.; Acids, I.; Acids, C.; Acids, C. D.H. Ripin, D.A. Evans. *Heterocycles*.

(5) Trumm, S.; Wipff, G.; Geist, A.; Panak, P.; Fanghaenel, T. Optimising BTP Ligands by Tuning Their Basicity. *Radiochim. Acta* **2011**, *99*, 13–16. https://doi.org/10.1524/ract.2011.1794.

(6) Afsar, A.; Laventine, D. M.; Harwood, L. M.; Hudson, M. J.; Geist, A. Utilizing Electronic Effects in the Modulation of BTPhen Ligands with Respect to the Partitioning of Minor Actinides from Lanthanides. *Chem. Commun.* **2013**, *49* (76), 8534–8536. https://doi.org/10.1039/C3CC45126G.

(7) Edwards, A. C.; Wagner, C.; Geist, A.; Burton, N. A.; Sharrad, C. A.; Adams, R. W.; Pritchard, R. G.; Panak, P. J.; Whitehead, R. C.; Harwood, L. M. Exploring Electronic Effects on the Partitioning of Actinides(III) from Lanthanides(III) Using Functionalised Bis-Triazinyl Phenanthroline Ligands. *Dalt. Trans.* **2016**, *45* (45), 18102–18112. https://doi.org/10.1039/c6dt02474b.

(8) Weßling, P.; Trumm, M.; Macerata, E.; Ossola, A.; Mossini, E.; Gullo, M. C.; Arduini, A.; Casnati, A.; Mariani, M.; Adam, C.; Geist, A.; Panak, P. J. Activation of the Aromatic Core of 3,3′-(Pyridine-2,6-Diylbis(1 H-1,2,3-Triazole-4,1-Diyl))Bis(Propan-1-Ol) - Effects on Extraction Performance, Stability Constants, and Basicity. *Inorg. Chem.* **2019**, *58* (21). https://doi.org/10.1021/acs.inorgchem.9b02325.

(9) Mongin, F.; Trécourt, F.; Gervais, B.; Mongin, O.; Quéguiner, G.; Que, G. First Synthesis of Caerulomycin B. A New Synthesis of Caerulomycin C. *J. Org. Chem.* **2002**, *67* (10), 3272–3276. https://doi.org/10.1021/jo010913r.

Chapter 4
Lipophilic Ligands for Selective An Separation

4.1 Introduction

As reported in the introductory chapter of this thesis, the SANEX process is the base of the European proposed strategy for the selective recovery of trivalent actinide. In recent years the SANEX has been widely studied in the frame of different European projects leading to the development of r-SANEX, i-SANEX and 1c-SANEX processes. Chapter 2 and 3 of this thesis were mainly focused on the progress in the field of hydrophilic ligands to be used in the i-SANEX, and EURO-GANEX processes. These technologies indeed, rely on the use of selective water-soluble ligands which can selectively extract An(III) from an organic phase containing An(III) and Ln(III) previously co-extracted by a lipophilic unselective ligand. Conversely, this chapter will be centered on the improvement of r-SANEX and 1c-SANEX processes. The regular SANEX technology is performed after an An(III) and Ln(III) co-extraction carried out through an independent DIAMEX/TODGA process. The raffinate downstream of DIAMEX containing trivalent An and Ln in HNO_3 aqueous solution is contacted with an organic phase consisting of a An(III) selective lipophilic ligand. A valuable improvement in the field of actinides separation is represented by the 1 cycle SANEX. The extraction of An(III) indeed takes place directly from the PUREX raffinate completely suppressing the previous coextraction step. In this circumstance, the PUREX raffinate containing trivalent An and Ln together with other fission products in acidic solution, is contacted with an organic phase consisting of an actinide selective lipophilic ligand. The current reference molecule of GENIORS for actinide separation in organic solvent is CyMe4-BTBP.[1]

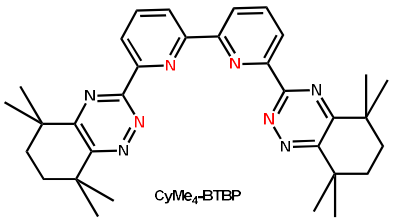

Figure 4.1. Chemical structure of CyMe$_4$-BTBP

Several different heterocycle N-donor ligands have been investigated to perform the An separation and among all the CyMe$_4$-BTBP showed the best radiolytic and hydrolytic stability together with interesting extraction properties.[2,3] The efficiency of this BTBP extractant has been successfully demonstrated by Magnusson et al. in 2009.[4] The used organic solvent was 0.015 M CyMe$_4$-BTBP + 0.25 M DMDOHEMA in n-octanol. The addition of a malonamide was necessary in order to increase the solubility of the heterocyclic ligand. Solubility indeed, is the main problematic issue related to the employ of lipophilic selective extractants. The SANEX feed (An + Ln) is 2 M HNO_3. This process enables the recovery of about 99.9 % of all the trivalent actinides present in solution showing also an excellent separation from Ln(III). Nevertheless, the limited loading capacity of the organic phase would be a drawback in the treatment of wastes at industrial scale.

Considering the remarkable results obtained employing the 2,6-bis(1,2,3-triazol-4-yl)pyridine, PyTri, chelating unit for the development of selective hydrophilic ligands, a lipophilic counterpart, BTTP (Figure 4.2) was recently proposed as an alternative to CyMe$_4$-BTBP.[5]

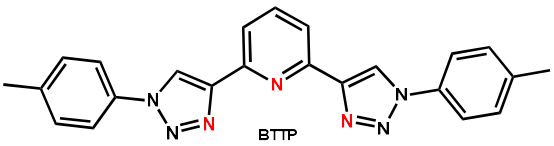

Figure 4.2. Chemical structure of 2,6-bis(1-(p-tolyl)-1H-1,2,3-triazol-4-yl)pyridine

In order to study the complexation performance of BTTP, TRLFS studies were conducted. Cm(III) and Eu(III) were selected as representative of trivalent An and Ln respectively. Table 4.1 shows the conditional stability constants for the formation of Cm(III) and Eu(III) BTTP complexes in ACN 5.0 vol % H_2O.

Table 4.1. Conditional stability constants for the formation of [Cm(BTTP)n] and [Eu(BTTP)n] (n =1–3)

Metal Ion	Logβ_1	Logβ_2	Logβ_3
Cm(III)		9.7 ± 0.2	14.0 ± 0.3
Eu(III)	2.8 ± 0.1		10.3 ± 0.2

In good agreement with the results obtained with PTD, the formation of the 1:3 Cm(III) complex with BTTP is favored compared to the 1:3 Eu(III) one. The stoichiometry of the species which appeared during fluorescence tritration were determined by slope analysis and conrespond to the 1:2 and 1:3 complexes for Cm(III) and to the 1:1 and 1:3 complexes for Eu(III). The difference in the determined logβ_3 values for Cm(III) and Eu(III) reflects the established selectivity of the hydrophilic 2,6-bis(1,2,3-triazol-4-yl)pyridine chelating unit found in aqueous solutions for An over Ln.[6,7] In order to evaluate the extraction selectivity and efficiency, liquid-liquid extraction tests were also performed with BTTP. Unfortunately, no extraction of Am(III) or Eu(III) into the organic phase was observed when using BTTP in 1-octanol with or without the presence of a lipophilic coadjuvant such as 2-bromodecanoic acid. Distribution ratios for both Am(III) and Eu(III) were indeed always below 0.001, meaning that less than 0.1% of the respective metal ions was extracted into the organic phase. The discrepancy between the high stability constants of BTTP in acetonitrile and its extraction behavior in biphasic octanol/water systems was hypothesized to be due to the strong solvation of metal ions by water molecules and therefore to the inability of BTTP to efficiently dehydrate and complex trivalent metal cations.

With the hypothesis that these poor extraction results obtained are also originated by the low solubility and compatibility of BTTP with the diluents used and considering the high selectivity previously demonstrated by the PyTri chelating units, PTD and PTD-OMe, even in water we have developed a series of N_3-core-based lipophilic ligands. The ligands were obtained by modifying the lateral substituents with alkyl chains (linear or branched) of different length (Figure 4.3) in order to increase their solubility in organic solvent, and especially in the preferred kerosene diluent. These ligands could hopefully also represent a solution to overcome the problems highlighted for the reference CyMe$_4$-BTBP ligand such as low solubility, slow kinetics and limited loading capability.

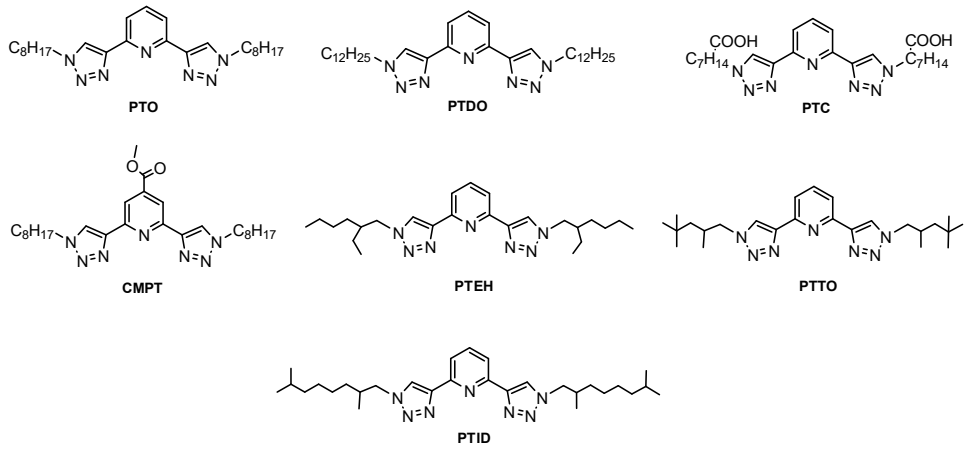

Figure 4.3. Molecular structures of the seven different lipophilic derivatives based on PyTri.

4.2 Results and discussion

We herein report the synthesis and extraction behavior of seven novel derivatives of PTD having the N_3 PyTri chelating core and functionalized on the 1-position of triazolyl moieties, and Py nucleus in one case, with different alkyl substituents. Solubility and extraction tests have been performed in collaboration with the Radiochemistry and Radiation Chemistry Lab. of Politecnico di Milano. The results obtained for PTEH, PTO, PTDO, PTC and CMPT have been published in a joint paper with the group of POLIMI.[6]

4.2.1 Synthesis

The synthetic pathway followed for the preparation of PTO, PTDO, PTC AND CMPT (compounds **7**-**10)** and of PTEH, PTTO and PTID (compounds **14**-**16)** is shown in Figure 4.5 and Figure 4.7. Precisely, Figure 4.5 represents the synthesis of the series of ligands bearing linear alkyl chains, while Figure 4.7 shows the synthesis of the ligands with branched alkyl chains.

In all these cases, the proposed PyTri chelating unit of the extractants were obtained under classical CuAAC reaction conditions starting from 2,6-diethynylpyridine **1** or methyl 2,6-diethynylisonicotinate **2** and the appropriate azide **3-5** and **11-13** (Figure 4.5 and 4.7). All the used azides were synthetized apart as not commercially available (Figure 4.4).

Linear azides **3-5** were prepared by direct azidation of commercially available

1-bromooctane, 1-bromododecane and 1-bromoctanoic acid according to literature procedure.[8,9] The corresponding bromo derivative was dissolved in dry DMF in order to obtain a nearly 0.4 M concentration, then NaN_3 (1.2 eq) was added, Figure 4.4. The mixture was stirred at 80 °C for 24 h then quenched with water. After the work up the azides were obtained pure in 64 % (**3**), 75 % (**4**) and 52 % (**5**) yield and subsequently used without further purification. Due to the length of the chains, no further studies on the hazard of the synthesized azides were undertaken or considered necessary (*see* Chapter 2 for consideration about the hazard of alkyl azydes). Care should be taken, in any case, when manipulating concentrated solutions or pure alkyl azides. The obtained azides were used in the next step as described below.

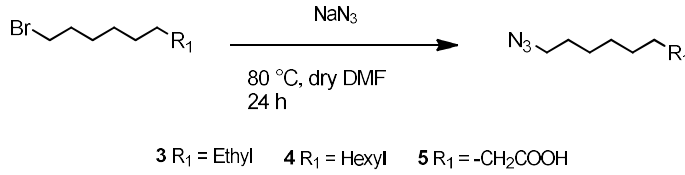

Figure 4.4. Synthesis of azides 3-5

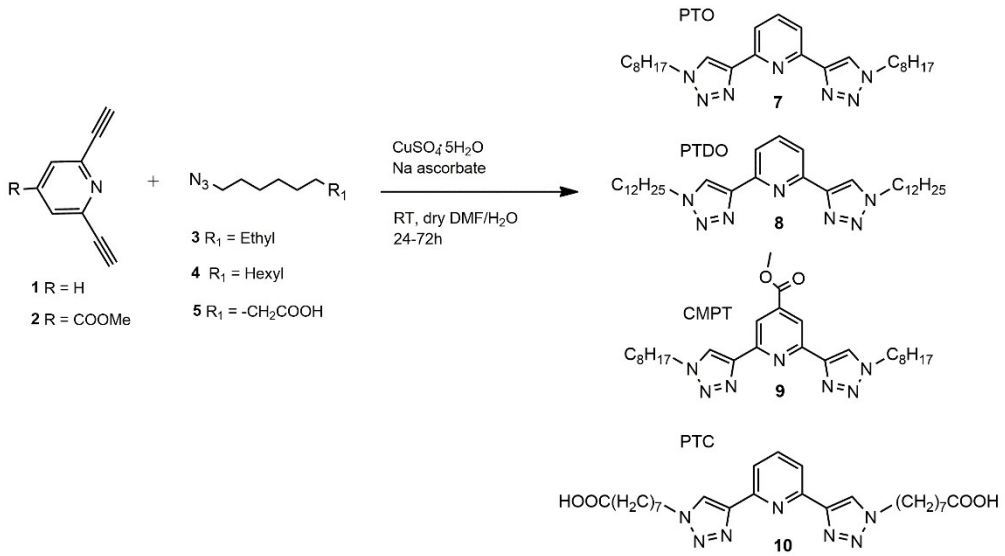

*Figure 4.5. Synthesis of PTO (**7**), PTDO (**8**), CMPT (**9**) and PTC (**10**)*

2,6-Diethynylpyridine (**1**) or methyl 2,6-diethynylisonicotinate (**2**) was dissolved in dry DMF under inert conditions. For the synthesis of PTC, H_2O was used as solvent. Then, $CuSO_4 \cdot 5H_2O$ (0.02 equiv.), Na ascorbate (0.2 equiv.) and the appropriate alkyl azide (2.5 equiv.) were added to the mixture. The resulting solution was stirred for 24 h (PTC), 48 h (PTO and PTDO), 72 h (CMPT) h at room temperature and then quenched

with water. The mixture was extracted three times with DCM. The combined organic phases were dried over anhydrous Na_2SO_4 and finally the solvents were evaporated under reduced pressure. The desired ligands were obtained without further purification in 50 % (PTDO), 55 % (PTO), 90 % (CMPT) and 40 % (PTC) yield.

The 1H NMR spectrum of PTO, as representative for all the series is reported. The NMR spectrum reflects the C_2 symmetry of the molecule. We can observe at 8.18 ppm the singlet related to the triazol protons and at 8.12 and 7.88 ppm the signals of the Py protons in meta and para position, respectively. The alkyl chains give rise to: two triplets at 4.45 and 0.90 ppm related to the protons close the N atom and to the methyl at the end of the chain, respectively; the quintuplet at 1.99 ppm due to the CH_2 protons in β respect to the N atom; finally, the central CH_2 groups give rise to the multiplet at 1.38-1.29 ppm.

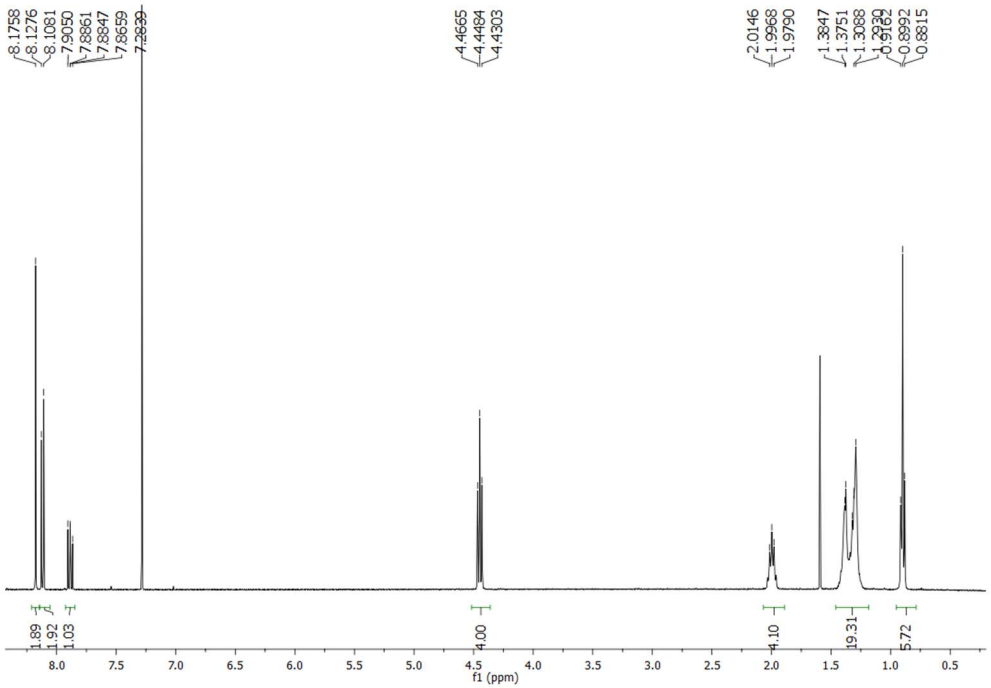

Figure 4.6. ^{1}H NMR ($CDCl_3$, 400 MHz) of PTO

Since the bromo derivatives are not commercially available, the branched alkyl azides **11**-**13** were prepared starting from the corresponding alcohols following the scheme in Figure 4.7. First, 2-ethyl-hexan-1-ol, 2,4,4-trimethyl-pentan-1-ol and 2,7-dimethyl-octan-1-ol were converted into their analogous tosylates (**11a**, **12a**, **13a**) in order to activate the substrates to the reaction of azidation.[10] The alcohol was dissolved in dry

DCM (0.2 M) then NEt_3 (3.2 equiv.) or Py, (2 equiv.) for **11,** was added under inert atmosphere. The mixture was cooled to 0 °C with an ice bath whereupon a solution of TsCl (0.98 equiv.) in dry DCM was added dropwise. When dropping was completed, a catalytic amount of DMAP (only for **12a** and **13a**) was added and the mixture was stirred for 24 h at room temperature. Since the purification of the product from an excess of TsCl demonstrated to be rather tricky even by chromatography, the molar ratio between alcohol and TsCl used is 1 : 0.98. The reaction was quenched with 1 M HCl in order to remove the excess of amine. After removal of solvent under reduced pressure the product **11a** was obtained pure as a colorless liquid 91 % yield while **12a** and **13a** needed a purification step. After flash column chromatography **12a** and **13a** were obtained in 80 % yield. Azides **11**, **12**, **13** were prepared by direct azidation of the tosylate intermediates with NaN_3 in DMF at room temperature until conversion completed (usually 24 h). The azides were all obtained and subsequently used without further purification, as colorless liquid in 78 % (**11**), 89 % (**12**), 81 % (**13**) yield. As for azides **3**-**5** no safety studies were conducted, but care should be taken in their handling.

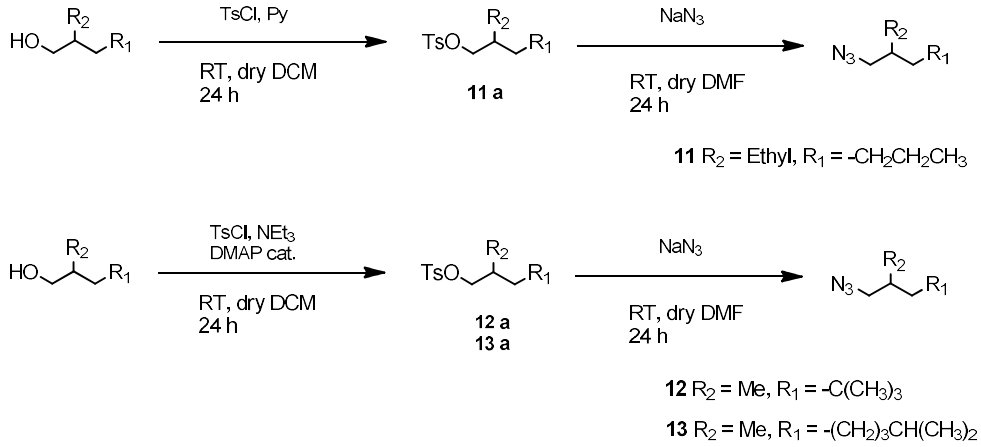

*Figure 4.7. Synthesis of azides **11**, **12**, **13***

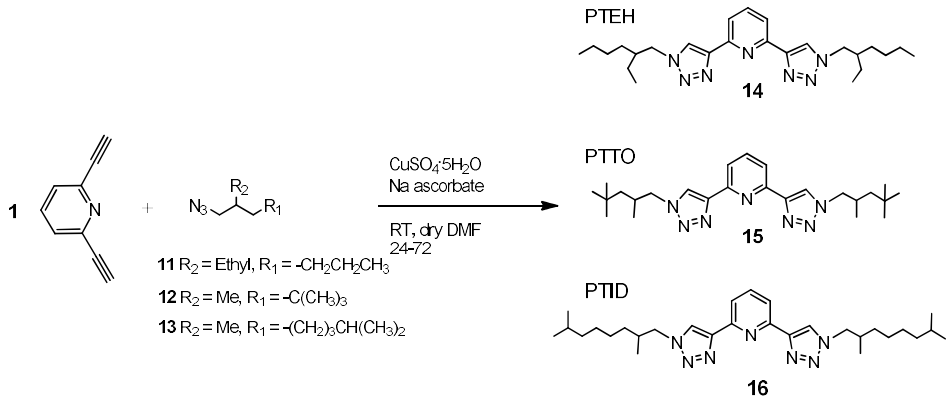

*Figure 4.8. Synthesis of PTEH (**14**), PTTO (**15**) and PTID (**16**)*

The obtained azides were used in the next step as follow.

2,6-Diethynylpyridine (**1**) was dissolved in dry DMF under inert conditions. Then, $CuSO_4 \cdot 5H_2O$ (0.06 equiv.), Na ascorbate (0.6 equiv.) and the appropriate alkyl azide (2.5 equiv.) were added to the mixture. The resulting solution was stirred for three (PTEH) or seven days (PTTO and PTID) at room temperature and then quenched with water. The ligands were purified by flash column chromatography using Hexane/AcOEt 8:2 (PTEH) or 7:3 (PTTO and PTID) as eluent. PTEH was obtained in 65 % yield while PTTO and PTID in 50 % yield. Only in those cases where the NMR spectrum revealed the presence of traces of azide left, the ligand was purified by trituration of the solid in n- hexane.

The ^1H NMR spectrum of PTEH, as representative of all the series, is reported in Figure 4.9. As for PTO, the spectrum reflects the C_2 symmetry of the molecule. At 8.16 ppm is possible to observe the singlet related to the triazol protons while at 8.12 and 7.88 ppm are present the signals of the Py protons in meta and para position, respectively. The alkyl chains give rise to: a doublet at 4.34 ppm related to the CH_2 close to the N atom; a quintuplet at 1.97 ppm due to the CH_2 protons in β respect to the N atom; the multiplet at 1.41-1.32 ppm due to the central CH_2 groups and finally the multiplet at 0.98-0.92 related to the methyl group present in the chains.

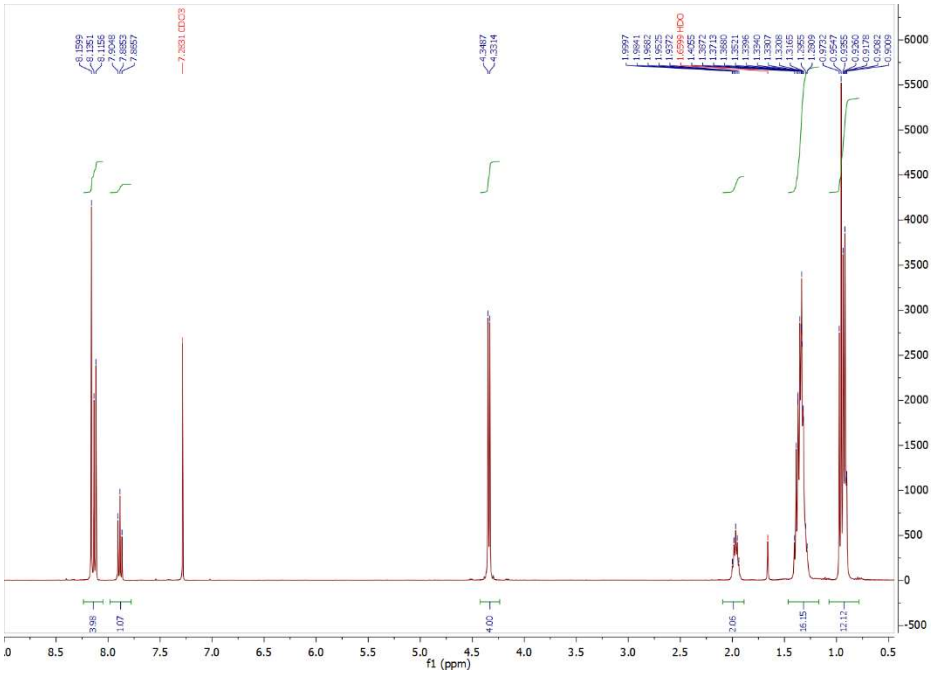

Figure 4.9. ^{1}HNMR (400 MHz, $CDCl_3$) spectrum of PTEH

4.2.2 Solubility tests

The synthetized lipophilic ligands have a common pyridine-bis-triazolyl, PyTri, core adorned by alkyl chains (linear or branched) of different lengths. PTO and CMPT show two n-octyl chains while PTDO two n-dodecyl chains. In CMPT the pyridine ring is para substituted with a methoxycarbonyl unit. In PTC the triazole units are functionalized with an ω-caprylic acid moiety. The series of ligands with branched chains PTEH and PTTO are decorated with two octyl chains. Both present a branching on the C2 atom of the chains. Moreover, PTTO has a further branched tert-butyl group on C3. PTID instead shows two decyl chains with branching on the C2 atom and an isopropyl group on C6. These modifications should not affect the selectivity properties of the core, except for CMPT where an electron-withdrawing group is present, but rather the solubility in organic diluents. Therefore, the solubility of the extractants were evaluated in different solvents, Table 4.2.

Since kerosene is commonly used in industrial hydrometallurgical processes, it has been chosen as reference solvent. Some tests were performed in a mixture of kerosene and 1-octanol. The addition of this alcohol has already been used in different separation processes in order to enhance ligand solubility and avoid third phase formation.[11] In order to further evaluate the effect of solvent compatibility and polarity, tests with

DCM and acetophenone were carried out as well.

Table 4.2. Solubility evaluation of PTO, PTDO, CMPT, PTEH, PTTO and PTID ligands in different diluents

[Ligand] M / Diluent	PTO	PTDO	CMPT	PTC	PTEH	PTT	PTI
Kerosene	≤ 0.01	0.01	0.025	0.01	0.2*	-	-
kerosene/1-octanol 95/5 % v/v	-	≤ 0.009	-	-	≥ 0.2	-	-
kerosene/1-octanol 90/10 % v/v	-	≤ 0.0085	-	-	≥ 0.2	0.12	0.12
kerosene/1-octanol 80/20 % v/v	-	≤ 0.0075	-	-	≥ 0.2	0.2	0.2
kerosene/1-octanol 70/30 % v/v	-	≤ 0.0066	-	-	≥ 0.2	-	-
kerosene/1-octanol 50/50 % v/v	-	≤ 0.01	-	-	≥ 0.2	-	-
1-octanol	0.05	≤ 0.0075	0.1*	0.01	≥ 0.2	-	-
DCM	-	≤ 0.1	0.01	**	≥ 0.2	-	> 0.2
DCM + 50 vol. % 1-octanol	-	≤ 0.05	-	0.02	≥ 0.2	-	-
acetophenone	-	-	-	-	-	> 0.4	> 0.4

* Third phase formation; ** Not soluble; - = not tested

Analyzing the data collected in Table 4.2, PTEH resulted the most soluble ligand in all the diluents though the formation of third phase was observed in pure kerosene. Nevertheless, even a small addition of 1-octanol solved this drawback. Contrary to the expectation that higher branching would have led to a higher solubility, PTTO and PTID were completely insoluble in pure kerosene. They start to dissolve at + 10

vol.% 1-octanol reaching a 0.2 M solubility at + 20 vol.%. However, they both show good solubility in cyclohexanone. PTDO reaches 0.01 M in pure kerosene, but the addition of 1-octanol seems to worse its solubility. PTO and CPT show scarce solubility in all the tested diluents, a quite good solubility in kerosene instead was observed for CMPT (0.025 M). The insertion of branched chains seems to more positively affect ligand solubility than the presence of longer but linear alkyl substituents. Nevertheless, PTID bringing more branched chains of the same length (C8) of PTEH shows lower solubility than PTEH.

The results obtained so far are encouraging since the ligands show higher solubility limit values than those reported for BTTP which has a solubility limit of 0.001 M in pure 1-octanol.[5]

4.2.3 Liquid-liquid extraction

The extracting properties of the novel ligands were studied trough liquid-liquid extraction tests. The scarce solubility of some ligands or their solubility in slightly different solvent mixtures limited a full evaluation of the extraction properties and hindered a direct comparison in the same diluents. Moreover, the analysis of a few extractants (e.g. PTID and PTTO) is in a preliminary stage and further, more detailed, studies are in due course.

Tables 4.3-4.6 report the D_{Am}, D_{Eu} and $SF_{Am/Eu}$ for the series of ligands bringing linear alkyl chains (PTDO, CMPT, PTC, PTO). As explained in Chapter 1 Paragraph 1.3.2, the D value is defined as the ratio between the concentrations of the metal of interest in the organic and in the aqueous phase, at the equilibrium. When a lipophilic ligand is used, a D value higher than 1 means that the ligand is efficient in the extraction of the metal in the organic phase. Therefore, contrarily as seen so far for hydrophilic stripping agents, the higher the D value is, the better is the complexation and extraction in the organic phase. At the same time, to have a good process selectivity, the separation factor ($SF_{An/Ln} = D_{An}/D_{Ln}$) values should be greater than 10 as for hydrophilic ligands.

Table 4.3. Distribution ratios and separation factors of PTDO ligand as a function of the diluent mixture composition and of the ligand concentration in the organic phase. Aqueous phase: HNO_3 solutions spiked with trivalent ^{241}Am and ^{152}Eu

PTDO					
[Ligand] M	Diluent	[HNO_3]	D_{Am}	D_{Eu}	$SF_{Am/Eu}$
0.075	DCM	1	0.014	<<0.001	>>1
		2.25	0.018	<<0.001	>>18
		3	0.074	0.0013	56
		4	0.059	0.001	41
0.02	octanol	1	<<0.001	<<0.001	-
0.01	Kerosene/Octanol 70/30 vol.%	1	<<0.001	<<0.001	-

Table 4.4. Distribution ratios and separation factors of CMPT ligand as a function of the diluent mixture composition and of the ligand concentration in the organic phase. Aqueous phase: HNO_3 solutions spiked with trivalent ^{241}Am and ^{152}Eu

CMPT					
[Ligand] M	Diluent	[HNO_3]	D_{Am}	D_{Eu}	$SF_{Am/Eu}$
0.05	octanol	0.01	<<0.001	<<0.001	-
		0.1	<<0.001	<<0.001	-
		1	<<0.001	<<0.001	-
		2	0.002	<<0.001	>>2
		3.82	0.005	0.002	2.5
0.1	DCM	3.82	0.067	0.0014	>>48

Note for Table 4.3-4.7

The error related to distribution ratios between 0.01 and 100 is around ± 5%, while it extends to ± 20% for smaller and larger values.

Table 4.5. Distribution ratios and separation factors of PTC ligand as a function of the diluent mixture composition and of the ligand concentration in the organic phase. Aqueous phase: HNO_3 solutions spiked with trivalent ^{241}Am and ^{152}Eu

PTC					
[Ligand] M	Diluent	[HNO_3]	D_{Am}	D_{Eu}	$SF_{Am/Eu}$
0.02	DCM/octanol 50/50 vol.%	1	0.0026	<<0.001	>>2
		3.82	0.0065	<<0.001	>>6

Table 4.6. Distribution ratios and separation factors of PTO ligand as a function of the diluent mixture composition and of the ligand concentration in the organic phase. Aqueous phase: HNO_3 solutions spiked with trivalent ^{241}Am and ^{152}Eu

PTO					
[Ligand] M	Diluent	[HNO_3]	D_{Am}	D_{Eu}	$SF_{Am/Eu}$
0.05	octanol	0.01	<<0.001	<<0.001	-
		0.1	<<0.001	<<0.001	-
		1	0.005	<<0.001	>>5
		2	0.009	<<0.001	>>9
		3.82	0.016	0.003	6

PTDO (Table 4.3) shows really low extraction efficiency (D_M<<0.001) for both trivalent Am and Eu in octanol and in Kerosene/octanol 7:3. Due to its better solubility in DCM, a higher ligand concentration could be used to perform the extraction tests and they revealed an interesting An selectivity, although D_{Am} remain far below the unit. At high nitric acid concentrations 3 and 4 M the $SF_{Am/Eu}$ values are 56 and 41, respectively. The same was observed for CMPT which, when dissolved in DCM and contacted with high HNO_3 concentration shows a $SF_{Am/Eu}$ greater than 48 (Table 4.4). Also in this case, however, D_{Am} remains below the unit. PTO (Table 4.6) was tested in octanol, where it showed the highest solubility, the extraction efficiencies for both Am(III) and Eu(III) are extremely low and no selectivity for Am over Eu could be calculated. Due to its very limited solubility, the behavior of ligand PTC was investigated only in few extracting conditions also resulting in a very low extraction efficiency (Table 4.5). On the other side and in sharp contrast to the results collected for PTDO, CMPT, PTC and PTO, PTEH showed remarkable outcomes in all the tested diluents, Table 4.7. Due to

the high solubility showed by the ligand, the extraction tests for all diluents were performed at 0.2 M ligand concentration. In kerosene, the higher D_{Am} value was obtained at $[HNO_3]$ = 1 ($SF_{Am/Eu}$ = 81.9) while increasing $[HNO_3]$ a third phase formation and a drop in D_{Am} and D_{Eu} values were observed. The D_{Am} values in DCM at $[HNO_3]$ = 3 and 4 are close to the unit and the $SF_{Am/Eu}$ are between 15 and 30. The efficiency increased more in octanol where, as the acid concentration increases, the D_{Am} values rise until 3.27 at $[HNO_3]$ = 3.93 M and the separation factors vary from 90 to 70. Notably the D_{Eu} values are always largely below 1. At $[HNO_3]$ = 3, PTEH exhibits good extracting performances in all the kerosene/1-octanol mixtures considered. The best result was obtained in kerosene/octanol 95/5 vol.% at $[HNO_3]$ ~ 3 M where D_{Am} is 9 and SF is almost 73.

Table 4.7. Distribution ratios and separation factors of PTEH ligand as a function of the diluent mixture composition and of the ligand concentration in the organic phase. Aqueous phase: HNO_3 solutions spiked with trivalent ^{241}Am and ^{152}Eu

PTEH					
[Ligand] M	Diluent	[HNO_3]	D_{Am}	D_{Eu}	$SF_{Am/Eu}$
0.2	kerosene	0.01	<<0.001	<<0.001	-
		1	0.0305	0.00037	81.9
		1.5*	<<0.001	<<0.001	-
		3*	<<0.001	<<0.001	-
		4*	<<0.001	<<0.001	-
0.2	DCM	2	0.141	0.0023	61.4
		3	1.039	0.039	26.5
		4	0.926	0.057	16.3
0.2	octanol	1	1.305	0.014	92.9
		2	3.239	0.037	88.8
		2.94	3.767	0.046	81.6
		3.93	3.270	0.046	71.2
0.2	Kerosene/octanol 70/30 vol. %	2.94	2.28	0.028	82.2
0.2	Kerosene/octanol 95/5 vol. %	2.94	9.09	0.13	72.7
0.2	Kerosene/octanol 50/50 vol. %	2.94	2.28	0.030	75.3

*third phase formation. D values are calculated as indicative ratio between $[Am]_{org}/[Am]_{aq}$ without taking into consideration the third phase

Due to solubility constraints the extraction tests for PTTO and PTID (Figure 4.10 and 4.12) were conducted only in kerosene/octanol 90/10 vol.%, kerosene/octanol 80/20 vol.% and acetophenone (still preliminary results). PTTO has D_{Am} values well above the unit in 0.2 M in kerosene/octanol 80/20 vol.% at all the [HNO_3] explored (Figure 4.10). These results are confirmed by the data obtained in acetophenone (Figure 4.11). The D values decrease a lot in kerosene/octanol 90/10 vol.%. In this mixture the ligand is less soluble so the concentration used for the extraction tests is 0.12 M. Reasonably, this lower concentration can be considered the cause of a lower efficiency.

Nevertheless, in both mixtures there are interesting selectivity values. D_{Eu} indeed are always well below the unit and the $SF_{Am/Eu}$ values are always between 60 and 80.

Conversely, PTID shows D_{Am} values below the unit in all the analyzed mixtures. Nevertheless, the D_{Am} values are significantly greater than those related to Eu and this disclosed $SF_{Am/Eu}$ values between 30 and 60. Despite the poor efficiency, PTID also shows an appealing selectivity, although worse than that of PTTO.

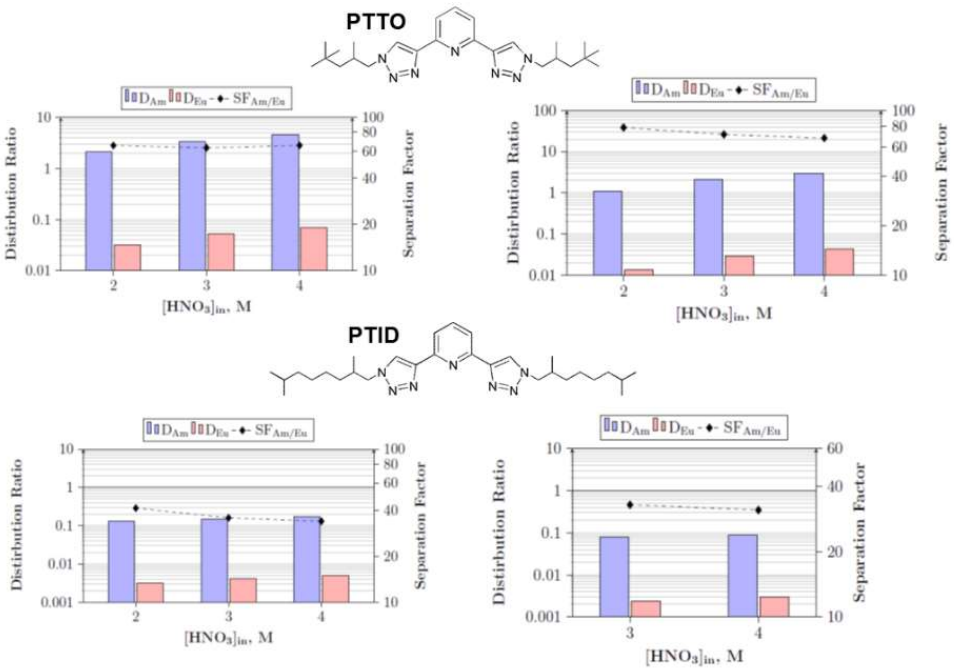

Figure 4.10. Distribution ratios and separation factors of PTTO (above) and PTID (below) ligands as a function of the HNO_3 concentrations spiked with trivalent ^{241}Am and ^{152}Eu. Diluent mixture: 0.2 M in kerosene/octanol 80/20 vol.% (right) and 0.12 M in kerosene/octanol 90/10 vol.%

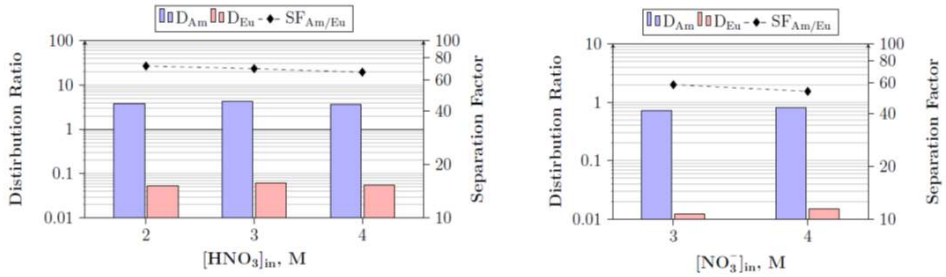

Figure 4.11. Distribution ratios and separation factors of PTTO (left) and PTID (right) ligands as a function of the HNO_3 concentrations spiked with trivalent ^{241}Am and ^{152}Eu. Diluent mixture compositions: 0.2 M in acetophenone

4.3 Identification of PTEH degradation products

The appealing extraction behavior of PTEH prompted us to further investigate its properties. Certainly, the hydrolytic and radiolytic stability is a key prerequisite in view of a possible employment of the ligand in industrial processes. Therefore, the ligand was exposed to tests which simulated the operating conditions of the industrial process. Ligand solutions were left to age for 169 days in contact with 3 M nitric acid in the dark at room temperature in order to evaluate its hydrolytic stability. At the same time, other solutions were subjected to gamma irradiation at 100 and 200 kGy (2.5 KGy/h), not in contact or in contact with an equal amount of 3 M nitric acid to value the radiolitic stability. Direct, and coupled with HPLC, ESI-MS analyses were performed (as for PTD) and few new peaks were identified in the chromatograms of the irradiated solutions. The separation and subsequent fragmentation of each by-product, at its specific *m*/*z*, was obtained by using the ESI-tandem mass (MS^2) spectrometry. This allowed to obtain several information about the structure of the observed species. Contrary to the results obtained with PTD which is predominantly present in water and reacts with nitric acid and hydroxo radicals, PTEH is present in the organic phase and apparently tends to react with octanol, kerosene or their decompositions products. Most of the products observed in the ESI-MS have m/z values significantly higher that of PTEH and corresponding to the addition of C8 or C12 chains. These chains may be attached to the pyridine or ethyl-hexyl lateral chains (Figure 4.1). Although both options are possible, the pioneering work by Minisci and co-workers in 1968[12] suggests that under strongly acidic conditions alkyl radicals, generated via radical rearrangements in situ, may add to the 2- or 4- positions of pyridines especially when protonated. Both protonation and presence of radical species are highly possible in the conditions used for these tests so that we are more favorable to consider that substitution on the pyridine nucleus takes place, in most of these decomposition products (Figure 4.2). The degradation product with m/z 563 can therefore be the outcome of a 1-octanol radical addition on the pyridine followed by oxidation. As well, DP with m/z 599 could result from the radical substitution of tetrapropylene (kerosene used for extraction has a branched C12 structure) on the pyridine.

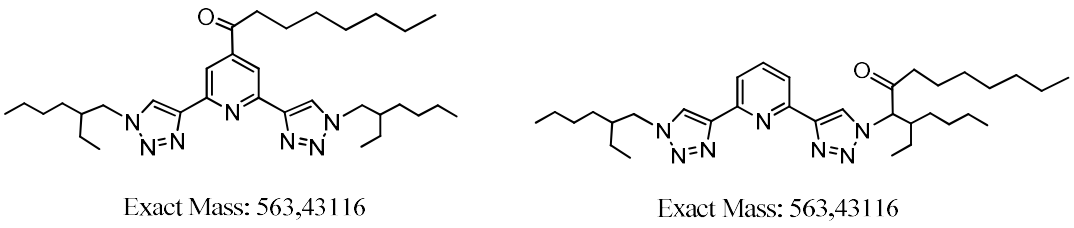

Figure 4.12. Possible addition of radicals originated by octanol to the pyridine nucleus (left) or ethyl-hexyl chain (right)

Also the tertiary C on the ethyl-hexyl chain, or the CH_2 group in α position to the triazol nucleus might be particularly reactive in radical reaction and this is the reason of the hypothesized presence of $-ONO_2$ or –OH groups in structures with m/z values of 498.30 and 581.44. In all the hypothesized degradation product structures, however, the chelating N_3 motif is preserved. Therefore, it is reasonable that the extraction behavior towards MA of aged and irradiated solutions is preserved.

The hydrolytic and radiolytic stability manifested by PTEH together with its exceptional extraction efficiency and selectivity towards An makes the new ligand a perfect candidate for its industrial implementation.

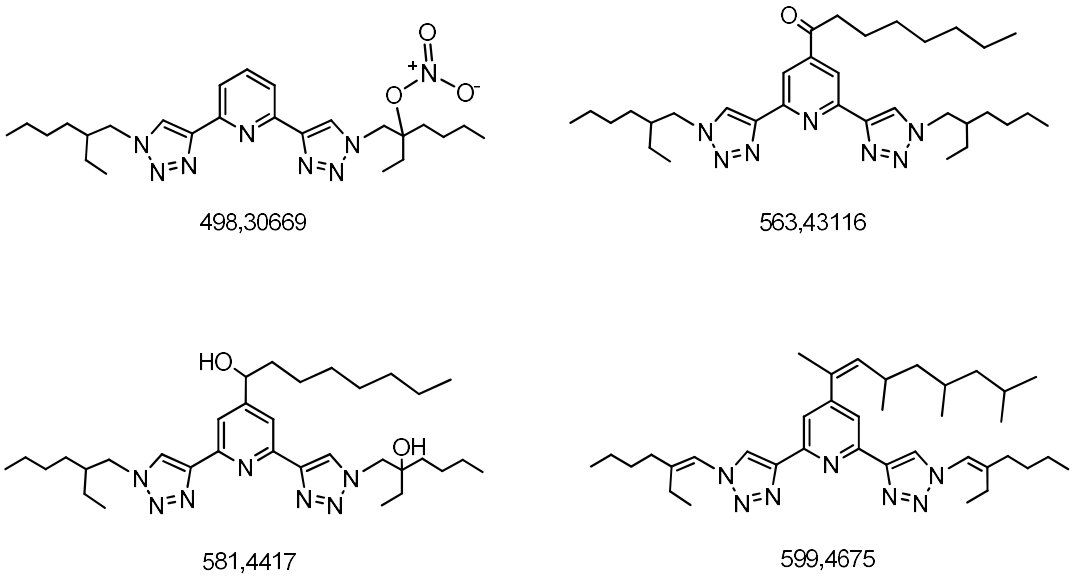

Figure 4.13. Molecular structure of the DPs as proposed by POLIMI and UNIPR

4.4 Multidentates Ligands

An and Ln are present in the nuclear waste in different oxidation states but most of them have oxidation state ≥ 3. They all show, however, high coordination number ≥ 5 and quite often 8, 9 or 10.[13] Therefore, to bind one of these f-metal ions several chelating units are needed at the same time and possibly each chelating unit needs to have at least three donor atoms. In order to improve the metal binding and extraction, the preorganization of the binding sites and especially chelating groups onto molecular platforms has been widely studied.[14] Moreover, the ligands performances can be influenced by the structure of the platform on which the chelating groups are bound. Preorganization usually reduces the entropy loss during complexation thus making free energy of binding more favorable. The preorganization effect indeed can lead not only to a better extraction but also to a higher metal selectivity.[14] Particularly, calix[n]arenes have been highly studied as platform for the development of selective metal chelating ligands.[15,16]

Calix[n]arenes are macrocycle made of a different number of phenyl ring (4-8) linked by a methylene bridge.[17] They present an upper (wide) rim and a lower (narrow) rim which can be both functionalized. The functionalization can be used to tune the solubility and/ or the conformation of the calixarene. Each phenyl ring indeed can rotate around the methylene bridge resulting in the existence of different conformations. With increasing the size of the macrocycle, a higher number of conformations are possible, and the platform becomes more flexible affecting its preorganization properties. Moreover, a high number of coordinating groups that can be linked to the platform can lead to a closely matching with the coordination number of the metal, thus raising the extraction efficiency of the ligand. Among all the macrocycles, the calix[4]arene scaffold, thanks to its easy synthesis and chemical modification, has been largely investigated and employed in organic-supramolecular chemistry. The free rotation can be hindered by full alkylation of the lower rim with groups larger than ethyl. In this way 4 conformers can be isolated: the cone, partial cone, 1,2- and 1,3-alternate. The calix[4]arene, blocked in the cone-shape conformer, still presents a certain mobility (C_{4v}, C_{2v}). This rotational freedom is transferred in a positive degree of flexibility of the chelating groups bound to it. A fully functionalized calix[4]arene at the lower rim can bring four chelating groups. Especially with the introduction of acetamide moieties (OCH_2CONR_2), valuable ligands for lanthanide ions were obtained, whose Tb(III) complexes are endowed with interesting

luminescent properties (Figure 4.14, right).[18]

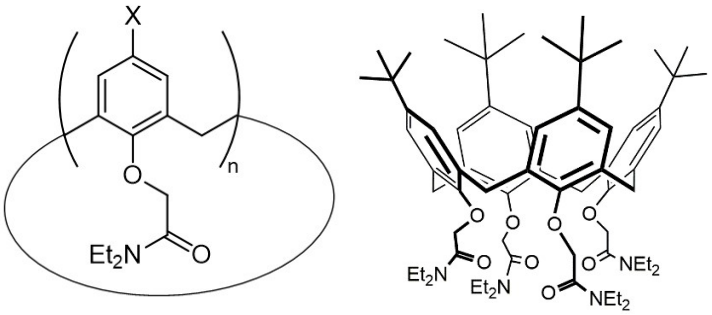

Figure 4.14. Structure of the calix[4]arene used for Tb(III) complexes (right) and of the calix[n]arenes (n = 6, 8) functionalized with acetamido groups. X = H, Bu^t (left)

The insertion of the same acetamido group at the lower rim of calix[6]- or calix[8]arenes (Figure 4.14, left) allowed to obtained interesting ligands potentially able to remove long-live Sr(II) radioisotopes from radioactive waste.[19] Very efficient ligands for the extraction of trivalent Ln and An from radioactive waste are calixarenes functionalized at the upper or lower rim with carbamoylmethylphosphine oxides (CMPO) functions[20–22] and that show a large cooperative effect in the binding. Another interesting class of ligands for the extraction of both Ln(III) and An(III) are those obtained by Iqbal et al. by adorning the calixarene with multiple tridentate diglycolamide chelating groups.[23]

However, probably the most remarkable industrial application of calixarenes is related to their use for the selective removal of long-lived Cesium ion from highly radioactive waste. The introduction of a penta-ethylene glycol bridge at the lower rim and the subsequent freezing of the calix[4]arene skeleton into the 1,3-alternate structure allowed to obtain a series of calix[4]arene-monocrown-6 (Figure 4.15) which are able to completely remove even small traces (10^{-4} M) of cesium nitrates from concentrated HNO_3 solution even when containing large amounts of $NaNO_3$ (2–4 M).[24] The efficiency and selectivity of this process is so remarkable that it was implemented industrially on real nuclear wastes by the DoE (Department of Energy – USA) which uses it to treat millions of gallons of waste per year.[25]

As far as concern the use of calixarenes in the selective An(III)/Ln(IIII) separation from radioactive wastes, rather few examples are reported in the literature. Picolinamide binding groups are used for this scope.

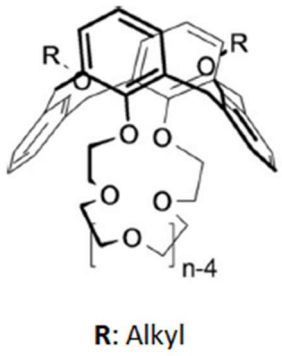

Figure 4.15. Structure of the cesium selective calix[4]arene-crown-6 with a penta-ethylene glycol bridge at the lower rim

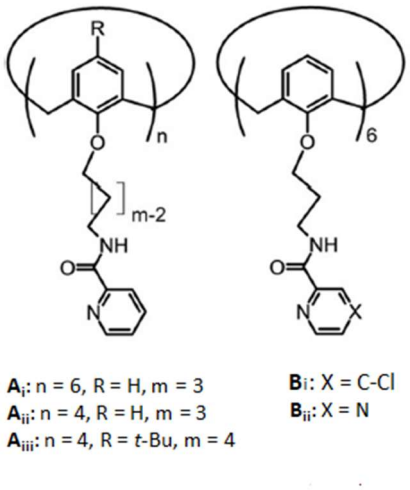

Figure 4.16. Structures of Calixarenes bearing picolinamide groups

Calixarenes bearing picolinamide groups (e.g., **A** in Figure 4.16)[26] show an An/Ln selectivity ($SF_{Am/Eu}$ up to 13.8). To increase the efficiency of extraction a lipophilic bromocosan anion is normally employed as synergizer with these ligands.[27] Quite remarkably, the presence of electron-withdrawing groups in the para positions of the pyridine rings (**B**$_i$, Figure 4.16) and the use of the aromatic units with the less basic pyrazine nuclei (**B**$_{ii}$, Figure 4.16) significantly increase the efficiency of these ligands especially at rather high HNO_3 concentrations.

The appealing results of selectivity obtained for PTEH ligands prompt therefore us to design a novel lipophilic ligand by anchoring three PTEH units onto a calix[4]arene platform. Preliminary molecular modeling studies carried out with SPARTAN suite and DFT using B3LYP as hybrid functional and as 6-31g** basis set, allowed to optimize the

length of the alkyl chain linking the PyTri units to the calix[4]arene lower rim oxygen atoms, Figure 4.17. As can be seen in Figure 4.16 the use of a butyl chains warrants a proper distance and reduces the tension in the aliphatic linear chain allowing all the three PyTri units to simultaneously interact with a La^{3+} metal ion used as model of the trivalent An/Ln ions.

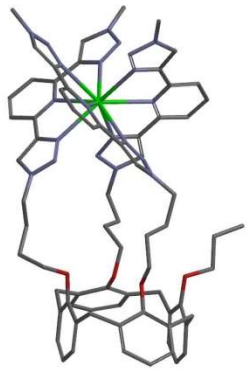

Figure 4.17. Molecular modeling. Ethyl-hexyl chains omitted for reduction of the computational resources

4.4.1 Synthesis

The synthetic pathway followed for the preparation of the Calix-PTEH is described in Figure 4.18. The first step is the tetralkylation of the 25,26,27,28-tetrahydroxycalix [4]arene with four propyl chains.[28] In order to obtain the full alkylation a strong base, NaH (4.5 equiv.), and an excess of alkylating agent (4.5 equiv.) were used. At low room temperature (room temperature) and with the use of sodium counterion the reaction turns stereoselective and the only cone structure can therefore be obtained. The calix[4]arene was dissolved in dry DMF and NaH was added. The mixture was stirred for one hour in order to favor the deprotonation of the reagent then the 1-iodopropane was added. After 4 days stirring, the reaction was quenched, and the product was obtained pure without further purification steps in 90 % yield. The monopropyl calixarene was obtained by adapting a literature procedure.[29] Intermediate **18** in figure 4.18 was dissolved in dry chloroform under inert atmosphere. The mixture was heated up to reflux and a solution of TMSI (3 equiv.) in chloroform was added dropwise. The reaction progression was checked by TLC. When the monoether was observed to be the only species present (usually 4 hours), the mixture was quenched with 3M HCl. The product was obtained as a white solid in 90 % yield. Intermediate **20** was then exhaustively alkylated adapting the procedure of step 1. 25,26,27-

trihydroxy-28-propyloxy-calix[4]arene was dissolved in dry DMF, then NaH (10 equiv.) was added under inert atmosphere. The mixture was stirred for 1 hour whereupon 1-azido-4-iodobutane (6 equiv.) was added. The mixture was stirred for 4 days at room temperature. The product was obtained in 94 % yield. Finally, the target compound was obtained by directly clicking the alkyl azide derivative **20** with the *mono*-PTEH **21**. Compound **21** was obtained as a byproduct of the synthesis of PTEH. The reaction between **20** and **21** was driven under classical CuAAC conditions with $CuSO_4 \cdot 5H_2O$ and sodium ascorbate in DMF. The final compound was purified by flash column chromatography and obtained in 56 % yield.

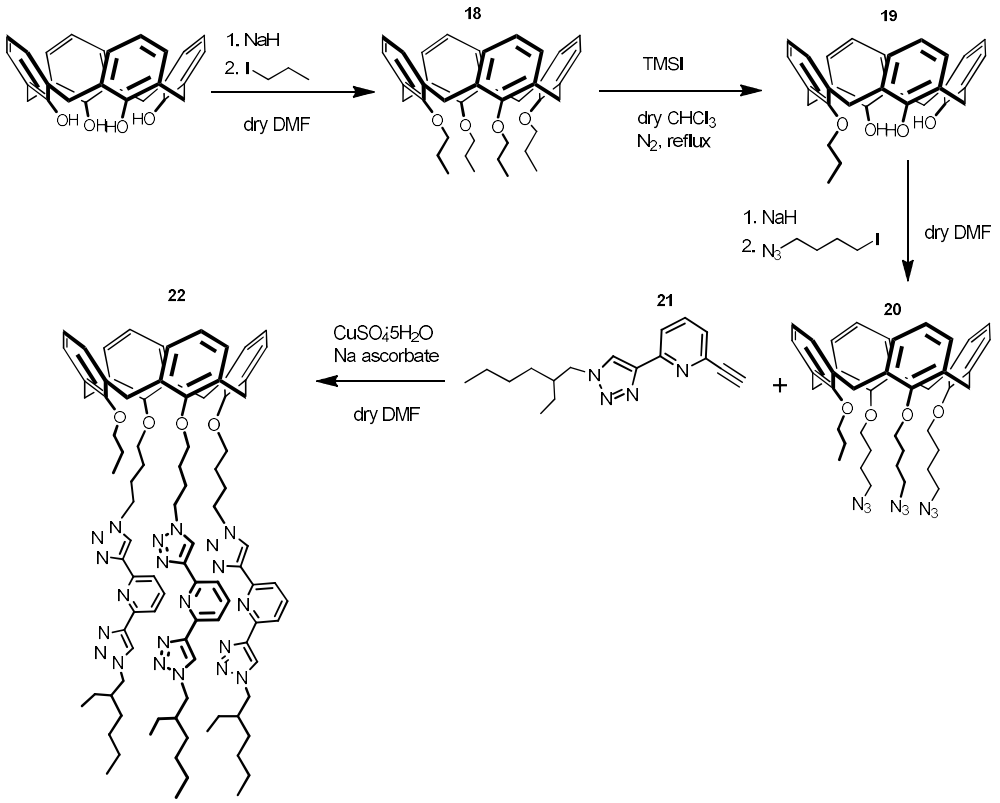

Figure 4.18. Synthesis of Calix-PTEH

The cone conformation of the calix[4]arene is confirmed by the ^{1}H NMR spectrum. When the calix[4]arene is in the cone conformation, the protons of the methylene bridges give rise to two doublets at 4.0-4.5 ppm and 3.0-3.3 ppm related to the axial and equatorial protons, respectively. Considering the asymmetry of the ring, the methylene bridges give rise to 4 doublets. The triazol protons of a single chelating unit are different from each other and give rise to two singlets in the range of 8.25-

8.50 ppm. The asymmetry of the cone determines the non-equivalency of the three chelating units. For this reason, the triazoles give rise to 4 different singlets (in a 1:2 ratio). The signals of the alkyl chains are at higher fields except for those close to O atoms and N atoms which give rise to signals at 3.98-3.7 ppm and 4.44-4.14 respectively.

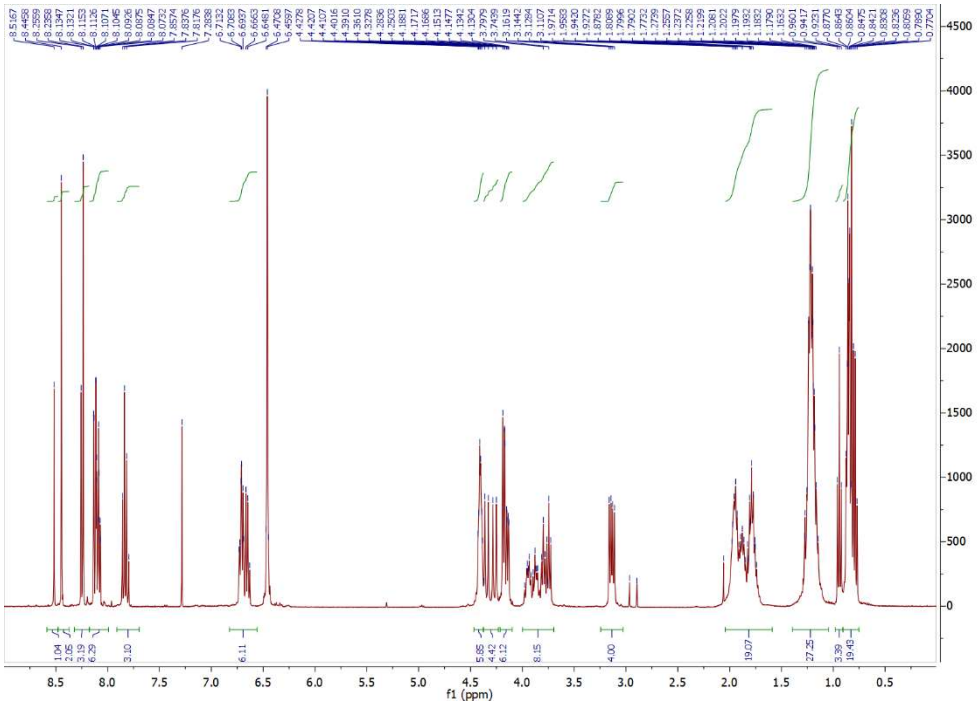

Figure 4.19. ^{1}H NMR ($CDCl_3$, 400 MHz) of Calix-PTEH

4.4.2 Solubility and extraction tests

In order to compare the novel ligand with PTEH, PTTO and PTID, Calix-PTEH was initially tested in k/o 80/20 vol.% and in acetophenone. PTEH showed its best performances at 0.2 M, therefore, since Calix-PTEH brings 3 chelating units, the latter ligand was tested at 0.08 M, which is roughly ⅓ the concentration of PTEH. In both mixtures D_{Am} ratios are well above the unit (Figure 4.20) and SF values are always greater than 40. Unfortunately, in acetophenone the D_{Eu} ratio increases thus originating a decrease of the SF values.

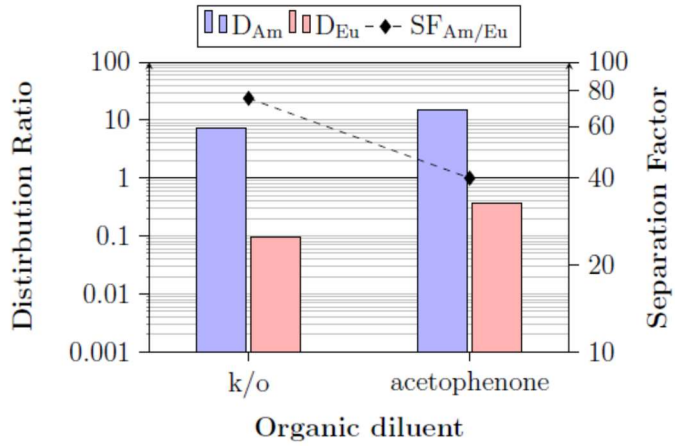

Figure 4.20. Distribution ratios and separation factors of Calix-PTEH ligand as a function of the diluent. Aqueous phase: 3M HNO_3 spiked with trivalent ^{241}Am and ^{152}Eu. Diluent mixture composition: 0.08 M in kerosene/octanol 80/20 vol.% (left) and 0.08 M in acetophenone (right)

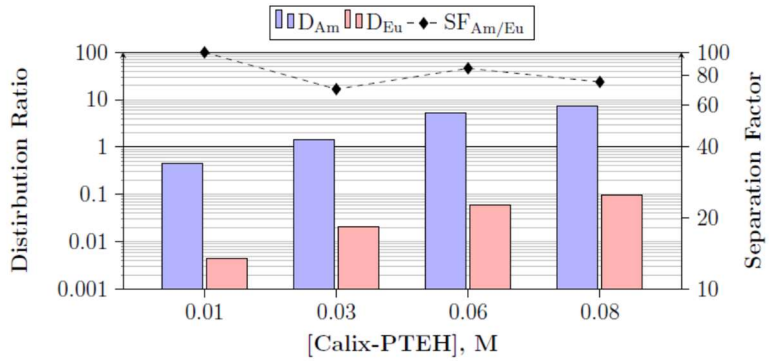

Figure 4.21. Distribution ratios and separation factors of Calix-PTEH as a function its concentration in kerosene/octanol 80/20 vol.%. Aqueous phase: 3M HNO_3 spiked with trivalent ^{241}Am and ^{152}Eu

As the k/o mixture was the most promising, further extraction tests, varying the ligand concentration, were carried out (Figure 4.21). As expected, greater concentrations give rise to better extraction efficiency. Nevertheless, with increasing concentration from 0.01 to 0.08 M the selectivity decreases.

Figure 4.22 shows the comparison of the extraction behavior of PTID, PTTO, PTEH and Calix-PTEH. At roughly the same PyTri concentrations (0.2 PTEH, PTID, PTTO and 0.08 Calix-PTEH) the Calix-PTEH shows higher D values than PTEH and SF up to 80. As expected, the preorganization effect indeed led not only to a better extraction efficiency but also to a higher Am(III) selectivity. Although this ligand appears quite

interesting certainly a drawback could be connected to the difficulty of its synthesis. Moreover, its radiolytically and chemical stability should be studied more in details.

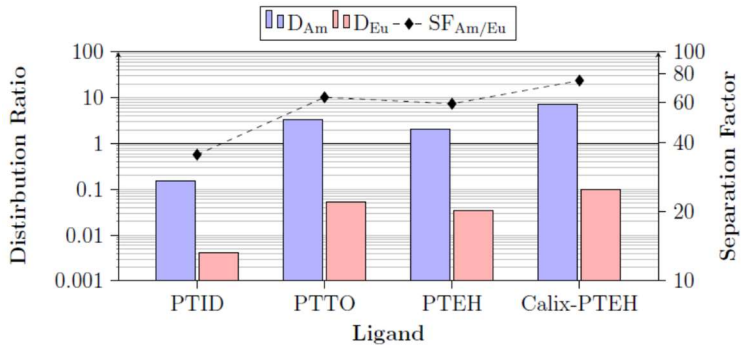

Figure 4.22. Distribution ratios and separation factors of PTID (0.2 M), PTTO (0.2 M), PTEH (0.2 M) and Calix-PTEH (0.08 M) in kerosene/octanol 80/20 vol.%. Aqueous phase: 3M HNO_3 spiked with trivalent ^{241}Am and ^{152}Eu

4.5 Experimental

4.5.1 General methods and chemicals

Reagents and solvents

All commercially available chemicals (Sigma-Aldrich, TCI, ChemPur, VWR) used in this study were analytical reagent grade and were used without further purification. All air sensitive reactions were carried out under nitrogen atmosphere using oven-dried glassware. All dry solvents were prepared according to standard procedures and stored over 3 or 4 Å molecular sieves.

Instrumentation, techniques, and common procedures

^{1}H NMR and ^{13}C NMR spectra were recorded on Bruker AV300 and AV400 or JEOL ECZ600R spectrometers (observation of ^{1}H at 300 MHz, 400 MHz and 600 MHz and of ^{13}C at 75 MHz, 100 MHz or 150 MHz). Partially deuterated solvents were used as internal standards to calculate the chemical shifts (δ values in ppm). J coupling constants are given in Hz. All ^{13}C NMR spectra were performed with proton decoupling. The used abbreviations in these spectra are singlet (s), doublet (d), triplet (t), quadruplet (q), quintuplet (quint) and multiplet (m).

In order to monitor the progress of reactions, aluminum sheets covered with silica gel 60 F-254 provided by Merck were used. All TLC s were revealed under an ultraviolet lamp

(λ= 254 nm) or using staining reagents. Merck silica gel 60 was used for flash chromatography (40-63 μm) and for preparative TLC plates 20x20cm (10-12 μm).

Electrospray ionization (ESI) mass analysis were performed on a Waters single- quadrupole instrument SQ Detector in positive mode using MeOH or CH_3CN as solvents. HR-MS spectra were registered by Dr. Andrea Faccini at "Centro Interdipartimentale Misure" of Università di Parma with an LTQ ORBITRAP XL Thermo instrument in positive mode using MeOH or CH_3CN as solvents.

Melting points were determined on an Electrothermal apparatus in sealed under nitrogen capillaries.

Solubility of extractants was evaluated by dissolving a weighed amount of compound in the chosen diluent at 22 ± 1 °C and by stepwise addition of a weighed amount of diluent until the solutions became clear. Sonication and heating were exploited to facilitate ligand dissolution only if necessary. Only the organic phases containing 1-octanol were pre-equilibrated with an equal volume of nitric acid of suitable concentration, before performing the liquid–liquid extraction tests, in order to ensure that the aqueous phase acidity did not change during the tests. The concentration of HNO_3 in the aqueous phase was checked by titration with NaOH before and after the extraction experiments. Besides that, all the extraction tests were carried out following a standard protocol. The organic phases were contacted in closed single-use Eppendorf microtubes with an equal volume of the aqueous phases containing the cations to be extracted and vigorously shaken at room temperature (22 ± 1 °C) with a mixer for 1 h, which proved to be sufficient to achieve the chemical equilibrium. An aliquot of 200 μL of each phase was sampled after centrifugation. The activity concentrations of ^{241}Am and ^{152}Eu in each phase were measured by γ-spectrometry (2'' x 2'' NaI(TI), Silena SNIP N MCA) exploiting the γ-lines at 59.5 keV and 121.8 keV, respectively. Following sample preparation by diluent evaporation to dryness on steel planchet, the activity concentrations of ^{241}Am were checked by α-spectrometry (ORTEC Octête PLUS) by exploiting the α-lines at about 5.4 MeV and 5.8 MeV, respectively. Each test was performed in duplicate. Extraction tests were performed only with the organic phases in which no precipitate or third phase formation were observed. Extraction data were considered reliable only if no third phase was observed during the tests and the mass balance was 100 ± 5%. Distribution ratios, D_M, were then calculated as the ratio between the activity concentration of the radiotracers (or the concentration of the stable elements) in the organic phase and that in the aqueous phase. In order to assess the extracting properties of the ligands, solvent

extraction tests were performed with aqueous phases at different HNO_3 concentrations spiked with a total activity of about 8000 Bq of ^{241}Am and ^{152}Eu.

4.5.2 Synthesis

2,6-Diethynylpyridine (**1**)[30] and methyl 2,6-diethynylisonicotinate (**2**)[31,32] were synthetized according to literature procedures starting from 2,6-dibromopyridine or isonicatinic acid, respectively.

2-ethylhexyl-4-methylbenzenesulfonate (11a)

Prepared according to literature procedure.[10] Pyridine (6 ml, 76 mmol) was added to a solution of 2-ethyl-hexan-1-ol (5 g, 38 mmol) in 25 ml of dry dichloromethane (DCM) under inert conditions. The reaction mixture was cooled to 0 °C and a solution of *p*-toluene sulfonylchloride (7.00 g in 25 ml DCM) was added drop-wise. The reaction mixture was stirred for 48 hours at room temperature then quenched with water and the aqueous layer extracted with DCM (3 x 20 ml). The organic phases were washed with HCl 1 M then dried over anhydrous Na_2SO_4 and the solvents evaporated *under vacuum* to get the final product as a colorless oil. Yield: 91%. ^1H NMR (300 MHz, $CDCl_3$): δ 7.81 (2H, d, *J* = 8.2 Hz, *H*Ar), 7.36 (2H, d, *J* = 8.2 Hz, *H*Ar), 3.98-3.89 (2H, m, C*H*$_2$Ts), 2.47 (3H, s, Ar-*CH*$_3$), 1.55 (1H, hept, *J* = 6.1 Hz, C*H*CH$_2$Ts), 1.38-1.11 (8H, m, C*H*$_2$), 0.88-0.78 (6H, m, C*H*$_3$).

General procedure for the synthesis of 2,4,4-trimethylpentyl 4-methylbenzenesulfonate (12a) and 2,7-dimethyloctyl 4-methylbenzenesulfonate (13a)

2,4,4-Trimethyl-pentan-1-ol and 2,7-dimethyl-octan-1-ol (1.00 g) was dissolved in dry DCM (0.2 M) then NEt_3 (3.2 equiv.) was added under inert conditions. The mixture was cooled to 0 °C with an ice bath whereupon a solution of TsCl (0.98 equiv.) in dry DCM was added dropwise. When dropping was completed DMAP (cat.) was added and the mixture was stirred for 24 h at room temperature. The reaction was quenched with 1 M HCl solution (30 ml) and the aqueous phase extracted with DCM (1 x 30 ml). The organic phases collected were washed with $NaHCO_3$ solution (1x 30 ml) and brine (1 x 30ml). The organic phase was dried over anhydrous Na_2SO_4 then the solvent was removed under reduced pressure. The crude was purified by flash column chromatography using hexane/Et_2O as eluent. product was obtained as a colorless liquid in 90 % and 80 % yield.

2,4,4-trimethylpentyl 4-methylbenzenesulfonate (12a)

Eluent: Hex/Et_2O 9:1, yield: 80%. ^1H NMR (400 MHz, $CDCl_3$): δ 7.77 (2H, d, *J* = 8.0 Hz, *H*Ar), 7.33 (2H, d, *J* = 8.0 Hz, *H*Ar), 3.85 (2H, dd, J_{vic} = 9.3 Hz J_{gem} = 5.5 Hz, CH_2OTs), 3.69 (2H, dd, J_{vic} = 9.3 Hz J_{gem} = 7.3 Hz, CH_2OTs), 2.43 (3H, s, Ar-CH_3), 1.81 (1H, oct., J = 5.4 Hz, C*H*CH_3, 1.15 (2H, dd, J_{vic} = 14.2 Hz J_{gem} = 4.1 Hz CH_2(*t*-but), 0.96 (2H, dd, J_{vic} = 14.1 Hz J_{gem} = 5.9 Hz CH_2(*t*-but), 0.91 (3H, d, *J* = 6.8 Hz, CHCH_3), 0.82 (9H, s, *t*-but). ^{13}C NMR (100 MHz, $CDCl_3$): δ 144.7, 133.4, 129.9, 128.0, 76.2, 46.5,30.8, 29.7, 29.5, 21.7, 19.5. HRMS: *m*/*z* calcd for $C_{15}H_{24}O_3SNa$: 307.1344; found: 307.1338. ESI-MS (+): 306.95 $[M+Na]^+$.

2,7-dimethyloctyl 4-methylbenzenesulfonate (13a)

Eluent: Hex/Et_2O 8:2, yield: 80%. ^1H NMR (400 MHz, $CDCl_3$): δ 7.81 (2H, d, *J* = 8.3 Hz, *H*Ar), 7.37 (2H, d, *J* = 7.7 Hz, *H*Ar), 4.13-4.04 (2H, m, CH_2OTs), 2.47 (3H, s, Ar-CH_3), 2.08-1.99 (2H, m, CH_2CHCH_2N), 1.84-1. 0.87 (3H, d, J = 6.6 Hz, CHCH_3), 0.82 (6H, d, J = 6.5 Hz, CH(CH_3)$_2$). ^{13}C NMR (100 MHz, $CDCl_3$): δ 144.7, 133.2, 129.8, 127.9, 69.2, 39.1, 36.8, 35.7, 29.2, 27.9, 24.5, 22.7, 22.6, 21.7, 19.2. HRMS: *m*/*z* calcd for $C_{15}H_{24}O_3SNa$: 335.1657; found: 335.1654. ESI-MS (+): 335.62 $[M+Na]^+$.

General procedure for the synthesis of 1-azidooctane (3), 1-azidododecane (4), 8-azidooctanoic acid (5). [8,9]

The corresponding commercially available bromo derivative (1 equiv) was dissolved in DMF (0.4 M). Then sodium azide was added (1.2 equiv) and the reaction was heated at 80 °C overnight. After completion of the reaction, water was added, and the desired product was extracted with diethyl ether (×3). The combined organic layers were washed with water (×3), brine (×1), dried over sodium sulfate, and concentrated in vacuo to give the desired azide, which was used in the next step without further purification.

1-azidooctane (3)

64 % yield. ^1H NMR (400 MHz, $CDCl_3$): δ 3.26 (2H, t, *J* = 7.0 Hz, CH_2N_3), 1.61 (2H, quint, *J* = 7.0 Hz, C$H_2CH_2N_3$), 1.34-1.30 (10H, m, CH_2), 0.90 (3H, t, *J* = 6.6 Hz, CH_3).

1-azidododecane (4)

Yield: 75%. ^1H NMR (400 MHz, $CDCl_3$): δ 3.07 (2H, t, *J* = 6.8 Hz, CH_2N_3,), 1.4 (2H, m, C$H_2CH_2N_3$), 1.18-1.08 (18H, m, CH_2), 0.69 (3H, bs, CH_3).

8-azidooctanoic acid (5)

Yield: 52%. ^{1}H NMR (400 MHz, $CDCl_3$): δ 3.26 (2H, t, *J* = 7.0 Hz, C*H*$_2$N$_3$,), 2.36 (2H, t, *J* = 7.4 Hz, C*H*$_2$COOH), 1.66-1.57 (4H, m, C*H*$_2$), 1.40-1.32 (6H, m, C*H*$_2$).

3-azidomethyl-heptane (11).

2-ethylhexyl 4-methylbenzenesulfonate (15.0 g, 52.7 mmol) were dissolved in 70 ml of dry dimethylformamide (DMF) with NaN_3 (6.8 g, 104.6 mmol) under inert conditions. The reaction was stirred for 48 h then quenched with water. The aqueous layer was extracted with DCM (3 x 25 ml), the collected organic phases were washed with water (3 x 50 ml) and then dried over anhydrous Na_2SO_4. The solvents were evaporated under reduced pressure to get the product as a colorless oil. Yield: 78%. ^{1}H NMR (400 MHz, $CDCl_3$): δ 3.25 (2H, d, *J* = 5.8 Hz, C*H*$_2$N$_3$), 1.51 (1H, hept, *J* = 6.1 Hz, C*H*CH$_2$N$_3$), 1.42-1.25 (8H, m, C*H*$_2$), 0.93-0.89 (6H, m, C*H*$_3$). ESI-MS (+): 184.1 $[M+H]^+$.

General procedure for the synthesis of 2,7-dimethyloctyl 4-methylazide (12) and 2-ethylhexyl 4-methylazide (13)

NaN_3 (2 equiv.) was dissolved in dry DMF (20 ml). The mixture was stirred at room temperature until dissolution completed. Whereupon, 12a or 13a (2.0 g) was added. The mixture was stirred at room temperature for 24 h then quenched with H_2O (5 ml). The aqueous pahse was extracted with AcOEt (3x 10 ml). The oragnica phases collected were washed with brine (5x 10 ml) then dried over anhydrous Na_2SO_4. The desired azide was obtained as a yellowish liquid without further purification.

2,7-dimethyloctyl 4-methylazide (12)

Yield: 90%. ^{1}H NMR (400 MHz, $CDCl_3$): δ 3.17 (1H, dd, J_{vic} = 11.9 Hz J_{gem} = 5.9 Hz, C*H*$_2$N$_3$), 3.04 (1H, dd, J_{vic} = 11.9 Hz J_{gem} = 7.4 Hz, C*H*$_2$N$_3$), 1.75 (1H, m, C*H*CH$_3$), 1.28-1.3 (1H, dd, J_{vic} = 14.1 Hz J_{gem} = 3.8 Hz, C*H*$_2$(*t*-but)), 1.04 (1H, dd, J_{vic} = 14.0 Hz J_{gem} = 6.2 Hz, C*H*$_2$(*t*-but), 0.99 (3H, d, *J* = 6.7 Hz, CHC*H*$_3$), 0.90 (9H, s, *t*-but). ^{13}C NMR (100 MHz, $CDCl_3$): δ 59.4, 48.0, 29.9, 30.1, 20.6. HRMS: *m*/*z* calcd for $C_8H_{18}N_3$:156.1501; found: 156.1495

2-ethylhexyl-4-methylazide (13)

Yield: 81.4 %. ^{1}H NMR (400 MHz, $CDCl_3$): δ 3.37-3.24 (2H, m, C*H*$_2$N$_3$), 1.7-1.11 (10H, m, C*H*$_2$CHCH$_2$N), 0.92 (3H, d, J = 6.6 Hz, CHC*H*$_3$), 0.89 (6H, d, J = 6.6 Hz, CH(C*H*$_3$)$_2$). ^{13}C NMR (100 MHz, $CDCl_3$): δ 49.6, 39.2, 37.0, 35.7, 30.3, 27.9, 24.6, 22.7, 22.6, 19.4.

1-azido-4-chlorobutane

1-bromo-4-chlorobutane (5.0 g, 29.2 mmol) was dissolved in dry DMF in order to obtain a 0.4 M concentration then NaN_3 (1.2 eq) was added under inert condition. The mixture

was stirred at room temperature for 48 h then quenched with water (20 ml). The aqueous phase was extracted with Et_2O (3 x 30 ml) then the organic phases collected were washed with brine (5 x 30 ml) and dried over anhydrous Na_2SO_4. The azide was obtained as a colorless liquid in 85 % yield.

^{1}H NMR (400 MHz, $CDCl_3$): δ 3.57 (2H, t, J = 6.1, CH_2Cl), 3.33 (2H, t, J = 6.6, CH_2N_3), 1.90-1.71 (4H, m, $ClCH_2CH_2CH_2CH_2N_3$).

***1-azido-4-iodobutane*[33]**

1-azido-4-chlorobutane (3.3 g, 24.7 mmol) was dissolved in acetone (100 ml) then NaI (2 equiv.) was added. The mixture was refluxed for 48 h then quenched with water (20 ml). The reaction mixture was extracted with AcOEt (3 x 20 ml) and the combined layer dried over anhydrous Na_2SO_4. After removal the solvent under reduced pressure the product was obtained as a brownish liquid in 75 % yield.

^{1}H NMR (400 MHz, $CDCl_3$): δ 3.35 (2H, t, J = 6.7, CH_2N_3), 3.23 (2H, t, J = 6.8 Hz, CH_2I), 1.94 (2H, quint., J = 7.6 Hz, CH_2CH_2I), 1.74 (2H, quint., J = 7.6 Hz, $CH_2CH_2N_3$).

General procedure for the synthesis of PTO, PTDO, CMPT and PTC

1.00 g of 2,6 diethynylpyridine (**1**) or methyl 2,6-diethynylisonicotinate (**2**) was dissolved in 35 ml of dry DMF under inert conditions. For the synthesis of **PTC**, H_2O was used as solvent. Then, $CuSO_4{\cdot}5H_2O$ (0.02 eq.), Na ascorbate (0.2 eq.) and the appropriate alkyl azide (2.5 eq.) were added to the mixture. The resulting solution was stirred for 24/72 hours at room temperature and then quenched with water. This mixture was extracted with DCM (3 x 15ml). The organic phases were then collected, dried over anhydrous Na_2SO_4 and finally the solvents were evaporated under reduced pressure.

2,6-bis(1-dodecyl-1H-1,2,3-triazol-4-yl)pyridine (PTDO)

Reaction time 48h; yield: 50 %. ^{1}H NMR (400 MHz, $CDCl_3$): δ 8.15 (2H, bs, Py$H_{3,5}$), 8.09 (2H, bs, Py$H_{3,5}$), 7.86 (1H, bs, PyH_4), 4.42 (4H, bs, CH_2N), 1.97 (4H, bs, CH_2CH_2N), 1.37-1.27 (36H, bs, CH_2), 1.97 (6H, bs, CH_3). ^{13}C NMR (100 MHz, $CDCl_3$): δ 150.2, 148.3, 137.6, 121.8, 119.3, 50.6, 31.9, 30.4, 29.6, 29.4, 29.3, 29.0, 26.5, 22.7, 14.1. ESI-MS (+): 572.7 $[M+Na]^+$, 1122.1 $[2M+Na]^+$. mp: 125.0-125.3 °C.

2,6-bis(1-octyl-1H-1,2,3-triazol-4-yl)pyridine (PTO)

Reaction time 48h; yield: 55 %. ^{1}H NMR (400 MHz, $CDCl_3$): δ 8.18 (2H, s, Triaz-*H*), 8.12 (2H, d, *J* = 7.7 Hz, Py$H_{3,5}$), 7.88 (1H, t, *J* = 7.7 Hz, PyH_4), 4.45 (4H, t, *J* = 7.2 Hz, CH_2N), 1.99 (4H, quint, *J* = 6.9 Hz, CH_2CH_2N), 1.38-1.29 (10H, m, CH_2), 0.89 (6H, t, *J* = 6.8 Hz, CH_2CH_3). ^{13}C NMR (100 MHz, $CDCl_3$): δ 150.1, 148.3, 137.7, 121.9, 119.2, 50.5, 31.7, 30.3,

29.02, 28.94, 26.5, 22.6, 14.0. ESI-MS (+): 460.2 $[M+Na]^+$, 897.5 $[2M+Na]^+$. mp: 117.0-117.6 °C

Methyl 2,6-bis(1-octyl-1H-1,2,3-triazol-4-yl)isonicotinate (CMPT)

Reaction time 72h; yield: 90 %. ^{1}H NMR (300 MHz, $CDCl_3$): δ 8.63 (2H, bs, Triaz-*H*), 8.24 (2H, bs, Py$H_{3,5}$), 4.44 (4H, bs, CH_2N), 4.00 (3H, bs, OCH_3), 1.98 (4H, bs, NCH_2CH_2), 1.35-1.66 (10H, bs, CH_2), 0.89-0.85 (6H, t, *J* = 6.1 Hz, CH_2CH_3).

8,8′-(4,4′-(pyridine-2,6-diyl)bis(1H-1,2,3-triazole-4,1-diyl))dioctanoic acid (PTC)

Reaction time 24h; yield: 40 %. 1H NMR (400 MHz, CD3OD): δ 8.61 (2H, s, Triaz-H), 7.94 (3H, m, PyH3,4,5), 4.49 (4H, t, J = 7.0 Hz, CH2N), 2.25 (4H, t, J = 7.3 Hz, CH2CO), 1.99 (4H, quint, J = 6.9 Hz, CH2CH2N3), 1.60 (4H, quint, J = 7.0 Hz, CH_2CH_2COOH), 1.38-1.27 (12H, m, CH_2). ^{13}C NMR (100 MHz, $CDCl_3$): 176.3, 163.5, 137.7, 137.6, 127.3, 123.3, 78.9, 33.5, 29.7, 28.8, 28.7, 28.6, 28.3, 25.9, 24.7, 24.5. ESI-MS: 498.60 $[M+H]^+$, 520.70 $[M+Na]^+$, 536.61 $[M+K]^+$.

General procedure for the synthesis of PTEH, PTTO and PTID

1.00 g of 2,6 diethynylpyridine (**1**) was dissolved in 35 ml of dry DMF under inert conditions. Then, $CuSO_4 \cdot 5H_2O$ (0.06 eq.), Na ascorbate (0.6 eq.) and the appropriate alkyl azide (2.5 eq.) were added to the mixture. The resulting solution was stirred for three days (PTEH) or seven days (PTTO and PTID) at room temperature and then quenched with water. This mixture was extracted with DCM (3 x 15 ml). The organic phases collected were washed with H_2O (3 x 30 ml) and dried over anhydrous Na_2SO_4. Finally, the solvents were evaporated under reduced pressure. The crude was purified by flash column chromatography using Hexane/AcOEt 8:2 (PTEH) or 7: 3 (PTTO and PTID) as eluent.

2,6-bis(1-(2-ethylhexyl)-1H-1,2,3-triazol-4-yl)pyridine (PTEH)

yield: 65 %. ^{1}H NMR (400 MHz, $CDCl_3$): δ 8.16 (2H, s, Triaz-*H*), 8.12 (2H, d, *J* = 7.8 Hz, Py$H_{3,5}$), 7.89 (1H, t, *J* = 7.8 Hz, PyH_4), 4.34 (4H, d, *J* = 6.9 Hz, CH_2N), 1.97 (2H, quint, *J* = 6.2 Hz, C*H*CH_2N), 1.41-1.32 (16H, m, CH_2), 0.98-0.92 (12H, t, *J* = 7.4 Hz, CH_3). ^{13}C NMR (100 MHz, $CDCl_3$): δ 150.1, 148.2, 137.7, 122.3, 119.3, 53.8, 40.5, 30.4, 28.5, 23.7, 22.9, 14.0, 14.05. ESI-MS (+): 438.7 $[M+H]^+$, 460.6 $[M+Na]^+$, 897.9 $[2M+Na]^+$. mp: 60.3-60.6 °C

2,6-bis(1-(2,4,4-trimethylpentyl)-1H-1,2,3-triazol-4-yl)pyridine (PTTO)

yield: 50 %. ^{1}H NMR (600 MHz, $CDCl_3$): δ 8.20 (2H, s, Triaz-*H*), 8.10 (2H, d, *J* = 7.8 Hz, Py$H_{3,5}$), 7.86 (1H, t, *J* = 7.8 Hz, PyH_4), 4.28-4.09 (4H, 2 x dd, J_{vic} = 13.5 Hz J_{gem} = 6.2 Hz, CH_2N),

2.19-2.15 (2H, m, C*H*CH$_2$N), 1.33-1.14 (4H, 2 x dd, J_{vic} = 13.5 Hz J_{gem} = 6.2 Hz CH_2(*t*-but), 0.94 (6H, t, *J* = 6.7 Hz, CHCH_3), 0.88 (18H, s, *t*-but). ^{13}C NMR (150 MHz, CDCl$_3$): δ 150.0, 148.0, 137.9, 122.5, 119.4, 57.8, 47.8, 31.1, 30.9, 29.8, 20.3. ESI-MS (+): 76% 438 $[M+H]^+$, 100% 460.6 $[M+Na]^+$. mp: 123.8-123.9 °C

2,6-bis(1-(2,7-dimethyloctyl)-1H-1,2,3-triazol-4-yl)pyridine (PTID)

yield: 50 %. 1H NMR (400 MHz, CDCl3): δ 8.28 (2H, s, Triaz-H), 8.14 (2H, d, J = 7.8 Hz, PyH3,5), 7.91 (1H, t, J = 7.8 Hz, PyH4), 4.54-4.42 (4H, m, CH2N), 2.08-1.99 (2H, m, CH2CHCH2N), 1.84-1.75 (2H, m, CH2CHCH2N), 1.54 (4H, ept., J = 6.6 Hz, CHCH3), 1.4-1.13 (12H, m,), 1.00 (6H, d, J = 6.6 Hz, CHCH3), 0.88 (12H, d, J = 6.6 Hz, CH(CH3)2) . 13C NMR (100 MHz, CDCl3): δ 150.0, 148.3, 137.8, 121.8, 119.3, 48.8, 39.1, 37.4, 36.9, 30.3, 27.9, 24.5, 22.7, 22.6, 19.3, ESI-MS (+): 494.5 [M+H]+, 516.03 [M+Na]+, 532 [M+K]+. mp: 84.0-84.8°C

25,26,27,28-tetrapropryl-calix[4]arene (18)

25,26,27,28-tetrahydroxycalix[4]arene (3.0 g, 7.0 mmol) was dissolved in dry DMF (60 ml) then 55% NaH (4.5 eq) was added. The mixture was stirred for 1 hour whereupon 1-iodopropane (4.5 equiv.) was added. The reaction was stirred for 4 days then quenched with 1 M HCl (50 ml). The precipitate formed was filtered off. The product was obtained as a white solid in 90 % yield. ^{1}H NMR (400 MHz, CDCl$_3$): δ 6.62-6.54 (12H, m, Ar-H), 4.45 (4H, d, J = 13.2 Hz, H_{ax}), 3.85 (8H, t, J = 7.4 Hz, OCH_2CH$_2$CH$_3$), 3.15 (4H, d, J = 13.4 Hz, H_{eq}), 1.93 (8H, hex, J = 7.5 Hz, OCH$_2$CH_2CH$_3$), 0.99 (12H, t, J = Hz, OCH$_2$CH$_2$CH_3).

25,26,27-tetrahydrossi-28-propryl-calix[4]arene (19)

25,26,27,28-tetrapropylcalix [4]arene (0.5 g, 0.84 mmol) was dissolved in dry CHCl$_3$ (25 ml) under inert atmosphere. The mixture was heated up until reflux then a solution of TMSI (3 equiv) in CHCl$_3$ (25 ml) was added dropwise. The dripping should be as slow as possible in order to disfavor the formation of the 25,26,27,28-tetrahydrossicalix[4]arene. The reaction progression is checked by TLC with Hex/AcOEt 9:1 as eluent. When the monoether was the only present species (usually 4 hours), the reaction was quenched with 3 M HCl (30 ml). The aqueous phase was extracted with DCM (3 x 25 ml). The organic phases collected where washed with a 0.5 M solution of $Na_2S_2O_3$ then dried over anhydrous Na_2SO_4. After removal the solvent under reduced pressure the product was obtained as a white solid in 90 % yield.

^{1}H NMR (400 MHz, $CDCl_3$): δ 9.75 (1H, s, Ar-OH), 9.44 (2H, s, Ar-OH), 7.11-6-67 (12 H, m, Ar-H), 4.4 (2H, d, J = 13 Hz, H_{ax}), 4.3 (2H, d, J = 13.7 Hz, H_{ax}), 4.15 (2H, t, J = 6.9 Hz, $OCH_2CH_2CH_3$), 3.48 (4H, d, J = 13.4 Hz, H_{eq}), 2.22 (2H, sest., J = 7.2 Hz, $OCH_2CH_2CH_3$),1.31 (3H, t, J = 7.4 Hz, $OCH_2CH_2CH_3$).

25,26,27-tetraazidobutyl-28-propryl-calix[4]arene (20)

25,26,27-tetrahydrossi-28-propryl-calix[4]arene (0.3 g, 0.64 mmol) was dissolved in dry DMF (40 ml) then NaH (10 equiv.) was added under inert condition. The mixture was stirred for 1 hour whereupon 1-azido-4-iodobutane (6 equiv.) was added. The mixture was stirred for 4 days at room temperature then quenched with 1 M HCl (15 ml). The aqueous layer was extracted with AcOEt (3 x 15 ml). The organic phases collected were washed with a 0.5 M solution of $Na_2S_2O_3$ (1x 30 ml) and brine (3x 30 ml) then dried over anhydrous Na_2SO_4. Yield: 94 %

^{1}H NMR (300 MHz, $CDCl_3$): δ 6.66-6.6 (12 H, m, Ar-H), 4.4 (2H, d, J = 13.4 Hz, H_{ax}), 4.4 (2H, d, J = 13.3 Hz, H_{ax}), 3.94 (6H, t, J = 7.3 Hz, $OCH_2CH_2CH_2N_3$), 3.85 (2H, t, J = 7.3 Hz, $OCH_2CH_2CH_3$), 3.39 (6H, t, J = 6.8 Hz, $OCH_2CH_2CH_2N_3$), 3.2 (4H, d, J = 13.4 Hz, H_{eq}), 2.05- 1.90 (8H, m, $OCH_2CH_2CH_3$ + $OCH_2CH_2CH_2N_3$), 1.73 (6H, quint., J = 7.0 Hz, $OCH_2CH_2CH_2N_3$), 1.03 (3H, t, J = 7.4 Hz, $OCH_2CH_2CH_3$). 13C (100 MHz, $CDCl_3$): δ 156.34, 156.26, 156.1, 135.1, 135.0, 134.9, 134.8, 128.4, 128.3, 128.2, 122.3, 122.26, 122.1, 74.3, 74.2, 51.52, 51.5, 31.03, 31.0, 29.7, 27.5, 27.1, 23.4, 10.5. ESI-MS (+): 780.5 $[M+Na]^+$, 796.5 [M+K]

Calix-PTEH (22)

25,26,27-tetraazidobutyl-28-propryl-calix[4]arene (0.25 g, 0.33 mmol) was dissolved in dry DMF (40ml) whereupon monoPTEH (6 equiv.), $CuSO_4 \cdot 5H_2O$ (0.12 equiv.) and Na ascorbate (1.2 equiv.) were added. The mixture was stirred for three days at 80 °C then quenched with water. The aqueous phase was extracted with AcOEt (3x). The organic phases collected were washed with brine (3x) then dried over anhydrous Na_2SO_4. The crude was purified by flash column chromatography using Hex/AcOET 7:3 + 1% MeOH to Hex/AcOET 1:1 + 1% MeOH as eluent. The product was obtained in 56 % yield. ^{1}H NMR (400 MHz, $CDCl_3$): δ 8.52 (1H, s, triaz-H), 8.45 (2H, s, triaz-H), 8.26 (1H, s, triaz-H), 8.24 (2H, s, triaz-H), 8.13 -8.07 (6H, m, Py-H_{meta}), 7.84 (3H, t, J = 7.9 Hz, Py-H_{para}), 6.73- 6.63 (6H, m, Ar-H), 6.47- 6.43 (6H, m, Ar-H), 4.44- 4.39 (6H, m, $OCH_2(CH_2)_2CH_2$Triaz), 4.34 (2H, d, J = 13.3 Hz, H_{ax}), 4.27 (2H, d, J = 13.3 Hz, H_{ax}), 4.18 (4H, d, J = 7.8 Hz, TriazCH_2CH), 4.14 (2H, d, J = 6.9 Hz, TriazCH_2CH), 3.98-3.73 (8H, m, $OCH_2CH_2CH_3$ + $OCH_2(CH_2)_2CH_2$Triaz), 3.2 (4H, d, J = 13.4 Hz, H_{eq}), 1.98-1.73 (17

H, $OCH_2CH_2CH_3$ + $OCH_2(CH_2)_2CH_2$Triaz), 1.27-1.45 (24 H, CH_2 ethyl-hexyl chains), 1.03 (3H, t, J = 7.4 Hz, $OCH_2CH_2CH_3$), 0.88-0.77 (18 H, m, CH_3).^{13}C NMR (100 MHz, $CDCl_3$): δ 156.3, 155.9, 155.6, 150.3, 150.1, 148.3, 148.27, 148.0, 147.9, 137.95, 137.9, 135.3, 135.2, 134.3, 134.26, 128.6, 128.4, 128.1, 128.0, 122.7, 122.6, 122.5, 122.4, 122.3, 122.27, 122.1, 119.3, 119.1, 73.9, 73.8, 53.7, 53.69, 50.4, 50.3, 40.3, 40.28, 31.0, 30.3, 30.2, 28.4, 28.37, 27.1, 27.01, 27.0, 23.6, 23.5, 23.3, 22.8, 22.79, 14.0, 10.6, 10.34, 10.3. ESI-MS (+): 1605.4 $[M+H]^+$, 1628.0 $[M+Na]^+$.

Mono-PTEH

Obtained as byproduct of the formation of PTEH.

^{1}H NMR (400 MHz, $CDCl_3$): δ 8.19 (1H, s, Triaz-H), 7.56 (1H, t, J = 7.8 Hz, Py-H_{para}), 7.42 (2H, d, J = 7.7 Hz, Py-H_{meta}), 4.31 (2H, d, J = 6.8 Hz, NCH_2), 3.2 (1H, s, $H_{acetylene}$), 1.93 (1H, ept. J = 6.3, $CHCH_2N$), 1.38-1.26 (8H, m, CH_2), 0.95-0.87 (6H, m, CH_3). ESI-MS (+): 283.5 $[M+H]^+$, 305.4 $[M+Na]^+$, 321.5 $[M+K]^+$.

4.6 References

(1) Geist, A.; Hill, C.; Modolo, G.; Foreman, M. R. S. J.; Weigl, M.; Gompper, K.; Hudson, M. J.; Madic, C. 6,6′-Bis(5,5,8,8-Tetramethyl-5,6,7,8-Tetrahydro- Benzo[1,2,4]Triazin-3-Yl) [2,2′]Bipyridine, an Effective Extracting Agent for the Separation of Americium(III) and Curium(III) from the Lanthanides. *Solvent Extr. Ion Exch.* **2006**, *24* (4), 463–483. https://doi.org/10.1080/07366290600761936.

(2) Magnusson, D.; Christiansen, B.; Glatz, J. P.; Malmbeck, R.; Modolo, G.; Serrano-Purroy, D.; Sorel, C. Towards an Optimized Flow-Sheet for a SANEX Demonstration Process Using Centrifugal Contactors. *Radiochim. Acta* **2009**, *97* (3), 155–159. https://doi.org/10.1524/ract.2009.1587.

(3) Schmidt, H.; Wilden, A.; Modolo, G.; Švehla, J.; Grüner, B.; Ekberg, C. Gamma Radiolytic Stability of CyMe4BTBP and the Effect of Nitric Acid. *Nukleonika* **2015**, *60* (4), 879–884. https://doi.org/10.1515/nuka-2015-0156.

(4) Magnusson, D.; Christiansen, B.; Foreman, M. R. S.; Geist, A.; Glatz, J. P.; Malmbeck, R.; Modolo, G.; Serrano-Purroy, D.; Sorel, C. Demonstration of a SANEX Process in Centrifugal Contactors Using the CyMe4-BTBP Molecule on a Genuine Fuel Solution. *Solvent Extr. Ion Exch.* **2009**, *27* (2), 97–106. https://doi.org/10.1080/07366290802672204.

(5) Kiefer, C.; Wagner, A. T.; Beele, B. B.; Geist, A.; Panak, P. J.; Roesky, P. W. A Complexation Study of 2,6-Bis(1-(p -Tolyl)-1 H -1,2,3-Triazol-4-Yl)Pyridine Using Single-Crystal X-Ray Diffraction and TRLFS. *Inorg. Chem.* **2015**, *54* (15), 7301–7308. https://doi.org/10.1021/acs.inorgchem.5b00803.

(6) Ossola, A.; Macerata, E.; Mossini, E.; Giola, M.; Gullo, M. C. M. C.; Arduini, A.; Casnati, A.; Mariani, M. 2,6-Bis(1-Alkyl-1H-1,2,3-Triazol-4-Yl)-Pyridines: Selective

Lipophilic Chelating Ligands for Minor Actinides. *J. Radioanal. Nucl. Chem.* **2018**, *318* (3), 2013–2022. https://doi.org/10.1007/s10967-018-6253-y.

(7) Wagner, C.; Mossini, E.; Macerata, E.; Mariani, M.; Arduini, A.; Casnati, A.; Geist, A.; Panak, P. J. Time-Resolved Laser Fluorescence Spectroscopy Study of the Coordination Chemistry of a Hydrophilic CHON [1,2,3-Triazol-4-Yl]Pyridine Ligand with Cm(III) and Eu(III). *Inorg. Chem.* **2017**, *56* (4), 2135–2144. https://doi.org/10.1021/acs.inorgchem.6b02788.

(8) Travelli, C.; Aprile, S.; Rahimian, R.; Grolla, A. A.; Rogati, F.; Bertolotti, M.; Malagnino, F.; Di Paola, R.; Impellizzeri, D.; Fusco, R.; Mercalli, V.; Massarotti, A.; Stortini, G.; Terrazzino, S.; Del Grosso, E.; Fakhfouri, G.; Troiani, M. P.; Alisi, M. A.; Grosa, G.; Sorba, G.; Canonico, P. L.; Orsomando, G.; Cuzzocrea, S.; Genazzani, A. A.; Galli, U.; Tron, G. C. Identification of Novel Triazole-Based Nicotinamide Phosphoribosyltransferase (NAMPT) Inhibitors Endowed with Antiproliferative and Antiinflammatory Activity. *J. Med. Chem.* **2017**, *60* (5), 1768–1792. https://doi.org/10.1021/acs.jmedchem.6b01392.

(9) Baek, S. Y.; Kim, Y. W.; Yoo, S. H.; Chung, K.; Kim, N. K.; Kim, J. S. Synthesis and Rust Preventing Properties of Dodecyl Succinate Derivatives Containing Triazole Groups. *Ind. Eng. Chem. Res.* **2012**, *51* (28), 9669–9678. https://doi.org/10.1021/ie300316f.

(10) Ulrich, S.; Petitjean, A.; Lehn, J.-M. Metallo-Controlled Dynamic Molecular Tweezers: Design, Synthesis, and Self-Assembly by Metal-Ion Coordination. *Eur. J. Inorg. Chem.* **2010**, *2010* (13), 1913–1928. https://doi.org/10.1002/ejic.200901262.

(11) Ishihara, T.; Ohawada, K. Chemical Degradation of Kerosene Diluent with Nitric Acid. *J. Nucl. Sci. Technol.* **1966**, *3* (1), 20–26. https://doi.org/10.1080/18811248.1966.9732267.

(12) Minisci, F.; Galli, R.; Cecere, M.; Malatesta, V.; Caronna, T. Nucleophilic Character of Alkyl Radicals: New Syntheses by Alkyl Radicals Generated in Redox Processes. *Tetrahedron Lett.* **1968**, *9* (54), 5609–5612. https://doi.org/https://doi.org/10.1016/S0040-4039(00)70732-5.

(13) Gorden, A. E. V. V.; DeVore, M. A.; Maynard, B. A. Coordination Chemistry with F-Element Complexes for an Improved Understanding of Factors That Contribute to Extraction Selectivity. *Inorg. Chem.* **2013**, *52* (7), 3445–3458. https://doi.org/10.1021/ic300887p.

(14) Dam, H. H.; Reinhoudt, D. N.; Verboom, W. Multicoordinate Ligands for Actinide/Lanthanide Separations. *Chem. Soc. Rev.* **2007**, *36* (2), 367–377. https://doi.org/10.1039/b603847f.

(15) Casnati, A. Calixarenes and Cations: A Time-Lapse Photography of the Big-Bang. *Chem. Commun.* **2013**, *49* (61), 6827. https://doi.org/10.1039/c3cc43165g.

(16) Baldini, L.; Sansone, F.; Casnati, A. Cation Complexation by Calixarenes. In *Reference Module in Chemistry, Molecular Sciences and Chemical Engineering*; Elsevier, 2013. https://doi.org/10.1016/B978-0-12-409547-2.05616-X.

(17) Mullins, S. Calixarenes By C. David Gutsche, Royal Society of Chemistry, Cambridge, 1989, Pp. 210. *J. Chem. Technol. Biotechnol.* **1991**, *50* (2), 293–294. https://doi.org/https://doi.org/10.1002/jctb.280500214.

(18) Sabbatini, N.; Guardigli, M.; Mecati, A.; Balzani, V.; Ungaro, R.; Ghidini, E.; Casnati, A.; Pochini, A. Encapsulation of Lanthanide Ions in Calixarene Receptors. A Strongly Luminescent Terbium(3+) Complex. *J. Chem. Soc.{,} Chem. Commun.* **1990**, No. 12, 878–879. https://doi.org/10.1039/C39900000878.

(19) Casnati, A.; Barboso, S.; Rouquette, H.; Schwing-Weill, M.-J.; Arnaud-Neu, F.; Dozol, J.-F.; Ungaro, R. New Efficient Calixarene Amide Ionophores for the Selective Removal of Strontium Ion from Nuclear Waste: Synthesis, Complexation, and Extraction Properties. *J. Am. Chem. Soc.* **2001**, *123* (49), 12182–12190. https://doi.org/10.1021/ja016597f.

(20) Sansone, F.; Galletta, M.; Macerata, E.; Trivellone, E.; Giola, M.; Ungaro, R.; Böhmer, V.; Casnati, A.; Mariani, M. Upper-Rim CMPO-Substituted Calix[6]- and Calix[8]Arene Extractants for the An3+/Ln3+ Separation from Radioactive Waste. *Radiochim. Acta* **2008**, *96* (4–5). https://doi.org/10.1524/ract.2008.1484.

(21) Arnaud-Neu, F.; Böhmer, V.; Dozol, J.-F.; Grüttner, C.; Jakobi, R. A.; Kraft, D.; Mauprivez, O.; Rouquette, H.; Schwing-Weill, M.-J.; Simon, N.; Vogt, W. Calixarenes with Diphenylphosphoryl Acetamide Functions at the Upper Rim. A New Class of Highly Efficient Extractants for Lanthanides and Actinides. *J. Chem. Soc., Perkin Trans. 2* **1996**, No. 6, 1175–1182. https://doi.org/10.1039/P29960001175.

(22) Barboso, S.; Carrera, A. G.; Matthews, S. E.; Arnaud-Neu, F.; Böhmer, V.; Dozol, J.-F.; Rouquette, H.; Schwing-Weill, M.-J. Calix[4]Arenes with CMPO Functions at the Narrow Rim. Synthesis and Extraction Properties. *J. Chem. Soc. Perkin Trans. 2* **1999**, No. 4, 719–724. https://doi.org/10.1039/a900210c.

(23) Iqbal, M.; Mohapatra, P. K.; Ansari, S. A.; Huskens, J.; Verboom, W. Preorganization of Diglycolamides on the Calix[4]Arene Platform and Its Effect on the Extraction of Am(III)/Eu(III). *Tetrahedron* **2012**, *68* (38), 7840–7847. https://doi.org/10.1016/j.tet.2012.07.036.

(24) Ugozzoli, F.; Casnati, A.; Pochini, A.; Ungaro, R.; Arnaud, F.; Fanni, S.; Schwing, M. J.; Egberink, R. J. M.; Jong, F. de; Reinhoudt, D. N. Synthesis, Complexation, and Membrane Transport Studies of 1,3-Alternate Calix[4]Arene-Crown-6 Conformers: A New Class of Cesium Selective Ionophores. *J. Am. Chem. Soc.* **1995**, *117* (10), 2767–2777. https://doi.org/10.1021/ja00115a012.

(25) Duncan, N. C.; Roach, B. D.; Williams, N. J.; Bonnesen, P. V; Rajbanshi, A.; Moyer, B. A. N, N′-Dicyclohexyl-N″-Isotridecylguanidine as Suppressor for the Next Generation Caustic Side Solvent Extraction (NG-CSSX) Process. *Sep. Sci. Technol.* **2012**, *47* (14–15), 2074–2087. https://doi.org/10.1080/01496395.2012.697517.

(26) Casnati, A.; Della Ca', N.; Fontanella, M.; Sansone, F.; Ugozzoli, F.; Ungaro, R.; Liger, K.; Dozol, J.-F. Calixarene-Based Picolinamide Extractants for Selective An/Ln Separation from Radioactive Waste. *European J. Org. Chem.* **2005**, *2005* (11), 2338–2348. https://doi.org/https://doi.org/10.1002/ejoc.200400793.

(27) Macerata, E.; Castiglione, F.; Panzeri, W.; Mariani, M.; Sansone, F.; Casnati, A.; Mele, A. Assessing the Mechanism of the Synergistic Action of Calixarenes and Co-Dicarbollides in Lanthanide Extractions. *New J. Chem.* **2010**, *34* (11), 2552. https://doi.org/10.1039/c0nj00269k.

(28) Dondoni, A.; Marra, A.; Scherrmann, M.-C.; Casnati, A.; Sansone, F.; Ungaro, R.

Synthesis and Properties OfO-Glycosyl Calix[4]Arenes (Calixsugars). *Chem. - A Eur. J.* **1997**, *3* (11), 1774–1782. https://doi.org/10.1002/chem.19970031108.

(29) Casnati, A.; Arduini, A.; Ghidini, E.; Pochini, A.; Ungaro, R. A General Synthesis of Calix[4]Arene Monoalkyl Ethers. *Tetrahedron* **1991**, *47* (12–13), 2221–2228. https://doi.org/10.1016/S0040-4020(01)96132-0.

(30) Mondal, T.; Basak, D.; Al Ouahabi, A.; Schmutz, M.; Mésini, P.; Ghosh, S. Extended Supramolecular Organization of π-Systems Using yet Unexplored Simultaneous Intra- and Inter-Molecular H-Bonding Motifs of 1{,}3-Dihydroxy Derivatives. *Chem. Commun.* **2015**, *51* (24), 5040–5043. https://doi.org/10.1039/C4CC10335A.

(31) Takashima, S.; Abe, H.; Inouye, M. Copper(Ii)-Mediated Chiral Helicity Amplification and Inversion of Meta-Ethynylpyridine Polymers with Metal Coordination Sites. *Chem. Commun.* **2011**, *47* (26), 7455. https://doi.org/10.1039/c1cc12358k.

(32) Ostermeier, M.; Berlin, M.-A.; Meudtner, R. M.; Demeshko, S.; Meyer, F.; Limberg, C.; Hecht, S. Complexes of Click-Derived Bistriazolylpyridines: Remarkable Electronic Influence of Remote Substituents on Thermodynamic Stability as Well as Electronic and Magnetic Properties. *Chem. - A Eur. J.* **2010**, *16* (33), 10202–10213. https://doi.org/10.1002/chem.201000721.

(33) Lowery, C. A.; Park, J.; Kaufmann, G. F.; Janda, K. D. An Unexpected Switch in the Modulation of AI-2-Based Quorum Sensing Discovered through Synthetic 4,5-Dihydroxy-2,3-Pentanedione Analogues. *J. Am. Chem. Soc.* **2008**, *130* (29), 9200–9201. https://doi.org/10.1021/ja802353j.

Chapter 5
Lipophilic Ligands for An and Ln Separation Based on DGA

5.1 Introduction

At the end of the 90s Sasaki and Choppin reported about the high affinity of diglycolamides (DGA, Figure 5.1) for both trivalent An and Ln.[1,2,3] Starting from the beginning of 2000's the family of diglycolamide ligands has therefore progressively replaced malonamides in the An and Ln coextraction from the nuclear waste (Chapter 1). The replacement of a bidentate ligand as malonamide with a tridentate DGA increases the affinity for An(III) and Ln(III) thus reducing the ligand concentration and amount needed for extraction. According to the Pearson's Hard Soft Acid Base theory,[4] the DGA interaction with metal ions takes place through the three hard donor oxygen atoms present in the structure. DGA ligands are therefore referred as O_3 based chelating unit.

Nowadays diglycolamides are considered an important class of extractants for actinide partitioning in the nuclear fuel cycle. As a matter of fact the current reference molecule in EURATOM project for the An/Ln co-extraction processes is the *N,N,N',N'*-tetraoctyldiglycolamide (TODGA).[5,6] The main drawback of TODGA is the tendency of third phase formation during ions complexation probably due to a scarce solubility in the industrial diluents used as organic solvents, mainly kerosene.[7] Therefore, recently lot of efforts have been done in order to increase the ligand lipophilicity and further improve its performances.

The efficiency and selectivity of DGA based ligands depend on the alkyl chains present on the amide-N atom and on the presence of additional alkyl chains inserted in the alpha position of the carboxy group (O-CH**R**C=O). Long alkyl side chains increase the solubility in organic solvents and, consequently, the loading capability. However linear and too long alkyl chains may lead to problems connected to aggregation of extractants and high viscosity of the solution. Moreover, the derivatization of the central backbone (CH**R**-O-CH**R**) can influence the extraction behavior of the ligand. In literature, several research works were proposed which study the possibility to tune the basicity of the central oxygen atom via structural modifications of the DGA structure.[8,9]

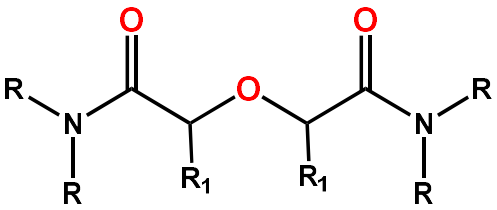

Figure 5.1. Structure of DGA based ligand

Since longer R side chains (Figure 5.1) can increase the loading capacity, two DGA derivatives, TDDGA and TDdGA, with a decyl and dodecyl chains respectively, were proposed. Among these TDDGA which showed a loading capability four times higher than TODGA and lower viscosity compare to TDdGA was selected as potential extractant in the GANEX process.[10] The increase in the loading capability determines an enhancement in the extraction efficiency. Nevertheless, a stronger extraction can lead to a high co-extraction of unwanted metal ions and to a more difficult back-extraction (stripping) process. In order to study the effect of structural modification on extraction efficiency, Iqbal et al. synthesized a series of modified DGA ligands with additional substituents on the methylene carbon atoms of the central backbone (CH_2-O-CH_2).[11] Particularly, Me-TODGA (CH_2-O-CH**Me**) and Me_2-TODGA (CH**Me**-O-CH**Me**), obtained by inserting, respectively, one methyl group on one of the two OCH_2 units of DGA or one methyl group on each of the two OCH_2 groups of DGA, showed lower distribution ratios for both An and Ln. The observed distribution ratios follow the order TODGA > Me-TODGA >, Me_2-TODGA. The lower extraction efficiency showed by the methylated TODGA derivatives determines also a reduction in the co-extraction of the unwanted fission metal ions (e.g. Sr, Mo, Zr). Also for this reason, Me-TODGA and Me_2-TODGA are promising candidate to replace TODGA in An/Ln coextraction processes. Demonstrating that the presence of alkyl groups in the backbone can deeply affect the extraction performances of the ligand, this study gave a breakthrough into the effect of structural changes of the TODGA chelating unit.

A significant development in understanding the extractant complexation mechanism of metal ions was proposed by Wilden et al.[12] with the discovery of an inversion of selectivity in the complexation of trivalent An and Ln by diastereomers of Me_2-TODGA (Figure 5.2). Even if the two diastereomers differ only in the orientation of a single methyl group, they show an unexpected difference in the extraction efficiency of trivalent f metal ions. The two diastereomers were separated in the first step of the

synthesis (*vide infra*), starting from enantiomerically pure (S)-lactate, in a molar ratio of 4:1. Since the stereochemical assignment was not immediate, the most abundant was referred as diastereomer A and the other as diastereomer B. In order to determine which of the two was the S,S and which the R,S, NMR studies were performed. Free ligands, due to the high conformational freedom of the C-C and C-O single bonds, show a rather similar ^{1}H NMR spectrum with a single multiplet for the C<u>H</u>-Me protons. Upon La^{3+} complexation the symmetry in the ^{1}H NMR spectrum was maintained for B, and the abovementioned multiplet was just shifted downfield, while the symmetry completely changed for for A, with the appearance at higher ppm of two distinct multiplets. This indicates that A and B have a Cs and C2 symmetry with R,S and S,S configuration respectively.

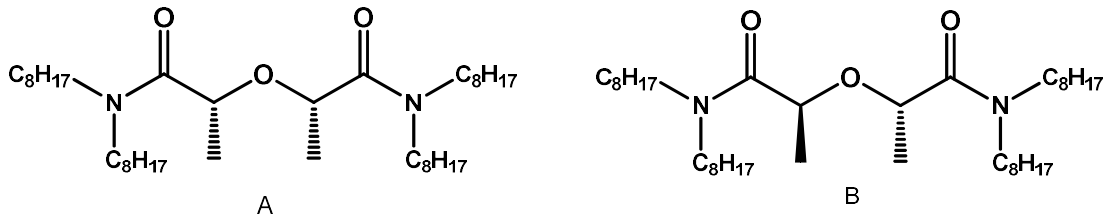

Figure 5.2. Structure of R,S-Me2TODGA (A) and S,S-Me2TODGA (B)

In order to evaluate their extraction properties, liquid-liquid extraction tests were performed. The extraction tests were conducted in 4.3 M HNO_3 with 0.1 M ligand A or ligand B in TPH. The data analysis, Figure 5.3, shows that the distribution ratios increase with decreasing ionic radius of the extracted metal ion as observed before for Me-TODGA. Evaluating the extraction behavior of both diastereomers A and B, A showed always D values higher than B with the largest difference observed for Ho. Notably, the variation in distribution ratios for Ln is greater for A than for B. Distribution ratios of Am and Cm, indicated in Figure 5.3 with filled symbols, highlight that diastereomers A and B exhibit an opposite behavior in their complexation. As expected, A shows a preference in the complexation of Cm(III) (preference always observed for DGA derivatives[13,14,15]). On the contrary, B reveals a higher D value for Am(III). Interestingly this study represents the first report of such an inversion of selectivity. In order to understand the marked different in extraction efficiency showed by diastereomers A and B, EXAFS analysis and DFT calculations were performed by the authors. The data collected showed that the difference in complexation is caused by a variation in the complexation of nitrate ions (used as counter ions) caused by the different orientation of the methyl groups in the ligand

back-bone.[12]

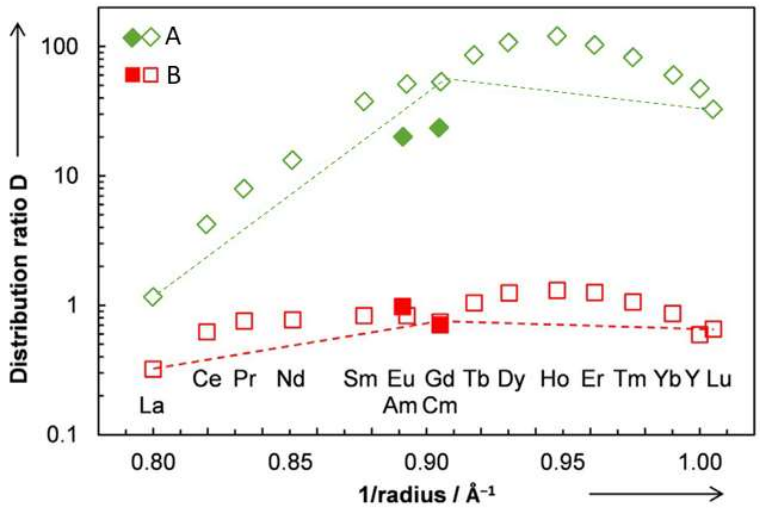

Figure 5.3. Distribution ratios of Am, Cm (filled symbols), Y, La, and other lanthanides (w/o Pm, open symbols) as a function of the inverse ionic radius. Green and red symbols represent diastereomer A and B respectively

The results obtained from the studies on dimethyl-TODGA (Me2-TODGA) demonstrated how the stereochemistry influenced ligands properties. This hypothesis is further evidenced from the extraction studies performed on a ligand with a five-membered tetrahydrofuran ring.[11] The presence of a ring in the TODGA backbone allowed to maintain the *cis*-disposition of the alpha substituents, influencing the binding behavior of the extractant. The tetrahydrofuran derivative performed worse than TODGA but better than Me_2-TODGA despite its high rigidification. The influence of structural changes in the TODGA ligand on its complexation and extraction behavior have been largely demonstrated. The evidence described so far can be the basis for further studies aiming to find better organic extractants which can overcome the weaknesses shown by TODGA.

The appeal to further understand the influence of structural changes in the central backbone of the DGAs led us to design and synthetize novel DGA-type ligands.

In this Chapter the synthesis of a derivative with **asymmetrical** substituents at the backbone, a methyl and an ethyl group (**4** and **5** in Figure 5.4), and with **symmetrical** ones, two propyl chains (**9** and **10** in Figure 5.4), at the backbone is described. In addition, considering the good results obtained with the tetrahydrofuran-DGA its derivative with bisdecylamine (**13** in Figure 5.4) has been synthesized.

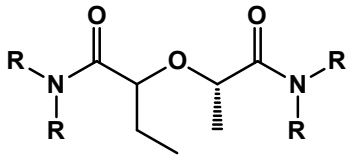

4: R = C_8H_{17}; e,m-TODGA
5: R = $C_{10}H_{21}$; e,m-TDDGA

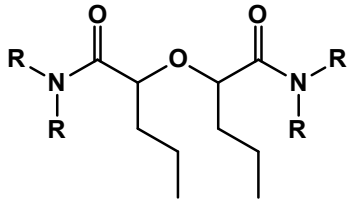

9: R = C_8H_{17}; p,p-TODGA
10: R = $C_{10}H_{21}$; p,p-TDDGA

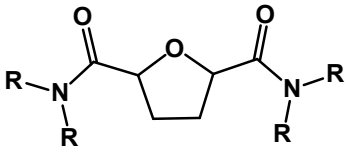

13: R = $C_{10}H_{21}$; THF-TDDGA

Figure 5.4. Structures of novel DGA-derivatives. R = C_8H_{17} or $C_{10}H_{21}$

5.2 Results and Discussion

In this chapter the synthesis of few novel An and Ln lipophilic ligands based on diglycolamide (DGA) chelating unit is presented. The experimental part was entirely carried out at the University of Twente (UTwente) during a three months secondment funded by the European GENIORS Horizon 2020 project. Due to reasons of time, the extraction results of the new DGA ligands could not yet be collected and reported in this thesis but they are expected in the next few months.

5.2.1 Synthesis

In order to study the effect of structural modifications at the backbone of the ligand on the extraction properties a symmetrical and asymmetrical DGA-derivatives were synthetized. Since the nature of the lateral chains has great influence on the extractant solubility the ligands were prepared with both C8 and C10 lateral chains. The DGAs were prepared via the Schotten-Baumann conditions.[16,17] This synthetic approach for the preparation of backbone functionalized DGAs was successfully introduced by Leoncini et al.[18] in 2016. This method is surely simpler compared the one used so far[11] which relies on the reaction between a dicarboxylic acid with the proper amine in presence of DCC. In their work Leoncini et al. focused on the synthesis of DGA bearing groups no longer than methyl at the backbone so what is herein presented is

the first attempt, to the best of our knowledge, to prepare DGAs having ethyl and propyl chains at the backbone.

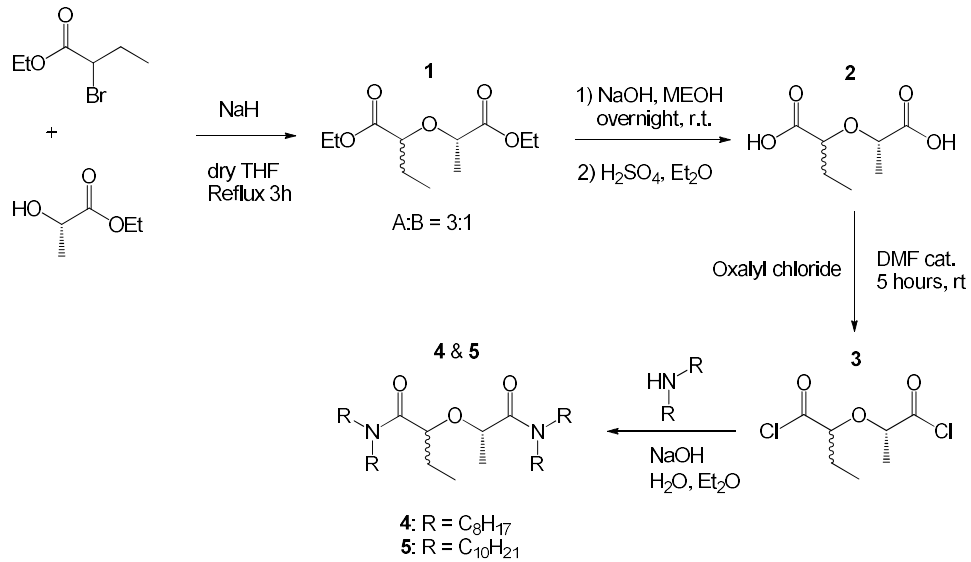

*Figure 5.5. Synthesis of e,m-TODGA (**4**) and e,m-TDDGA (**5**)*

For the synthesis of the asymmetrical derivative (e,m-TODGA and e.m-TDDGA in Figure 5.5) we started from racemic ethyl 2-bromobutanoate and (S)-ethyl lactate. NaH (1.1 equiv.) was suspended in dry THF and the mixture was cooled to 0°C with an ice bath. Then, a solution of ethyl (S)-lactate (1 equiv.) in dry THF and of racemic ethyl 2-bromobutanoate (1 equiv.) were added dropwise and sequentially. The mixture was stirred at room temperature for 1 h and then refluxed for 3 h. After removal of solvent under reduced pressure the crude was obtained as a yellowish liquid. The reaction gives rise to a mixture of diastereomers, A and B, which were separated by flash column chromatography using heptane/AcOEt 75 : 25 as eluent. Compounds A and B were obtained in 52.5 % and 17.4 % yield respectively with a ratio of 3 to 1. The separated diastereomers A and B were analyzed through NMR, Figure 5.6. The diagnostic signals are referred to the CH in the alpha position of the carboxy group (O-C*H*RC=O). The proton close to the ethyl chain gives rise to a triplet at 3.95 or 3.89 for compounds **1** A and **1** B respectively. The proton close to the methyl gives rise to a quadruplet at 4.05 or 4.07 for compounds **1** A and **1** B, respectively. Therefore, the main difference among the two spectra is the Δ between the triplet and the quadruplet signals which is 0.1 ppm for **1** A and 0.18 ppm for **1** B. A slightly difference can be observed also in the signals related to the alkylamine chains. Since no further studies on the stereochemistry of the compounds were made, we cannot assert which one of

the two diastereomers is the cis (R, S) one and which on is the trans (S, S). For this reason, we refer as A to the compound with higher RF on TLC and as B to the other one.

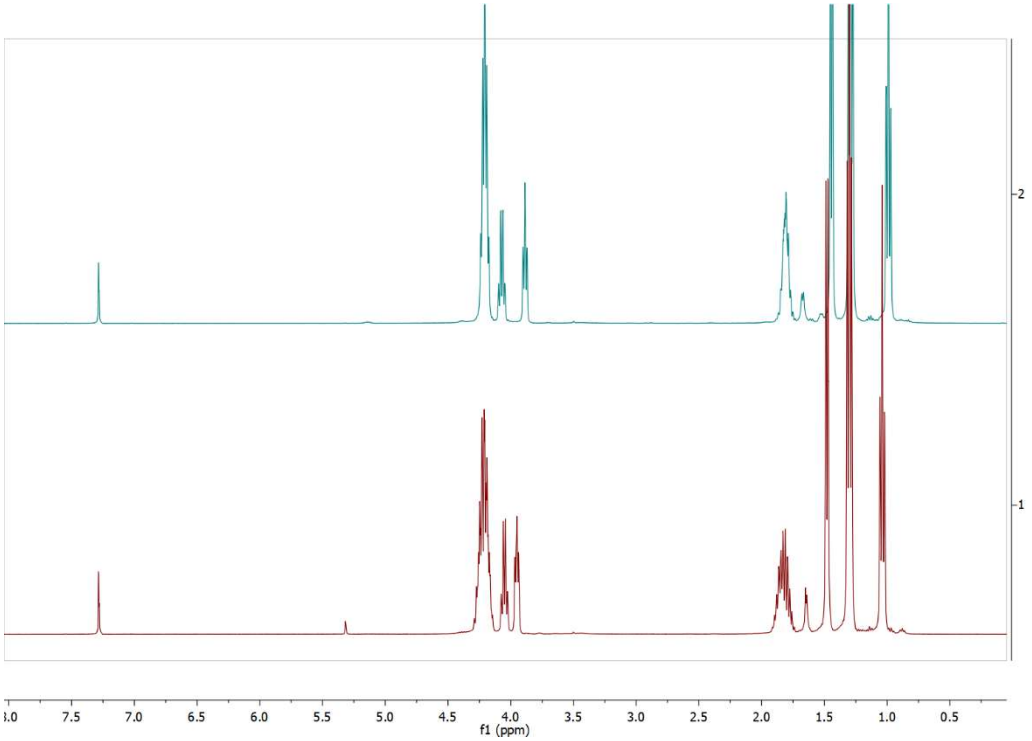

*Figure 5.6. ^{1}H NMR ($CDCl_3$, 400 MHz) of diesters **1** A (below) and **1** B (above)*

Starting from this point in the synthetic pathway (Figure 5.5), the same reactions were performed on the diastereomers A and B but, obviously, separately. Intermediates **2** were obtained through the saponification of the diesters **1**. Compound **1** and NaOH (5.6 equiv.) was dissolved in MeOH. The reaction mixture was stirred at room temperature overnight, then the solvent was evaporated under reduced pressure. The white solid obtained was kept under high vacuum in order to completely remove the methanol whereupon, the flask was cooled using an ice bath and cold 20% H_2SO_4 was added dropwise until the solid was completely dissolved. The product was extracted with AcOEt and the diacids **2** obtained pure in quantitative yield without further purification steps. The diacyl chlorides were obtained by direct chlorination of the diacids with excess of oxalyl chloride. Some drops of dry DMF were used as catalyst. After removal of the excess of oxalyl chloride, the dichlorides **3** were used directly in the following step. A solution of **3** (1 equiv. of A or B) in Et_2O was added dropwise to a solution of diamine (2.5 equiv.) in 0.8 M NaOH at 0° C over 30 minutes. The mixture

was stirred at 0° C for 2 h then the phases were separated. HCl was added to the organic layer and the solution was shaken vigorously in order to form clumps of ammonium salts which were filtered off. The organic layer was washed two more times with 10% HCl, then filtered through a glass frit (G3). Treatment with poly(4-styrenesulfonic acid) solution in water was accomplished in order to remove the excess of diamine. Then the mixture was washed with water. After removing the solvent under vacuum, the crude was purified by flash column chromatography using Heptane/AcOEt 1:1 as eluent. The products **4** A and **4** B were obtained in 56 % and 42 % yield respectively. Products **5** A and **5** B instead, were obtained in 30 % and 23 % yield.

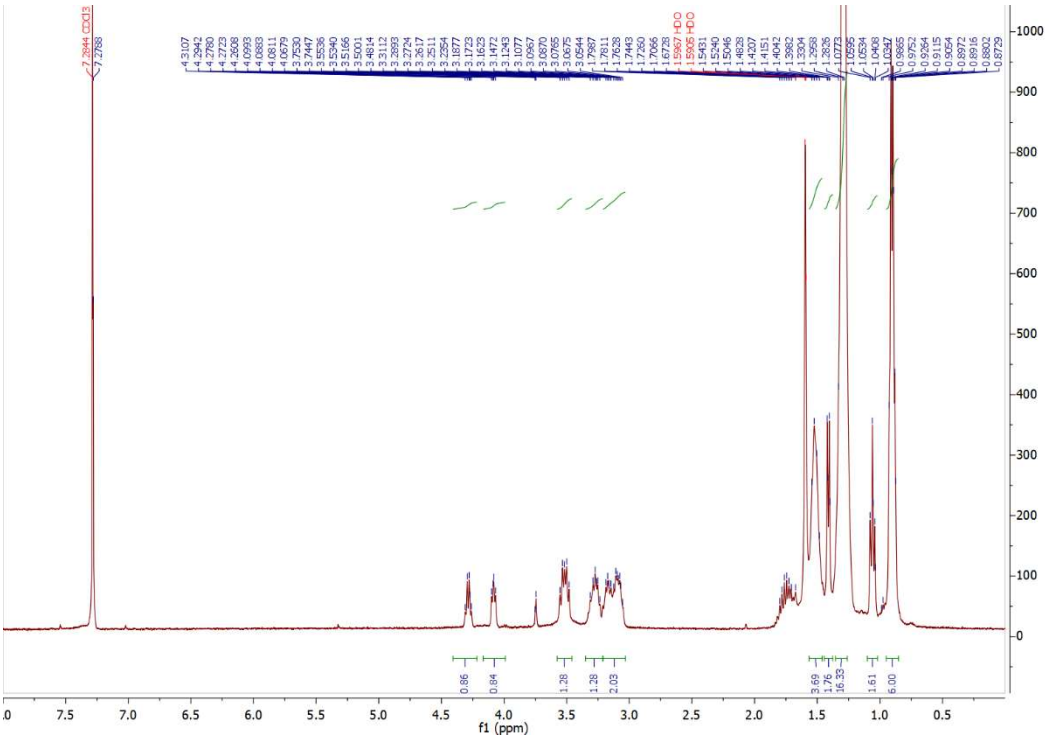

*Figure 5.7. ^{1}H NMR ($CDCl_3$, 400 MHz) of e,m-TODGA (**4** A)*

In Figure 5.7 is reported the ^{1}H NMR spectrum of e,m-TODGA **4** A which shows the presence of two different –CHR signals. At 4.28 ppm is present a quartet for the methyne proton coupled with the methyl group while at 4.08 resonates the –CHR proton (a triplet) of the methyne close to the ethyl group.

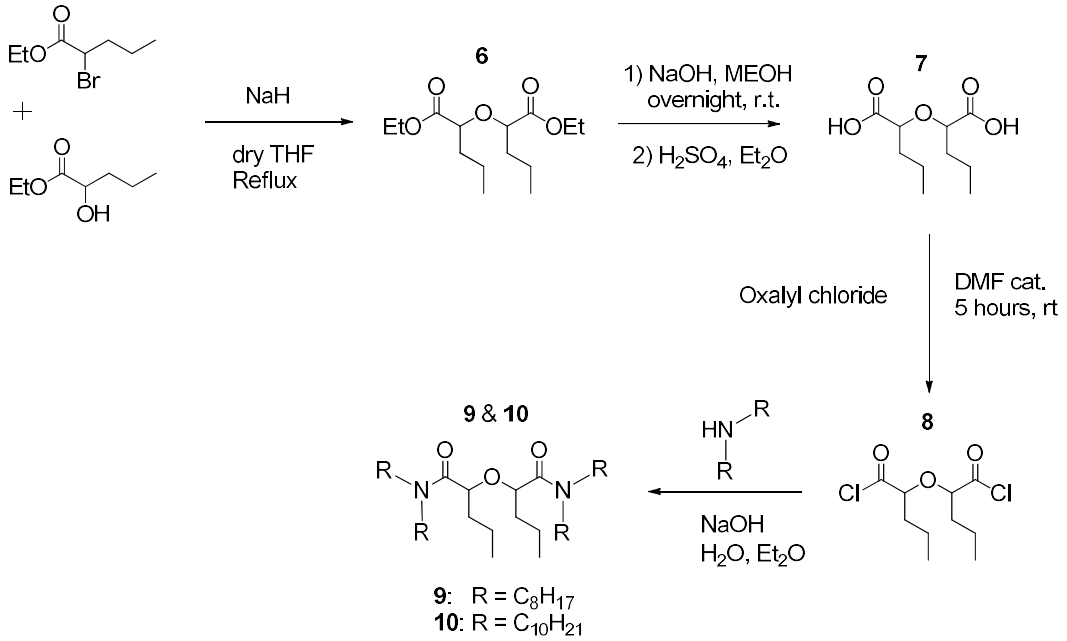

*Figure 5.8. Synthesis of p-TODGA (**9**) and p-TDDGA (**10**)*

A further modification obtained is that of p,p-TODGA derivatives **9** and **10** bearing two propyl groups in the DGA-backbone. The synthesis was performed in the same way as described for e,m-TODGA and e,m-TDDGA, now starting from racemic ethyl 2-bromopentanoate and racemic ethyl 2-hydroxypentanoate, Figure 5.8. The diastereomers **6** A and **6** B were separated at the diester stage in 59 % and 11 % yield, respectively. This time the ratios among the two diastereomers is 5 : 1 always in favor of the fastest diastereomers in the chromatographic separation. As for e,m-TODGA/TDDGA, no further studies on the stereochemistry of the compounds have been made. We refer as A to the compound with higher RF on TLC and as B to the other one. Considering the symmetry of the molecule, the diagnostic signals referred to the CH groups in the alpha position of the carboxy groups (O-C*H*RC=O) in the ^{1}H NMR spectra (Figure 5.9) give rise to a single triplet at 3.96 and to a multiplet at 3.88-3.9 for **6** A and **6** B respectively.

In the last step, intermediates **8** A and **8** B were reacted with dioctylamine and didecylamine in order to obtained compounds **9**, A and B, and compounds **10**, A and B, in 54 % and 24 % yield respectively.

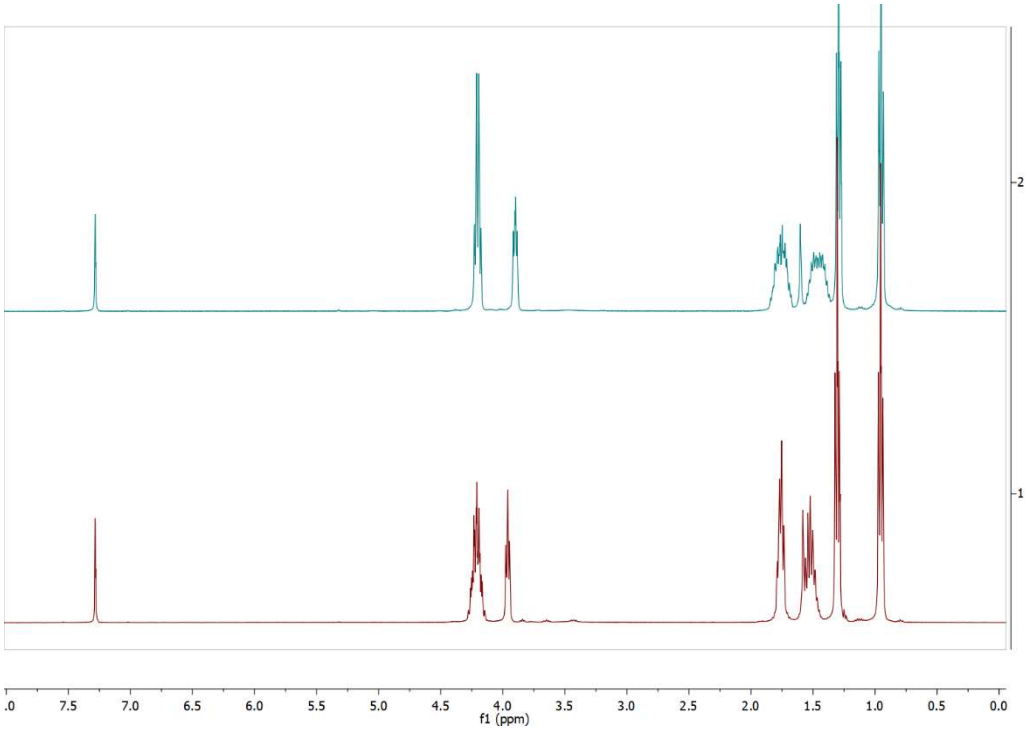

*Figure 5.9. ^{1}H NMR ($CDCl_3$, 400 MHz) of diesters **6** A (below) and **6** B (above)*

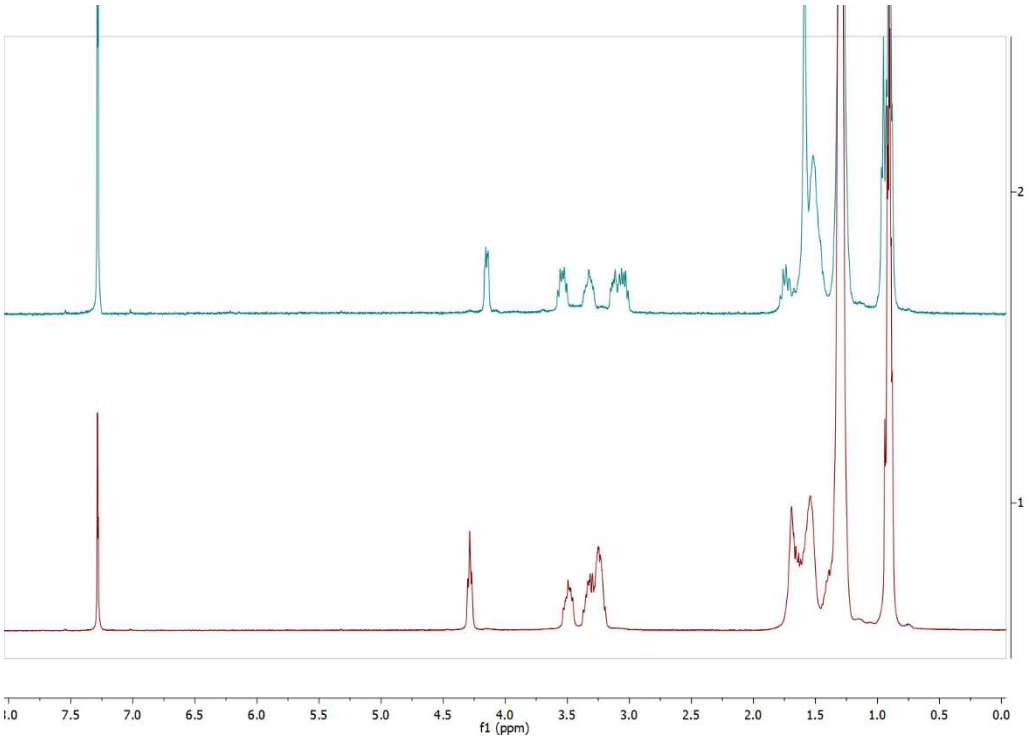

*Figure 5.10. ^{1}H NMR ($CDCl_3$, 400 MHz) of **9** A (above) and **9** B (below)*

In Figure 5.10 is reported the ^{1}H NMR spectrum of p,p-TODGA **9** A and **9** B. The single signal related to the–CHR protons at 4.14 (**9** A) and 4.29 (**9** B) confirms the symmetry of the molecule.

In order to study the effect of rigidification and preorganization of the ligand structure, the tetrahydrofuran-TODGA was synthetized by Iqbal et al.[19] Considering the appealing results obtained with this derivative, in order to enhance its properties we report the synthesis of a tetrahydrofuran-TDDGA derivative, Figure 5.11. The ccommercially available furan 2,5-dicarboxylic acid was converted into the corresponding dichloride (**11**) in excess of oxalyl chloride and DMF as catalyst. The intermediate was immediately reacted with the didecylamine (2.5 equiv.) in order to give the corresponding diamide derivative **12** in 47 % yield. Subsequent reduction with H_2 using Pd/C as a catalyst afforded the target ligand **13** in quantitative yield. The reduction was conducted in autoclave under 8 bar.

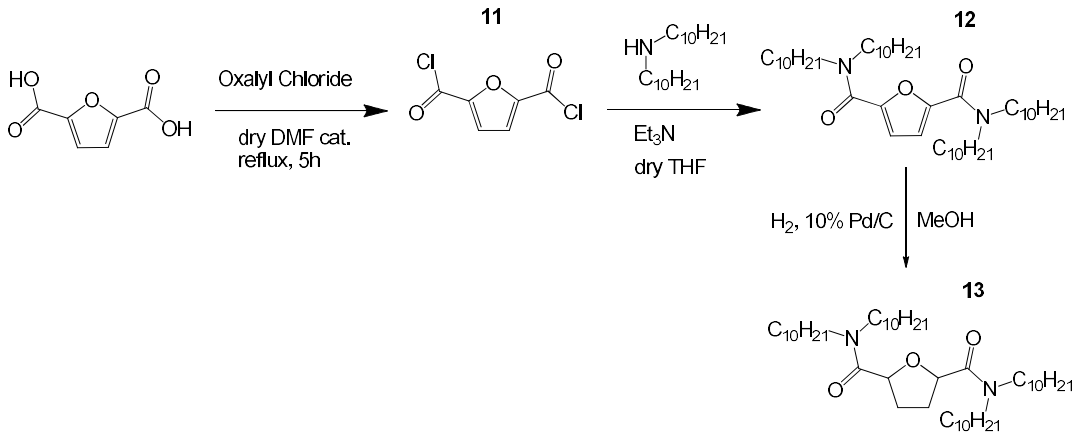

*Figure 5.11. Synthesis of tetrahydrofuran-TDDGA (**13**)*

The reduction reaction was checked by ^{1}H NMR, Figure 5.12. The absence of aromatic signals together with the appearance of a large signal of the aliphatic –CHR-O at 4.7 ppm indeed, confirms the complete conversion of the aromatic reagent **12** into the desired aliphatic cycle **13**.

The collaboration with the University of Twente has successfully led to the synthesis of 5 new DGA-based ligands. The Schotten-Baumann approach demonstrated to be a valid method for the preparation of DGAs bringing substituents at the central backbone. The prepared ligands will soon be tested in the extraction in order to evaluate their efficiency and selectivity towards trivalent An and Ln.

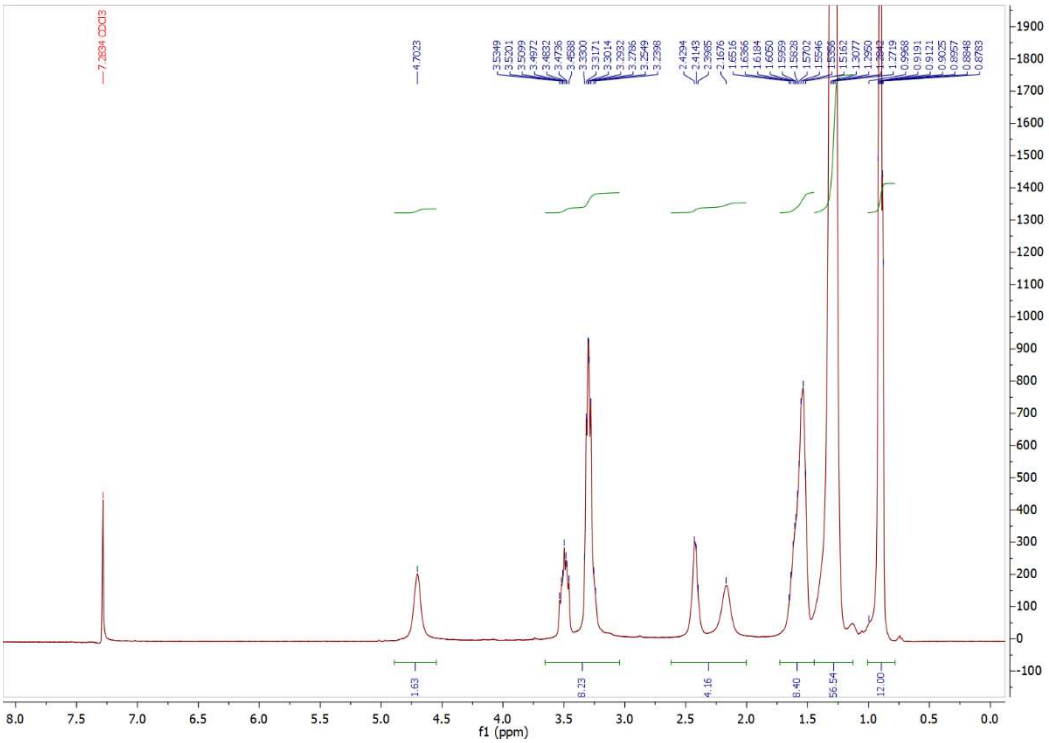

*Figure 5.12. ^{1}H NMR ($CDCl_3$, 400 MHz) of tetrahydrofuran-TDDGA **13***

5.3 Experimental part

5.3.1 General methods and chemicals

Reagents and solvents

All commercially available chemicals (Sigma-Aldrich, TCI, ChemPur, VWR) used in this study were analytical reagent grade and were used without further purification. All air sensitive reactions were carried out under nitrogen atmosphere using oven-dried glassware. All dry solvents were prepared according to standard procedures and stored over 3 or 4 Å molecular sieves.

Instrumentation and techniques

^{1}H NMR and ^{13}C NMR spectra were recorded on Bruker AscendeTM 400 MHz NMR spectrometer (observation of ^{1}H at 400 MHz and of ^{13}C at 100 MHz). Partially deuterated solvents were used as internal standards to calculate the chemical shifts (δ values in ppm). J coupling constants are given in Hz. All ^{13}C NMR spectra were performed with proton decoupling. The used abbreviations in these spectra are

singlet (s), doublet (d), triplet (t), quadruplet (q), quintuplet (quint) and multiplet (m).

In order to monitor the progress of reactions, aluminum sheets covered with silica gel 60 F-254 provided by Merck were used. All aluminum sheets were revealed under an ultraviolet lamp (λ= 254 nm) or using staining reagents.

Electrospray ionization (ESI) mass analysis were performed on a Waters micromass LCT mass spectrometer SQ Detector in positive mode using MeOH or CH_3CN as solvents. HR-MS spectra were recorded on a Waters Micromass LCT mass spectrometer with time-of-flight analyzer.

Ethyl (S)-2-(((S)-1-ethoxy-1-oxopropan-2-yl)oxy)butanoate (1 A) and ethyl (R)-2-(((S)-1-ethoxy-1-oxopropan-2-yl)oxy)butanoate (1 B)

A suspension of sodium hydride (2.2 g, 55 mmol) in hexane (10 ml) was stirred for 15 min, whereupon the solvent was removed using a pipette. Dry THF (20 ml) was added and the suspension was cooled to 0 °C using an ice bath. Then, a solution of ethyl (S)-lactate (5.7 ml, 50 mmol) in dry THF and of racemic ethyl 2-bromobutanoate (7.3 ml, 50 mmol) were added dropwise and sequentially. The mixture was stirred at room temperature for 1 h and then refluxed for 3 h. The reaction was quenched by evaporating the solvent under reduced pressure.

The crude was dissolved in water (50 ml) and the aqueous phase extracted with diethyl ether (3 x 50 ml). The organic phases collected were washed with brine (50 ml) and dried over anhydrous $MgSO_4$. The solvent was evaporated in vacuum to obtain a yellowish liquid. The crude was purified by flash column chromatography using heptane/AcOEt 75:25. Diastereomer A was obtained in 52.5 % yield while diastereomer B in 17.4 % yield.

Diasteromer A: ^{1}H NMR (400 MHz, $CDCl_3$): δ 1.04 (3H, t, *J* = 7.4 Hz, C*H*$_3$CH$_2$CH), 1.30 (6H, t, *J* = 7.2 Hz, C*H*$_3$CH$_2$OCO), 1.48 (3H, t, *J* = 6.8 Hz, C*H*$_3$CH), 1.74-1.91 (2H, m, *J* = 7.3 Hz, CH$_3$C*H*$_2$CH), 3.95 (1H, t, J = 5.0 Hz, CH$_3$CH$_2$C*H),* 4.05 (1H, q, *J* = 6.8 Hz, CH$_3$C*H*), 4.15-4.29 (4H, m, *J* = 7.2 Hz, CH$_3$C*H*$_2$OCO). ^{13}C NMR (100 MHz, $CDCl_3$): δ 172.9, 172.6, 79.1, 74.0, 60.85, 60.79, 26.4, 18.7, 14.2, 14.19, 9.7. IR (υ_{max}/cm^{-1}): 2981.8, 2937.5, 1730.3, 1447.6, 1369.9, 1268.4, 1192.5, 1127.1, 1045.9, 1022.3. ESI-MS: *m*/*z* 255.61 [100%; (M+Na)$^+$]. HRMS: *m*/*z* calcd for $C_{11}H_{20}O_5$: 255.1208; found: 255.6004.

Diasteromer B: ^{1}H NMR (400 MHz, $CDCl_3$): δ 0.99 (3H, t, *J* = 7.4 Hz, C*H*$_3$CH$_2$CH), 1.29 (6H, t, *J* = 7.2 Hz, C*H*$_3$CH$_2$OCO), 1.44 (3H, t, *J* = 6.8 Hz, C*H*$_3$CH), 1.75-1.86 (2H, m, *J* = 7.3 Hz, CH$_3$C*H*$_2$CH), 3.89 (1H, t, J = 5.8 Hz, CH$_3$CH$_2$C*H),* 4.07 (1H, q, *J* = 6.8 Hz, CH$_3$C*H*), 4.21 (4H, quint, *J* = 7.2 Hz, CH$_3$C*H*$_2$OCO). ^{13}C NMR (100 MHz, $CDCl_3$): δ 172.4, 172.0, 80.1, 75.2, 60.9, 60.8, 26.0, 18.1, 14.2, 14.1, 9.6. IR (υ_{max}/cm^{-1}): 2981.8, 2937.5, 1730.3,

1447.6, 1369.9, 1268.4, 1192.5, 1127.1, 1045.9, 1022.3. ESI-MS: *m*/*z* 255.61 [100%; $(M+Na)^+$]. HRMS: *m*/*z* calcd for $C_{11}H_{20}O_5$: 255.1208; found: 255.6047.

(S)-2-((S)-1-carboxyethoxy)butanoic acid (2 A)and (R)-2-((S)-1-carboxyethoxy)butanoic acid (2 B)

A solution of ethyl 2-(((S)-1-ethoxy-1-oxopropan-2-yl)oxy)butanoate A (2.66g, 11.45 mmol) and NaOH (2.6 g, 65 mmol) in MeOH (50 ml) was stirred overnight. Then, the solvent was evaporated under reduced pressure and the white solid obtained was kept under high vacuum in order to completely remove the solvent. The flask was cooled using an ice bath and cold 20% H_2SO_4 were added dropwise. The aqueous phase was extracted with Et_2O (3x 50 ml) then the combined organic phases were dried over anhydrous $MgSO_4$. The solvent was removed under vacuum to obtain the product in quantitative yield.

Diasteromer A: ^{1}H NMR (400 MHz, MeOD): δ 1.02 (3H, t, *J* = 7.4 Hz, C*H*$_3$CH$_2$CH), 1.43 (3H, d, J = 6.8 Hz, C*H*$_3$CH), 1.71-1.9 (2H, m, *J* = 7.1 Hz, CH$_3$C*H*$_2$CH), 3.96 (1H, t, *J* = 6.8 Hz, CH$_3$CH$_2$C*H*), 4.06 (1H, q, *J* = 6.8 Hz, CH$_3$C*H*). ^{13}C NMR (100 MHz, MeOD): δ 175.0, 174.7, 78.5, 73.6, 25.9, 17.6, 8.5. ESI-MS: *m*/*z* 199.53 [100%; $(M+Na)^+$]. IR (υ_{max}/cm^{-1}): 2980.3, 1704.7, 1465.2, 1450.4, 1419.5, 1246.2, 1161.8, 1131.7, 1069.8.

The compound was prepared following the same procedure as for ethyl 2-(((S)-1-ethoxy-1-oxopropan-2-yl)oxy)butanoate A, starting from ethyl 2-(((S)-1-ethoxy-1-oxopropan-2-yl)oxy)butanoate B (0.76 g, 3.27 mmol) and NaOH (0.75g, 18.7mmol) in MeOH (20 ml). The solvent was removed under vacuum to obtain the product in quantitative yield.

Diasteromer B: ^{1}H NMR (400 MHz, MeOD): δ 0.89 (3H, t, *J* = 7.4 Hz, C*H*$_3$CH$_2$CH), 1.31 (3H, d, J = 6.8 Hz, C*H*$_3$CH), 1.59-1.8 (2H, m, *J* = 7.1 Hz, CH$_3$C*H*$_2$CH), 3.92 (1H, t, *J* = 7.0 Hz, CH$_3$CH$_2$C*H*), 4.04 (1H, q, *J* = 6.8 Hz, CH$_3$C*H*). ^{13}C NMR (100 MHz, MeOD): δ 174.2, 173.4, 79.3, 74.7, 25.4, 17.0, 8.3. IR (υ_{max}/cm^{-1}): 2980.3, 1704.7, 1465.2, 1450.4, 1419.5, 1246.2, 1161.8, 1131.7, 1069.8. ESI-MS: *m*/*z* 199.53 [100%; $(M+Na)^+$].

General procedure 1: In situ preparation of diacyl chlorides

To a solution of a substituted dicarboxylic acid (1 mmol) dissolved in pure oxalyl chloride (2 mL), DMF (some drops) was added. The mixture was stirred under nitrogen for 4 hours, whereupon the oxalyl chloride was removed under vacuum. The product was obtained in a quantitative yield and immediately dissolved in Et_2O in order to be used for the synthesis of DGAs.

(S)-2-(((S)-1-(dioctylamino)-1-oxopropan-2-yl)oxy)-N,N-dioctylbutanamide (4 A) and (R)-

2-(((S)-1-(dioctylamino)-1-oxopropan-2-yl)oxy)-N,N-dioctylbutanamide (4 B)

A solution of diglycolyl chloride **3 A** (1.7 g, 8.0 mmol) in Et_2O (60 ml) was added dropwise to a solution of amine (4.8 g, 20.0 mmol) in 0.8 M NaOH (70 ml) at 0°C over 30 minutes. The mixture was stirred at 0° C for 2 h then the phases were separated. The aqueous layer was extracted three times (50 ml) with Et_2O. 10% HCl (40 ml) was added to the combined organic phases and the solution was shaken vigorously in order to form clumps of ammonium salts which were filtered off. The organic layer was washed with 10% HCl (2 x 30 ml) then filtered through a glass frit (G3) when necessary. A poly(4-styrenesulfonic acid) solution in water (20 ml) was added to the organic layer. The mixture was shaken vigorously to form polymeric salts as an amorphous material floating between the layers. The organic layer was washed three times with water and then separated from the polymeric salt. It was dried over anhydrous $MgSO_4$ and the solvent was evaporated under vacuum to afford a viscous oil.

The crude was purified by flash column chromatography using Heptane/AcOEt 1:1 as eluent. The product was obtained as a yellowish oil in 56 % yield.

Diasteromer A: ^{1}H NMR (400 MHz, $CDCl_3$): δ 0.89-0.91 (12H, bs, $N(CH_2)_7CH_3$), 1.06 (3H, t, *J* = 7.2 Hz, CH_3CH_2CH), 1.29 (40 H, s, $NCH_2CH_2CH_3$), 1.41 (3H, d, J = 6.4 Hz, CH_3CH), 1.53 (8H, bs, NCH_2CH_2), 1.67-1.8 (2 H, m, CH_3CH_2CH), 3.07-3.31 + 3.48-3.56 (8H, m, $NCH_2CH_2CH_3$), 4.07-4.1 (1H, broad triplet, CH_3CH_2CH), 4.28 (1H, q, *J* = 6.5 Hz, CH_3CH). IR (υ_{max}/cm^{-1}): 2956.3, 2923.5, 2854.4, 1653.2, 1458.2, 1425.7, 1377.4, 1120.0. ESI-MS: *m*/*z* 646.81 [100%; $(M+Na)^+$]. HRMS: *m*/*z* calcd for $C_{39}H_{78}N_2O_3Na$: 645.5910; found: 645.5751

A solution of diglycolyl chloride **3** B (0.5 g, 2.44 mmol) in Et_2O (20 ml) was added dropwise to a solution of amine (1.5 g, 6.1 mmol) in 0.8 M NaOH (40 ml) at 0°C over 30 minutes. The mixture was stirred at 0° C for 2 h then the phases were separated. The aqueous layer was extracted three times (20 ml) with Et_2O. 10% HCl (20 ml) was added to the combined organic phases and the solution was shaken vigorously in order to form clumps of ammonium salts which were filtered off. The organic layer was washed with 10% HCl (2 x 20 ml) then filtered through a glass frit (G3) when necessary. A poly(4-styrenesulfonic acid) solution in water (10 ml) was added to the organic layer. The mix was shaken vigorously to form polymeric salts as an amorphous material floating between the layers. The organic layer was washed three times with water and then separated from the polymeric salt. It was dried over anhydrous $MgSO_4$ and the solvent was evaporated under vacuum to afford a viscous oil.

The crude was purified by flash column chromatography using Heptane/AcOEt 1:1 as

eluent. The product was obtained as a yellowish oil in 42 % yield.

Diasteromer B: ^{1}H NMR (400 MHz, $CDCl_3$): δ 0.88-0.92 (12H, bs, $N(CH_2)_7CH_3$), 1.54 (3H, t, *J* = 7.2 Hz, CH_3CH_2CH), 1.29 (40H, s, $NCH_2CH_2(CH_2)_5CH_3$), 1.41 (3H, d, J = 6.4 Hz, CH_3CH), 1.52 (8H, bs, NCH_2CH_2), 1.67-1.83 (2H, m, CH_3CH_2CH), 3.05-3.32 + 3.48-3.55 (8H, m, $NCH_2CH_2(CH2)_5CH_3$), 4.09 (1H, broad triplet, CH_3CH_2CH), 4.28 (1H, q, *J* = 6.6 Hz, CH_3CH). IR (υ_{max}/cm^{-1}): 2954.9, 2922.9, 2854.6, 1646.1, 1464.1, 1427.0, 1376.5, 1110.9. ESI-MS: *m*/*z* 646.83 [100%; $(M+Na)^+$]. HRMS: *m*/*z* calcd for $C_{39}H_{78}N_2O_3Na$: 645.5910; found: 645.5796.

N,N-didecyl-2-(((S)-1-(N,N-didecylamino)-1-oxopropan-2-yl)oxy)butanamide (5 A)

A solution of diglycolyl chloride **3** A (1.5 g, 7.04 mmol) in Et_2O (60 ml) was added dropwise to a solution of amine (5.24 g, 17.6 mmol) in 0.8 M NaOH (60 ml) at 0°C over 30 minutes. The mixture was stirred at 0° C for 2 h then the phases were separated. The aqueous layer was extracted three times (30 ml) with Et_2O. 10% HCl (20 ml) was added to the combined organic phases and the solution was shaken vigorously in order to form clumps of ammonium salts which were filtered off. The organic layer was washed with 10% HCl (2 x 30 ml) then filtered through a glass frit (G3) when necessary. A poly(4-styrenesulfonic acid) solution in water (10 ml) was added to the organic layer. The mix was shaken vigorously to form polymeric salts as an amorphous material floating between the layers. The org layer was washed three times with water and then separated from the polymeric salt. It was dried over anhydrous $MgSO_4$ and the solvent was evaporated under vacuum to afford a viscous oil.

The crude was purified by flash column chromatography using Heptane/AcOEt 1:1 as eluent. The product was obtained as a yellowish oil in 30 % yield.

Diasteromer A: ^{1}H NMR (400 MHz, $CDCl_3$): δ 0.88-0.92 (12H, m, $NCH_2CH_2(CH_2)_7CH_3$), 1.06 (3H, t, *J* = 7.2 Hz, CH_3CH_2CH), 1.29 (56 H, s, $NCH_2(CH_2)_7CH_3$), 1.41 (3H, d, J = 6.3 Hz, CH_3CH), 1.52 (8H, bs, $NCH_2CH_2(CH_2)_7CH_3$), 1.68-1.85 (2 H, m, CH_3CH_2CH), 3.05-3.32 + 3.48-3.56 (8H, m, $NCH_2CH_2(CH_2)_7CH_3$), 4.08 (1H, broad triplet, CH_3CH_2CH), 4.28 (1H, q, *J* = 6.5 Hz, CH_3CH). IR (υ_{max}/cm^{-1}): ESI-MS: 757.65 *m*/*z* [100%; $(M+Na)^+$]. HRMS: *m*/*z* calcd for $C_{47}H_{94}N_2O_3Na$: 757.7162 found: 757.6318.

N,N-didecyl-2-(((S)-1-(N,N-?didecylamino)-1-oxopropan-2-yl)oxy)butanamide (5 B)

A solution of diglycolyl chloride 3 B (1.6 g, 7.5 mmol) in Et2O (50 ml) was added dropwise to a solution of amine (5.6 g, 18.8 mmol) in 0.8 M NaOH (50 ml) at 0°C over 30 minutes. The mixture was stirred at 0° C for 2 h then the phases were separated. The aqueous

layer was extracted three times (3 x 30 ml) with Et_2O. 10% HCl (20 ml) was added to the combined organic phases and the solution was shaken vigorously in order to form clumps of ammonium salts which were filtered off. The organic layer was washed with 10% HCl (2 x 30 ml) then filtered through a glass frit (G3) when necessary. A poly(4-styrenesulfonic acid) solution in water (10 ml) was added to the organic layer. The mix was shaken vigorously to form polymeric salts as an amorphous material floating between the layers. The org layer was washed three times with water and then separated from the polymeric salt. It was dried over anhydrous $MgSO_4$ and the solvent was evaporated under vacuum to afford a viscous oil.

The crude was purified by flash column chromatography using Heptane/AcOEt 1:1 as eluent. The product was obtained as a yellowish oil in 23 % yield.

Diasteromer B: ^{1}H NMR (400 MHz, $CDCl_3$): δ 0.88-0.95 (15H, m, $NCH_2CH_2(CH_2)_7CH_3$ + CH_3CH_2CH), 1.32 (59 H, s, $NCH_2(CH_2)_7CH_3$ + CH_3CH_2CH), 1.53 (8H, bs, $NCH_2CH_2(CH_2)_7CH_3$), 1.69-1.81 (2H, m, CH_3CH_2CH), 3.16-3.59 (8H, m, $NCH_2CH_2(CH_2)_7CH_3$), 4.16-4.21 (1H, broad triplet, CH_3CH_2CH), 4.42-4.46 (1H, q, J = 6.5 Hz, CH_3CH). IR (υ_{max}/cm^{-1}): 2921.3, 2852.5, 1750.7, 1649.8, 1464.3, 1375.8, 1200.9, 1112.2. ESI-MS: 757.45 *m*/*z* [100%; $(M+Na)^+$]. HRMS: *m*/*z* calcd for $C_{47}H_{94}N_2O_3Na$: 757.7162 found: 757.6376.

Diethyl 2,2'-oxydipentanoate (6 A and 6 B)

A suspension of sodium hydride (1.5 g, 37.6 mmol) in hexane (10 ml) was stirred for 15 min, whereupon the solvent was removed using a pipette. Dry THF (20 ml) was added and the suspension was cooled to 0° C using an ice bath. Then, a solution of ethyl (±)-2-hydroxyvalerate (5.0 g, 34.2 mmol) in dry THF and of ethyl 2-bromovalerate (7.15 g, 34.2) were added dropwise and sequentially. The mixture was stirred at room temperature for 1 h and then refluxed for 3 h. The solvent was evaporated under reduced pressure. The crude was dissolved in water (50 ml) and the aqueous phase extracted with diethyl ether (3x50 ml). The combined organic phases were washed with brine (50 ml) and dried over anhydrous $MgSO_4$. The solvent was evaporated in vacuum to obtain a yellowish liquid. The crude was purified by flash column chromatography using Heptane/AcOEt 9:1 as eluent. Diastereomer A was obtained in 59 % yield while diastereomer B in 11.0 % yield.

Diastereomer A: ^{1}H NMR (400 MHz, $CDCl_3$): δ 0.95 (3H, t, J = 7.4 Hz, CH_3CH_2OCO), 1.3 (3H, t, J = 7.2, CH_3CH_2), 1.46-1.56 (2H, m, $CH_3CH_2CH_2CH$), 1.74-1.79 (2H, m, $CH_3CH_2CH_2CH$), 3.96 (1H, t, J = 6.2 Hz, $COCHO$), 4.15-4.28 (2H, m, CH_3CH_2OCO). ^{13}C NMR (100 MHz, $CDCl_3$): δ 172.7, 77.7, 60.7, 35.3, 18.5, 14.2, 13.8. IR (υ_{max}/cm^{-1}): 2962.5,

2874.7, 1747.6, 1732.2, 1466.6, 1380.8, 1265.03, 1190.1, 1130.5, 1096.3, 1025.2. ESI-MS: *m*/*z* 297.64 [100%; $(M+Na)^+$]. HRMS: *m*/*z* calcd for $C_{14}H_{26}O_5Na$ 297.1678; found: 297.11.

Diastereomer B: ^1H NMR (400 MHz, $CDCl_3$): δ 0.95 (3H, t, J = 7.4 Hz, CH_3CH_2OCO), 1.3 (3H, t, J = 7.2, CH_3CH_2), 1.37-1.55 (2H, m, $CH_3CH_2CH_2CH$), 1.98-1.84 (2H, m, $CH_3CH_2CH_2CH$), 3.88-3.9 (1H, m, COCHO), 4.2 (2H, q, J = 7.1 Hz, CH_3CH_2OCO). ^{13}C NMR (100 MHz, $CDCl_3$): δ 172.2, 79.7, 60.8, 34.9, 18.5, 14.2, 13.8. IR (υ_{max}/cm^{-1}): 2960.8, 2875.2, 1750.4, 1730.8, 1466.5, 1368.3, 1271.5, 1185.6, 1128.3, 1028.2. ESI-MS: *m*/*z* 297.66 [100%; $(M+Na)^+$]. HRMS: *m*/*z* calcd for $C_{14}H_{26}O_5Na$: 297.1678; found: 297.1217.

2,2'-oxydipentanoic acid (7 A and 7 B)

A solution of **diethyl 2,2'-oxydipentanoate 6 A** (4.2 g, 15.3 mmol) and NaOH (3.4 g, 85.7 mmol) in MeOH (80 ml) was stirred overnight. Then, the solvent was evaporated under reduced pressure and the white solid obtained was kept under high vacuum in order to completely remove the solvent. The flask was cooled using an ice bath and cold 20% H_2SO_4 (20 ml) were added dropwise. The aqueous phase was extracted with Et_2O (3x 50 ml) then the combined organic phases were dried over anhydrous $MgSO_4$. The solvent was removed under vacuum to obtain the product in quantitative yield.

Diastereomer A: ^1H NMR (400 MHz, $CDCl_3$): δ 0.97 (3H, t, *J* = 7.0 Hz, $CH_3CH_2CH_2CH$), 1.56 (2H, sest, *J* = 7.7 Hz, $CH_3CH_2CH_2CH$), 1.84 (2H, q, *J* = 6 Hz, $CH_3CH_2CH_2CH$), 4.1 (1H, t, *J* = 6.0 Hz, $CH_3CH_2CH_2CH$). ^{13}C NMR (100 MHz, $CDCl_3$): δ 178.3, 77.3, 35.1, 18.3, 13.7. IR (υ_{max}/cm^{-1}): 2963.7, 2875.4, 1717.7, 1455.0, 1420.9, 1254.2, 1208.7, 1132.3, 1094.5. ESI-MS: *m*/*z* 241.57 [100%; $(M+Na)^+$]. HRMS: *m*/*z* calcd for $C_{10}H_{18}O_5Na$: 241.2371; found: 241.2011.

The compound was prepared following the same procedure as for **2,2'-oxydipentanoic acid 7 A**, starting from diethyl 2,2'-oxydipentanoate **6 B** (0.76 g, 3.27 mmol) and NaOH (0.75g, 18.7mmol) in MeOH (20 ml). The solvent was removed under vacuum to obtain the product in quantitative yield.

Diastereomer B: ^1H NMR (400 MHz, $CDCl_3$): δ 0.99 (3H, t, *J* = 7.4 Hz, $CH_3CH_2CH_2CH$), 1.50 (2H, sest, *J* = 7.4 Hz, $CH_3CH_2CH_2CH$), 1.82-1.87 (2H, q, *J* = 6 Hz, $CH_3CH_2CH_2CH$), 4.01 (1H, t, *J* = 6 Hz, $CH_3CH_2CH_2CH$). ^{13}C NMR (100 MHz, $CDCl_3$): δ 175.8, 80.0, 34.5, 18.22, 13.8. IR (υ_{max}/cm^{-1}): 2960.6, 2875.4, 1715.6, 1380.24, 1212.7, 1123.8, 1092.7. ESI-MS: *m*/*z* 241.59 [100%; $(M+Na)^+$]. HRMS: *m*/*z* calcd for $C_{10}H_{18}O_5Na$: 241.2371; found: 241.1947.

2,2'-oxybis(N,N-dioctylpentanamide) (9 A and 9 B)

Diglycolyl chloride **8 A** and **8** B were obtained following the general procedure 1.

A solution of diglycolyl chloride **8 A** (3.2 g, 12.5 mmol) in Et_2O (90 ml) was added dropwise

to a solution of amine (76 g, 31.3 mmol) in 0.8 M NaOH (100 ml) at 0°C over 30 minutes. The mixture was stirred at 0° C for 2 h then the phases were separated. The aqueous layer was extracted three times (50 ml) with Et_2O. 10% HCl (40 ml) was added to the combined organic phases and the solution was shaken vigorously in order to form clumps of ammonium salts which were filtered off. The organic layer was washed with 10% HCl (2 x 30 ml) then filtered through a glass frit (G3) when necessary. A poly(4-styrenesulfonic acid) solution in water (20 ml) was added to the organic layer. The mix was shaken vigorously to form polymeric salts as an amorphous material floating between the layers. The org layer was washed three times with water and then separated from the polymeric salt. It was dried over anhydrous $MgSO_4$ and the solvent was evaporated under vacuum to afford a viscous oil.

The crude was purified by flash column chromatography using Heptane/AcOEt 8:2 as eluent. The product was obtained as a yellowish oil in 54 % yield.

Diastereomer A: ^{1}H NMR (400 MHz, $CDCl_3$): δ ^{1}H NMR (400 MHz, $CDCl_3$): 0.85-0.97 (18H, m, N $CH_2CH_2(CH_2)_5CH_3$ + $CHCH_2CH_2CH_3$), 1.28-1.33 (44H, s, $NCH_2CH_2(CH_2)_5CH_3$, $CHCH_2CH_2CH_3$), 1.44-1.55 (8H, m, $NCH_2CH_2(CH_2)_5CH_3$), 1.67-1.78 (4H, m, $CHCH_2CH_2CH_3$), 3.00-3.08, 3.09-3.15, 3.28-3.36, 3.50-3.57 (2H each, m, $CH_2CH_2(CH_2)_5CH_3$), 4.14 (2H, t, J = 6.4 Hz, $CHCH_2CH_2CH_3$). ^{13}C NMR (100 MHz, $CDCl_3$): δ 171.4, 75.5, 47.1, 46.1, 35.7, 31.8, 29.4, 29.3, 29.29, 29.2, 27.7, 27.1, 26.9, 22.6, 18.9, 14.1, 18.9, 14.1, 14.0. IR (υ_{max}/cm^{-1}): 2956.3, 2923.5, 2854.4, 1653.2, 1458.2, 1425.7, 1377.4, 1120.1, 1091. ESI-MS: m/z 687.61 [100%; $(M+Na)^+$]. HRMS: m/z calcd for $C_{42}H_{84}N_2O_3Na$: 688.1995; found: 687.6371.

Diastereomer B: A solution of diglycolyl chloride **8 B** (0.8 g, 3.13 mmol) in Et_2O (25 ml) was added dropwise to a solution of amine (1.9 g, 7.8 mmol) in 0.8 M NaOH (25 ml) at 0°C over 30 minutes. The mixture was stirred at 0° C for 2 h then the phases were separated. The aqueous layer was extracted three times (3x20 ml) with Et_2O. 10% HCl (20 ml) was added to the combined organic phases and the solution was shaken vigorously in order to form clumps of ammonium salts which were filtered off. The organic layer was washed with 10% HCl (2 x 30 ml) then filtered through a glass frit (G3) when necessary. A poly(4-styrenesulfonic acid) solution in water (10 ml) was added to the organic layer. The mix was shaken vigorously to form polymeric salts as an amorphous material floating between the layers. The org layer was washed three times with water and then separated from the polymeric salt. It was dried over anhydrous $MgSO_4$ and the solvent was evaporated under vacuum to afford a viscous

oil. The crude was purified by flash column chromatography using Heptane/AcOEt 8:2 as eluent. The product was obtained as a yellowish oil in 24 % yield.

^{1}H NMR (400 MHz, $CDCl_3$): ^{1}H NMR (400 MHz, $CDCl_3$): 0.89-0.95 (18 H, m, $N(CH_2)_7CH_3$ + $CHCH_2CH_2CH_3$), 1.3 (40 H, s, $NCH_2CH_2(CH_2)_5CH_3$), 1.3-1.4 (4H, m, $CHCH_2CH_2CH_3$), 1.5-1.73 (12H, m, $NCH_2CH_2(CH_2)_5CH_3$ + $CHCH_2CH_2CH_3$), 3.21-3.53 (8H, m, $NCH_2CH_2(CH_2)_5CH_3$), 4.29 (2H, t, J = 6.5 Hz), $CHCH_2CH_2CH_3$). ^{13}C NMR (100 MHz, $CDCl_3$): δ 171.62, 76.054, 46.8, 34.8, 31.8, 31.77, 29.4, 29.3, 27.4, 27.1, 26.9, 22.6, 18.9, 14.1, 14.0. IR (υ_{max}/cm^{-1}): 2956.1, 2923.6, 2854.2, 1651.9, 1458.8, 1426.7, 1377.3, 1111.2, 1085.3. ESI-MS: *m*/*z* 688.18 [100%; $(M+Na)^+$]. HRMS: *m*/*z* calcd for $C_{42}H_{84}N_2O_3Na$: 688.1995; found: 687.6543.

2,2'-oxybis(N,N-didecylpentanamide) (10 A)

A solution of diglycolyl chloride (1.1 g, 4.3 mmol) in Et_2O (40 ml) was added dropwise to a solution of amine (3.2 g, 10.7 mmol) in 0.8 M NaOH (40 ml) at 0°C over 30 minutes. The mixture was stirred at 0° C for 2 h then the phases were separated. The aqueous layer was extracted three times (30 ml) with Et_2O. 10% HCl (20 ml) was added to the combined organic phases and the solution was shaken vigorously in order to form clumps of ammonium salts which were filtered off. The organic layer was washed with 10% HCl (2 x 20 ml) then filtered through a glass frit (G3) when necessary. A poly(4-styrenesulfonic acid) solution in water (20 ml) was added to the organic layer. The mix was shaken vigorously to form polymeric salts as an amorphous material floating between the layers. The org layer was washed three times with water and then separated from the polymeric salt. It was dried over anhydrous $MgSO_4$ and the solvent was evaporated under vacuum to afford a viscous oil.

The crude was purified by flash column chromatography using Heptane/AcOEt 9:1 as eluent. The product was obtained as a yellowish oil in 45 % yield.

^{1}H NMR (400 MHz, $CDCl_3$): δ 0.88-0.97 (18 H, m, $N(CH_2)_7CH_3$ + $CHCH_2CH_2CH_3$), 1.29 (56 H, s, $NCH_2CH_2(CH_2)_7CH_3$), 1.44-1.78 (16H, m, N $CH_2CH_2(CH_2)_6CH_3$ + $CHCH_2CH_2CH_3$), 3.01 -3.57 (8 H, m, $NCH_2CH_2(CH_2)_7CH_3$), 4.13 – 4.16 (2H, m, $CHCH_2CH_2CH_3$). ^{13}C NMR (100 MHz, $CDCl_3$): 171.4, 75.4, 47.2, 46.1, 35.6, 31.9, 29.64, 29.59, 29.6, 29.5, 29.44, 29.41, 29.3, 27.6, 27.1, 27.0, 22.7, 18.9, 14.1, 14.0. IR (υ_{max}/cm^{-1}): 2956.2, 2921.4, 2852.8, 1653.3, 1465.4, 1425.7, 1376.9, 1121.0, 1089.7. ESI-MS: *m*/*z* 799.6162 [100%; $(M+Na)^+$]. HRMS: *m*/*z* calcd for $C_{50}H_{100}N_2O_3Na$: 799.7632; found: 799.6131.

2,2'-oxybis(N,N-didecylpentanamide) (10 B)

A solution of diglycolyl chloride **8 B** (1.3 g, 5.3 mmol) in Et_2O (40 ml) was added dropwise

to a solution of amine (3.9 g, 13.2 mmol) in 0.8 M NaOH (40 ml) at 0°C over 30 minutes. The mixture was stirred at 0° C for 2 h then the phases were separated. The aqueous layer was extracted three times (30 ml) with Et_2O. 10% HCl (20 ml) was added to the combined organic phases and the solution was shaken vigorously in order to form clumps of ammonium salts which were filtered off. The organic layer was washed with 10% HCl (2 x 20 ml) then filtered through a glass frit (G3) when necessary. A poly(4-styrenesulfonic acid) solution in water (20 ml) was added to the organic layer. The mix was shaken vigorously to form polymeric salts as an amorphous material floating between the layers. The org layer was washed three times with water and then separated from the polymeric salt. It was dried over anhydrous $MgSO_4$ and the solvent was evaporated under vacuum to afford a viscous oil.

The crude was purified by flash column chromatography using Heptane/AcOEt 8:2 as eluent. The product was obtained as a yellowish oil in 50 % yield.

^{1}H NMR (400 MHz, $CDCl_3$): δ 0.89-0.95 (18H, m, $N(CH_2)_7CH_3$ + $CHCH_2CH_2CH_3$), 1.29 (56 H, s, $NCH_2CH_2(CH_2)_7CH_3$), 1.5-1.73 + 2.00 (16H, m, $N\ CH_2CH_2(CH_2)_6CH_3$ + $CHCH_2CH_2CH_3$), 3.21-3.53 (8H, m, $NCH_2CH_2(CH_2)_7CH_3$), 4.33 (2H, t, J = 6.5 Hz), $CHCH_2CH_2CH_3$). ^{13}C NMR (100 MHz, $CDCl_3$): 171.1, 75.4, 47.41, 46.42, 34.54, 31.9, 31.88, 29.62, 29.60, 29.57, 29.53, 29.45, 29.42, 29.41, 29.31, 27.5, 27.1, 27.0, 22.7, 18.9, 14.1, 14.0. IR (υ_{max}/cm^{-1}): 2956.6, 2921.4, 2852.7, 1652.7, 1465.2, 1427.0, 1377.4, 1110.7, 1079.9. ESI-MS: *m*/*z* 799.58 [100%; $(M+Na)^+$]. HRMS: *m*/*z* calcd for $C_{50}H_{100}N_2O_3Na$: 799.7632; found: 799.6083.

Furan-2,5-dicarbonyl dichloride (FDCA-Cl_2)

Prepared in situ according to **General procedure 1**.

N,N,N',N'-Tetradecylfuran-2,5-dicarboxamide (MC 12)

To a solution of FDCA-Cl_2 (0.5 g, 2.6 mmol) in 50 ml dry THF were added didecylamine (1.9 g, 6.5 mmol) and triethylamine (1.2 ml). The solution was stirred at room temperature over week-end then quenched removing the solvent under reduced pressure. The crude was dissolved in DCM and washed with HCl 5% (3x) and with water (3x). The organic phase was dried over anhydrous $MgSO_4$ and evaporated in vacuum.

The crude was purified by flash column chromatography using DCM/MeOH 98:2 as eluent. The product was obtained as a yellow in 47 % yield

^{1}H NMR: δ 0.90 (12 H, t, $CH_3(CH_2)_7$), 1.17-1.43 (56 H, m, $CH_3(CH_2)_7$), 1.56-1.69 (8H, m, NCH_2CH_2), 3.37-3.59 (8H, m, NCH_2), 6.95 (2H, s, CH); ^{13}C NMR: δ 14.1, 22.7, 29.3, 29.4, 29.5, 29.6, 115.7, 148.6, 159.6.

N,N,N′,N′-Tetradecyltetrahydrofuran-2,5-dicarboxamide (13)

To a solution of N,N,N′,N′-Tetradecylfuran-2,5-dicarboxamide (0.87 g, 1.21 mmol) in 40 ml MeOH was added 10% Pd/C after bubbling N_2 for 10 minutes. The solution was kept under 8 bar H_2 in an autoclave overnight. After removal of the catalyst by filtration the solvent was evaporated under reduced pressure. The filtration was made through a glassfilter using hyflo as filter-aid. The product was obtained as a pale yellow oil in quantitative yield. ^{1}H NMR: δ 0.90 (12 H, m, C*H*$_3$(CH$_2$)$_7$), 1.52-1.3 (56 H, m, CH$_3$(C*H*$_2$)$_7$), 1.65-1.56 (8H, m, NCH$_2$C*H*$_2$), 2.43-2.17 (4H, m, CH$_2$ ring), 3.53-3.24 (8H, m, NC*H*$_2$), 4.7 (2H, s, OC*H*CO). ^{13}C NMR: δ 77.87, 47.6, 46.5, 31.9, 29.62, 29.58, 29.47, 29.42, 29.32, 29.1, 27.5, 27.1, 26.9, 22.7, 14.1. IR (υ_{max}/cm^{-1}). 2920.8, 2852.2, 1653.6, 1457.1, 1377.4, 1059.2. ESI-MS: *m*/*z* 741.71 [100%; (M+Na)$^+$]. HRMS: *m*/*z* calcd for $C_{46}H_{90}N_2O_3Na$: .741.6849; found: 741.6407.

5.4 References

(1) Sasaki, Y.; Choppin, R. Solvent Extraction of Eu, Th, U, Np and Am with N,N′-Dimethyl-N,N′-Dihexyl-3-Oxapentanediamide and Its Analogous Compounds. *Anal. Sci.* **1996**, *12* (2), 225–230. https://doi.org/10.2116/analsci.12.225.

(2) Sasaki, Y.; Tachimori, S. Extraction of Actinides (III), (IV), (V), (VI), and Lanthanides (III) by Structurally Tailored Diamides. *Solvent Extr. Ion Exch.* **2002**, *20* (1), 21–34. https://doi.org/10.1081/SEI-100108822.

(3) Sasaki, Y.; Choppin, G. R. Extraction of Np(V) by N,N′-Dimethyl-N,N′-Dihexyl-3-Oxapentanediamide. *Radiochim. Acta* **1998**, *80* (2). https://doi.org/10.1524/ract.1998.80.2.85.

(4) Pearson, R. G. Hard and Soft Acids and Bases. *J. Am. Chem. Soc.* **1963**, *85* (22), 3533–3539.

(5) Modolo, G., Vijgen, H., Schreinemachers,C., Baron, P., Dinh, B. Proceedings of GLOBAL, New Orleans, Louisiana, USA, 16-20 November. **2003**, 1926–1930.

(6) Modolo, G.; Wilden, A.; Geist, A.; Magnusson, D.; Malmbeck, R. A Review of the Demonstration of Innovative Solvent Extraction Processes for the Recovery of Trivalent Minor Actinides from PUREX Raffinate. *Radiochimica Acta*. August 2012, pp 715–725. https://doi.org/10.1524/ract.2012.1962.

(7) Brown, J.; McLachlan, F.; Sarsfield, M.; Taylor, R.; Modolo, G.; Wilden, A. Plutonium Loading of Prospective Grouped Actinide Extraction (GANEX) Solvent Systems Based on Diglycolamide Extractants. *Solvent Extr. Ion Exch.* **2012**, *30* (2), 127–141. https://doi.org/10.1080/07366299.2011.609378.

(8) Sasaki, Y.; Sugo, Y.; Morita, K.; Nash, K. L. The Effect of Alkyl Substituents on Actinide and Lanthanide Extraction by Diglycolamide Compounds. *Solvent Extr. Ion Exch.* **2015**, *33* (7), 625–641. https://doi.org/10.1080/07366299.2015.1087209.

(9) Malmbeck, R.; Magnusson, D.; Geist, A. Modified Diglycolamides for Grouped

Actinide Separation. *J. Radioanal. Nucl. Chem.* **2017**, *314* (3), 2531–2538. https://doi.org/10.1007/s10967-017-5614-2.

(10) Sasaki, Y.; Sugo, Y.; Suzuki, S.; Kimura, T. A Method for the Determination of Extraction Capacity and Its Application to N,N,N′,N′-Tetraalkylderivatives of Diglycolamide-Monoamide/n-Dodecane Media. *Anal. Chim. Acta* **2005**, *543* (1–2), 31–37. https://doi.org/10.1016/j.aca.2005.04.061.

(11) Iqbal, M.; Huskens, J.; Verboom, W.; Sypula, M.; Modolo, G. Synthesis and Am/Eu Extraction of Novel TODGA Derivatives. *Supramol. Chem.* **2010**, *22* (11–12), 827–837. https://doi.org/10.1080/10610278.2010.506553.

(12) Wilden, A.; Kowalski, P. M.; Klaß, L.; Kraus, B.; Kreft, F.; Modolo, G.; Li, Y.; Rothe, J.; Dardenne, K.; Geist, A.; Leoncini, A.; Huskens, J.; Verboom, W. Unprecedented Inversion of Selectivity and Extraordinary Difference in the Complexation of Trivalent f Elements by Diastereomers of a Methylated Diglycolamide. *Chem. - A Eur. J.* **2019**, *25* (21), 5507–5513. https://doi.org/10.1002/chem.201806161.

(13) Chapron, S.; Marie, C.; Arrachart, G.; Miguirditchian, M.; Pellet-Rostaing, S. New Insight into the Americium/Curium Separation by Solvent Extraction Using Diglycolamides. *Solvent Extr. Ion Exch.* **2015**, *33* (3), 236–248. https://doi.org/10.1080/07366299.2014.1000792.

(14) Sasaki, Y.; Sugo, Y.; Suzuki, S.; Tachimori, S. The novel extractants, diglycolamides, for the extraction of lanthanides and actinides in HNO_3-n-dodecane system. *Solvent Extr. Ion Exch.* **2001**, *19* (1), 91–103. https://doi.org/10.1081/SEI-100001376.

(15) Ansari, S. A.; Pathak, P.; Mohapatra, P. K.; Manchanda, V. K. Chemistry of Diglycolamides: Promising Extractants for Actinide Partitioning. *Chem. Rev.* **2012**, *112* (3), 1751–1772. https://doi.org/10.1021/cr200002f.

(16) Schotten, C. Ueber Die Oxydation Des Piperidins. *Berichte der Dtsch. Chem. Gesellschaft* **1884**, *17* (2), 2544–2547. https://doi.org/https://doi.org/10.1002/cber.188401702178.

(17) Baumann, E. Ueber Eine Einfache Methode Der Darstellung von Benzoësäureäthern. *Berichte der Dtsch. Chem. Gesellschaft* **1886**, *19* (2), 3218–3222. https://doi.org/https://doi.org/10.1002/cber.188601902348.

(18) Leoncini, A.; Huskens, J.; Verboom, W. Preparation of Diglycolamides via Schotten-Baumann Approach and Direct Amidation of Esters. *Synlett* **2016**, *27* (17), 2463–2466. https://doi.org/10.1055/s-0035-1561495.

(19) Wilden, A.; Modolo, G.; Lange, S.; Sadowski, F.; Beele, B. B.; Skerencak-Frech, A.; Panak, P. J.; Iqbal, M.; Verboom, W.; Geist, A.; Bosbach, D. Modified Diglycolamides for the An(III) + Ln(III) Co-Separation: Evaluation by Solvent Extraction and Time-Resolved Laser Fluorescence Spectroscopy. *Solvent Extr. Ion Exch.* **2014**, *32* (2), 119–137. https://doi.org/10.1080/07366299.2013.833791.

Conclusions

Independently from the political decision to adopt or not nuclear power as source for the production of electrical energy, the recycle of upcoming or already existing nuclear wastes is one of the current worldwide scientific, and social challenges.

The spent nuclear fuel contains Minor Actinides which are recognized as the main responsible for the long-term radiotoxicity of the waste. Accordingly, the recovery of MAs can be considered the key step to reduce the radioactive hazard related to the spent nuclear fuel. In Europe three alternatives processes *r*-SANEX, *i*-SANEX and *1c*-SANEX which exploit lipophilic or hydrophilic An(III) selective ligands have been proposed for the selective extraction of An from the waste.

In this thesis we focused on the synthesis and the extraction properties of both hydrophilic and lipophilic ligands based on the PyTri chelating unit. In particular, the effect of substitutes on the pyridine core or triazoles units were studied.

The developed of a "*three steps, one pot*" procedure which allows to directly isolate PTD without further intermediate purification steps and without the handling of the hazardous 3-azidopropan-1-ol discloses a key step for the industrial scale implementation of PTD. The investigated PTD degradation products DP1 and DP2 were successfully synthetized and preliminary extraction tests were performed. The data collection confirms the exceptional ability of the PyTri chelating unit as effective and selective stripping agent for trivalent actinide ions in acidic water solution.

In order to enhance PTD complexation properties, a revised ligand was designed and synthetized, PTD-OMe. The obtained data demonstrate that the presence of an electron donating group enhance the basicity of the Py core thus making PTD-OMe a better ligand than PTD. Nevertheless, in the acidic conditions used in the extraction experiments (0.44 M HNO_3) PTD-OMe is protonated to a larger extent than PTD and therefore shows e lower stripping abilities. These results are of great importance for the development of novel hydrophilic ligands aim to the improvement of PTD extraction behavior.

Considering the high selectivity of the water-soluble pyridine-bis-triazole demonstrated by PTD and PTD-OMe we developed a series of N_3-core-based lipophilic ligands, obtained by modifying the lateral substituents with alkyl chains. Among all PTEH showed the best properties in term of solubility and extraction behavior. This is the first example of a lipophilic extractants based on the PyTri unit able to selectively extract An(III) ions from a rafioactive waste and this opens the way to a possible industrial implementation of such ligands in the r-SANEX and 1c-SANEX processes.

The last part of the work was carried out at the University of Twente during a three months secondment. The collaboration successfully led to the synthesis of 5 new DGA-based ligands. The Schotten-Baumann approach demonstrated to be a valid method for the preparation of DGAs bringing substituents at the central backbone. The prepared ligands will soon be tested in the extraction in order to evaluate their efficiency and selectivity towards trivalent An and Ln. These studies will help to better understand the effect of substituents at the central backbone on the extraction behavior of DGAs.

List of Publications

1. Vu, T. H.; Simonin, J.-P.; Rollet, A. L.; Egberink, R. J. M.; Verboom, W.; Gullo, M. C.; Casnati, A. **Liquid/Liquid Extraction Kinetics of Eu(III) and Am(III) by Extractants Designed for the Industrial Reprocessing of Nuclear Wastes**. *Ind. Eng. Chem. Res.* **2020**, *59* (30). https://doi.org/10.1021/acs.iecr.0c02401.
2. Gullo, M. C.; Baldini, L.; Casnati, A.; Marchiò, L. **Halogen Bonds Direct the Solid State Architectures of a Multivalent Iodopropargylcalix[4]Arene**. *Cryst. Growth Des.* **2020**, *20* (6). https://doi.org/10.1021/acs.cgd.0c00442.
3. Weßling, P.; Trumm, M.; Macerata, E.; Ossola, A.; Mossini, E.; Gullo, M. C.; Arduini, A.; Casnati, A.; Mariani, M.; Adam, C.; Geist, A.; Panak, P. J. **Activation of the Aromatic Core of 3,3′-(Pyridine-2,6-Diylbis(1 H-1,2,3-Triazole-4,1-Diyl))Bis(Propan-1-Ol) - Effects on Extraction Performance, Stability Constants, and Basicity**. *Inorg. Chem.* **2019**, *58* (21). https://doi.org/10.1021/acs.inorgchem.9b02325.
4. Ossola, A.; Macerata, E.; Mossini, E.; Giola, M.; Gullo, M. C.; Arduini, A.; Casnati, A.; Mariani, M. **2,6-Bis(1-Alkyl-1H-1,2,3-Triazol-4-Yl)-Pyridines: Selective Lipophilic Chelating Ligands for Minor Actinides.** *J. Radioanal. Nucl. Chem.* **2018**, *318* (3), 2013–2022. https://doi.org/10.1007/s10967-018-6253-y.
5. Souto, M.; Gullo, M. C.; Cui, H.; Casati, N.; Montisci, F.; Jeschke, H. O.; Valentí, R.; Ratera, I.; Rovira, C.; Veciana, J. **Role of the Open-Shell Character on the Pressure-Induced Conductivity of an Organic Donor–Acceptor Radical Dyad**. *Chem. - A Eur. J.* **2018**, *24* (21). https://doi.org/10.1002/chem.201800881.